

Copyright Warning & Restrictions

The copyright law of the United States (Title 17, United States Code) governs the making of photocopies or other reproductions of copyrighted material.

Under certain conditions specified in the law, libraries and archives are authorized to furnish a photocopy or other reproduction. One of these specified conditions is that the photocopy or reproduction is not to be “used for any purpose other than private study, scholarship, or research.” If a user makes a request for, or later uses, a photocopy or reproduction for purposes in excess of “fair use” that user may be liable for copyright infringement,

This institution reserves the right to refuse to accept a copying order if, in its judgment, fulfillment of the order would involve violation of copyright law.

Please Note: The author retains the copyright while the New Jersey Institute of Technology reserves the right to distribute this thesis or dissertation

Printing note: If you do not wish to print this page, then select “Pages from: first page # to: last page #” on the print dialog screen

The Van Houten library has removed some of the personal information and all signatures from the approval page and biographical sketches of theses and dissertations in order to protect the identity of NJIT graduates and faculty.

INFORMATION TO USERS

This was produced from a copy of a document sent to us for microfilming. While the most advanced technological means to photograph and reproduce this document have been used, the quality is heavily dependent upon the quality of the material submitted.

The following explanation of techniques is provided to help you understand markings or notations which may appear on this reproduction.

1. The sign or "target" for pages apparently lacking from the document photographed is "Missing Page(s)". If it was possible to obtain the missing page(s) or section, they are spliced into the film along with adjacent pages. This may have necessitated cutting through an image and duplicating adjacent pages to assure you of complete continuity.
2. When an image on the film is obliterated with a round black mark it is an indication that the film inspector noticed either blurred copy because of movement during exposure, or duplicate copy. Unless we meant to delete copyrighted materials that should not have been filmed, you will find a good image of the page in the adjacent frame. If copyrighted materials were deleted you will find a target note listing the pages in the adjacent frame.
3. When a map, drawing or chart, etc., is part of the material being photographed the photographer has followed a definite method in "sectioning" the material. It is customary to begin filming at the upper left hand corner of a large sheet and to continue from left to right in equal sections with small overlaps. If necessary, sectioning is continued again—beginning below the first row and continuing on until complete.
4. For any illustrations that cannot be reproduced satisfactorily by xerography, photographic prints can be purchased at additional cost and tipped into your xerographic copy. Requests can be made to our Dissertations Customer Services Department.
5. Some pages in any document may have indistinct print. In all cases we have filmed the best available copy.

University
Microfilms
International

300 N. ZEEB RD., ANN ARBOR, MI 48106

8121969

McGOVERN, PAUL ALOYSIUS

STATISTICAL AVERAGING IN POSITION DETERMINATION BY
HOLOGRAPHY UNDER TURBULENCE CONDITIONS

New Jersey Institute of Technology

D.ENG.SC.

1981

**University
Microfilms
International** 300 N. Zeeb Road, Ann Arbor, MI 48106

PLEASE NOTE:

In all cases this material has been filmed in the best possible way from the available copy. Problems encountered with this document have been identified here with a check mark .

1. Glossy photographs or pages
2. Colored illustrations, paper or print _____
3. Photographs with dark background
4. Illustrations are poor copy _____
5. Pages with black marks, not original copy _____
6. Print shows through as there is text on both sides of page _____
7. Indistinct, broken or small print on several pages _____
8. Print exceeds margin requirements _____
9. Tightly bound copy with print lost in spine _____
10. Computer printout pages with indistinct print _____
11. Page(s) _____ lacking when material received, and not available from school or author.
12. Page(s) _____ seem to be missing in numbering only as text follows.
13. Two pages numbered _____. Text follows.
14. Curling and wrinkled pages _____
15. Other _____

STATISTICAL AVERAGING
IN POSITION DETERMINATION
BY HOLOGRAPHY
UNDER TURBULENCE CONDITIONS

by

Paul Aloysius McGovern

This dissertation is to be used only with due regard to the rights of the author. Bibliographical references may be noted, but passages must not be copied without permission of the Institute and without credit being given in subsequent written or published work.

Dissertation submitted to the Faculty of the Graduate School
of the New Jersey Institute of Technology in partial fulfillment
of the requirements for the degree of
Doctor of Engineering Science
1981

APPROVAL SHEET

Title of Thesis: Statistical Averaging In Position
Determination By Holography Under
Turbulence Conditions

Name of Candidate: Paul Aloysius McGovern
Doctor of Engineering Science, 1981

Thesis and Abstract Approved:

Mauro Zambuto Date
Professor
Electrical Engineering Department

Date

Date

Date

VITA

Name: Paul Aloysius McGovern.

Degree and date to be conferred: D. Eng. Sc., 1981.

<u>Collegiate institutions attended</u>	<u>Dates</u>	<u>Degree</u>	<u>Date of Degree</u>	
Newark College of Engineering	1960/65	B.S.E.E.	June	1965
Michigan State University	1965/66	M.S.	September	1966
New Jersey Institute of Technology	1971/81	D.Eng.Sci.	May	1981

Major: Electrical Engineering.

Publications: "Composite Miniature Special Effects by Holography," by Mauro Zambuto and Paul McGovern, The Acts of the 14th Congress of UNIATEC.

Positions held: Senior Engineer, The Port Authority of New York and New Jersey, One World Trade Center, Room 58S, New York, New York 10048.

ABSTRACT

Title of Thesis: Statistical Averaging In Position
Determination By Holography Under
Turbulence Conditions.

Paul Alyious McGovern, Doctor of Engineering Science, 1981.

Thesis directed by: Professor Mauro Zambuto

An investigation of several, disparate phenomena is conducted with the aim of developing a novel surveying system capable of overcoming the limitations imposed by turbulence in modern surveying. This method incorporates standard holographic techniques and time domain statistical averaging of survey data.

Some pertinent characteristics of atmospheric turbulence are reviewed, and the restrictions imposed on standard surveying practices by such turbulence are identified. A model for the turbulent medium is proposed on the basis of previous work and several theoretical results are summarized and extended.

On this basis the technical characteristics of the proposed technique are developed and each step analyzed in detail and design procedures established.

A specific surveying task is selected and the new method is applied.

Experimental verification of each of the techniques employed in the new surveying method is presented. To this end techniques for the laboratory production of the desired condition and for the analysis of the method for recording survey data under turbulence are developed and their validity tested. Statistical analysis of the recorded survey data is presented to verify the accuracy of the results.

As a second application of the holography principles and techniques described, a novel methodology is proposed, capable of overcoming inherent restrictions of the miniature techniques presently used by the motion picture industry.

The existing use of miniature techniques is reviewed and the benefits of the holographic techniques are identified. The process by which the new method is implemented is described. The mathematics for determining the dimensions of the miniature objects and the locations of all the components utilized in making the hologram and reconstructing and magnifying its image are presented.

Sources of distortion are also discussed and methods for avoiding them are indicated.

Experimental verification is cited.

PREFACE

The study of optical propagation in turbulent media is, at the present state of the art, an open subject of research. For many years researchers have investigated turbulence in optical transmission media, endeavoring to define appropriate parameters to characterize the phenomenon and to develop techniques for their measurement in an attempt to obviate the degradation of optical images resulting from the effects of turbulence on the optical transfer characteristics of gaseous and liquid media. Most researchers have found the structure function formulation to be particularly well suited to the description of such effects.

Previous work by other investigators has proposed a specific model of the turbulent medium and derived theoretically several statistical properties of the resulting structure function. These properties appeared to suggest a promising approach to several practical engineering applications of optical image analysis, so that it was considered expedient to develop an evaluation of these results, together with possible further extension of the attending theory and proper experimental support.

The investigation presented in this thesis is mainly concerned with the effects of atmospheric turbulence on an optical path when viewing objects at a relatively long distance in surveying applications. Standard surveying

practices are severely hampered by atmospheric turbulence since the only techniques available to deal with it are mostly qualitative and empirical and offer cumbersome and economically onerous, impractical applications. Effective use of these statistical properties also requires the use of other techniques, such as holographic image magnification and spatial positioning, which, for this application, have to be refined, so that a revision and expansion of previously developed holographic theory is mandated.

A synthesis of such theories and techniques indicates several promising avenues of approach to a rather large variety of problems.

As a result a novel surveying process is proposed, which provides the capability for performing accurate surveys under turbulence conditions at observation distances much greater than those heretofore permitted by the state of the art.

In Chapter I, the characteristics of atmospheric turbulence are reviewed and some useful properties of a mathematical structure function are analyzed.

The effects of such turbulence on standard surveying practices are identified and a novel method for conducting a survey of an airport runway is defined. This new procedure utilizes the holographic technique for magnification of a reconstructed image and time domain statistical averaging of optically acquired data to relieve the maximum

distance constraints placed on standard surveying applications by atmospheric turbulence.

In Chapter II, the theory of magnification of a reconstructed hologram image is reviewed in its general form. Two specific areas are then developed. The first area deals with the inherent lateral distortion which results from magnification of an image. Two methods for removing or avoiding this distortion are presented. The second area addresses the variables in holographic equipment locations during the recording of a hologram and the subsequent magnification of its reconstructed image. The optimum parameters for the surveying application are developed.

Chapter III discusses the requirements to be met by the new surveying method with particular regard to the experimental arrangements for a laboratory feasibility study. The characteristics of the hologram to be used in the laboratory verification of the principles are developed. The construction of the object for the hologram is detailed, as is the procedure for making the hologram.

Experimental results are presented verifying the validity of the theory in obtaining a hologram suitable for its intended surveying use; in controlling the magnification of the reconstructed image to the desired dimensions; and in spatially locating the reconstructed image at the required location with suitable accuracy.

In particular the chapter describes the method used to spatially locate a hologram's reconstructed image at any

predetermined position and how the exact fact of magnification of the image is determined after its spatial location has been altered, since longitudinal and lateral magnification are altered proportionately. The laboratory equipment required for the verification of the new method for recording survey data is described.

Chapter IV describes several methods used to simulate random atmospheric turbulence together with the optical distortion effects associated with the location in the optical path at which the turbulence occurs. Experimental verification is presented of the time domain statistical averaging of photographically recorded survey data. The validity of these averaging techniques and of the theoretical assumptions on which they are based is verified on the basis of these experimental results.

Chapter V refers to the miniature techniques used by the motion picture industry to avoid movie-set construction costs. The inherent limitations of the method commonly used at the present state of the art are reviewed and a novel holographic method for removing many of these restrictions is proposed. This method is based on the theory previously described in connection with the development of the holographic surveying techniques.

Longitudinal distortion associated with the magnification of a hologram's reconstructed image is reviewed in detail. A method for compensation for this distortion by appropriate geometric predistortion during the construction

of the miniature set is proposed along with the mathematics and a set of geometrical rules for its design and implementation.

Chapter VI presents conclusions and recommendations for future work.

DEDICATION

To My Wife

ACKNOWLEDGMENT

My sincere thanks to Professor Mauro Zambuto; without his patience, sacrifice and consultation, this work would not have been completed.

Further, the research would not have been possible without the facilities provided by the Electrical Engineering Department of New Jersey Institute of Technology.

TABLE OF CONTENTS

Chapter	Page
PREFACE.	ii
DEDICATION	vii
ACKNOWLEDGMENT	viii
TABLE OF CONTENTS.	ix
LIST OF FIGURES.	x
LIST OF PHOTOGRAPHS.	xii
I. PRECISION SURVEYING IN TURBULENT CONDITIONS. A PROPOSED SYSTEM.	1
II. DISTORTION AND ACCURACY IN HOLOGRAPHIC IMAGE MAGNIFICATION.	32
III. EXPERIMENTAL ARRANGEMENT FOR A FEASIBILITY STUDY.	57
IV. EXPERIMENTAL SIMULATION OF TURBULENCE CONDITIONS	84
V. MINIATURE AND SPECIAL EFFECTS (AN APPLICATION TO MOTION PICTURE TECHNIQUES).	111
VI. CONCLUSIONS AND RECOMMENDATIONS.	125
APPENDIX A. Computation of expected values of A and B in Photograph IV-3.	133
SELECTED BIBLIOGRAPHY.	136

LIST OF FIGURES

Figure		Page
I.1	Optical paths in the absence of turbulence	6
I.2	Optical paths through a turbulent medium	7
I.3	The path of a light ray through a refractive surface.	10
I.4	The projection of triangle PVU on the X axis . .	12
I.5	The path of a light ray through a homogeneous medium	14
I.6	A water pipe method for providing an absolute reference	25
I.7	Airport runway preparation for the proposed survey process	26
I.8	A holographic image superimposed on a runway cross section.	28
I.9	Plan view of a runway and hologram image reconstruction equipment.	30
II.1	Coordinate system for the parameters of holographic wave recording and reconstruction. . . .	34
II.2	Plan view of the locations of the reference and reconstruction light sources	42
II.3	Plot of the values of image displacement (magnification) as a function of Z_r	47
II.4	Plot of the values of image displacement (magnification) as a function of Z_c	48
II.5	Plot of the values of image displacement (magnification) as a function of Z_1	50
III.1a	Elements for recording a hologram.	63
III.1b	Elements for reconstruction of hologram image. .	63
III.2	Equipment arrangement for recording hologram of vertical scale.	65
III.3	Dimensions of vertical scale used for recording hologram	69

LIST OF FIGURES
(continued)

Figure		Page
III.4	Locations of principle elements in recording and reconstruction of hologram image	79
III.5	Translation and rotation of reconstructed image.	83
IV.1a	Two point arrangement for survey subject	85
IV.1b	Three point arrangement for survey subject	85
IV.2	Distortion as a function of the location of turbulence	89
IV.3	Equipment arrangement for optical path thru water	99
IV.4	Equipment arrangement for generating turbulence in water	101
V.1	Miniature shooting using standard techniques	113
V.2	Miniature shooting using holographic techniques.	114
V.3	Coordinate system for the parameters of holographic wave recording and reconstruction.	116
V.4	Longitudinal distortion in magnified image	118
V.5	Starting point for construction of a pre-distorted miniature set.	121
V.6	Predistorted miniature set and undistorted magnified hologram image	124

LIST OF PHOTOGRAPHS

Photograph	Page
III.1 Equipment arrangement for recording hologram . .	72
III.2 Equipment arrangement for recording hologram . .	73
III.3 Reconstructed image juxtaposed to hologram model.	74
III.4 Equipment arrangement for reconstruction of hologram image	75
III.5 Reconstructed image used as measurement scale. .	77
III.6 Reconstructed image superimposed in cross section.	78
III.7 Reconstructed image magnified by a factor of five (5)	80
III.8 Equipment arrangement for magnification of hologram image	81
IV.1 Two point survey subject with scale in the absence of turbulence.	87
IV.2a Equipment arrangement for generating turbulence with open flame.	91
IV.2b Turbulent medium	92
IV.3 Statistical stationary sample through a turbulent medium	94
IV.4 Equipment arrangement for generating turbulence in water.	103
IV.5 Three point survey subject with scale observed through water medium	104
IV.6 Multiple exposures of precise point positions thru turbulent water	105

CHAPTER I

PRECISION SURVEYING IN TURBULENT CONDITIONS. A PROPOSED SYSTEM

The methods utilized in modern surveying have evolved from the need to keep the inevitable measurement errors within acceptable boundaries. The concepts of "accuracy" and "precision" are paramount in classifying possible errors in measurement where "accuracy" is defined as "the degree of absolute nearness to the truth" and "precision" means "the degree of refinement in the performance of an operation." The independent constraints determining the above parameters are in fact the three sources of error, namely, atmospheric conditions, instruments, and humans.

Consider the instrumentation presently available. Tape measures and rods whose lengths are grossly dependent on temperature; transits wherein the relative location and orientation of lenses, scales and levels are subject to temperature variations, manufacturing tolerances and each transit's history of physical handling, and where the tolerances in the mechanical stages produce unavoidable play in the movements.

Also to be considered are the expected human errors in reading and recording the transit, rod and tape data, and the additional errors resulting from the change in the focal length of the surveyor's eyes, due to fatigue, as the work progresses.

As an "error-free" survey is, of course, inconceivable, standards have been established for the degrees of accuracy and precision required in different types of surveys, and accepted practices have been devised for obtaining these standards (broadly described as first, second and third cut accuracies or specific values of allowable error per thousand feet measured). The resulting "state of the art" in surveying is an ingenious complex of geometric measurements, counter measurements, and re-measurements of both, carried on until the required accuracies are obtained.¹

One area of application on which the complexities of surveying techniques have serious impact is in airport runway testing and maintenance. The need for recurrent surveys generally arises from uneven settling of the runways, which generates surface and support bed deterioration.

The gravity of this condition is determined by the impact of the unevenness on aircraft. Very short wavelength grade variations, or bumps, constitute the most easily observable deviation from a flat runway, but aircraft suspension systems effectively smooth out bumps, and these grade variations are generally not critical.

Medium wavelength, or gradual, changes in grade are mostly not absorbed by suspension systems, but rather, tend to cause a change in the attitude of the aircraft. The

¹ Davis, Foote & Kelly, Surveying: Theory and Practice, Fifth Edition, New York: McGraw-Hill, 1968.

resultant change in windload forces is a condition which, if not corrected for by the ship's pilot, can be quite dangerous. These gradual grade variations have always been the most difficult to detect and remove, and now the recent advent of large tail heavy planes has increased flatness requirements to the extent that even grade variations with wavelengths in excess of 2,000' have become critical.

At this writing, the effort to detect and correct such grade variations involves a survey of the entire 10,000' x 150' area of a runway, on 20' centers, attempting to attain a first cut accuracy of less than 1/10 of a foot vertical error per 1,000 feet measured. The execution of this type survey is a painstaking and expensive operation. Utilizing 4 man-teams, it takes as many as 500 man-days to complete, and the runway must be shut down for this period. Also, the resultant data acquired from these surveys is often of marginal quality.

Due to atmospheric turbulence, which produces intolerable optical errors at viewing distances in excess of 400' on a still winter night, and in excess of 50' on a hot summer day, the number of transit sightings possible from one reference transit location is severely limited, and the coordinates of each additional transit location are determined by dependent calculations, with all the inherent error propagation. The calculated 'less than 1/10' error per 1,000'' results are therefore questionable.

The impact of closing a runway on an airport's

operating capacity is so severe that management is reluctant to do so until surface conditions deteriorate to the point where they present a greater hazard to aircraft than the traffic congestion resulting from a shutdown. Extensive efforts have been put forth by many agencies toward improving 'state-of-the-art' conditions for runway surveys with little success to date.

What is needed most is an accurate means of spot-checking flatness conditions without interrupting runway operations. Attempts to develop new techniques, such as equipping surface vehicles with altimeters and vibration detectors/recorders and driving them down runways at different speeds, and investigations of alternate optical techniques have been unsuccessful.

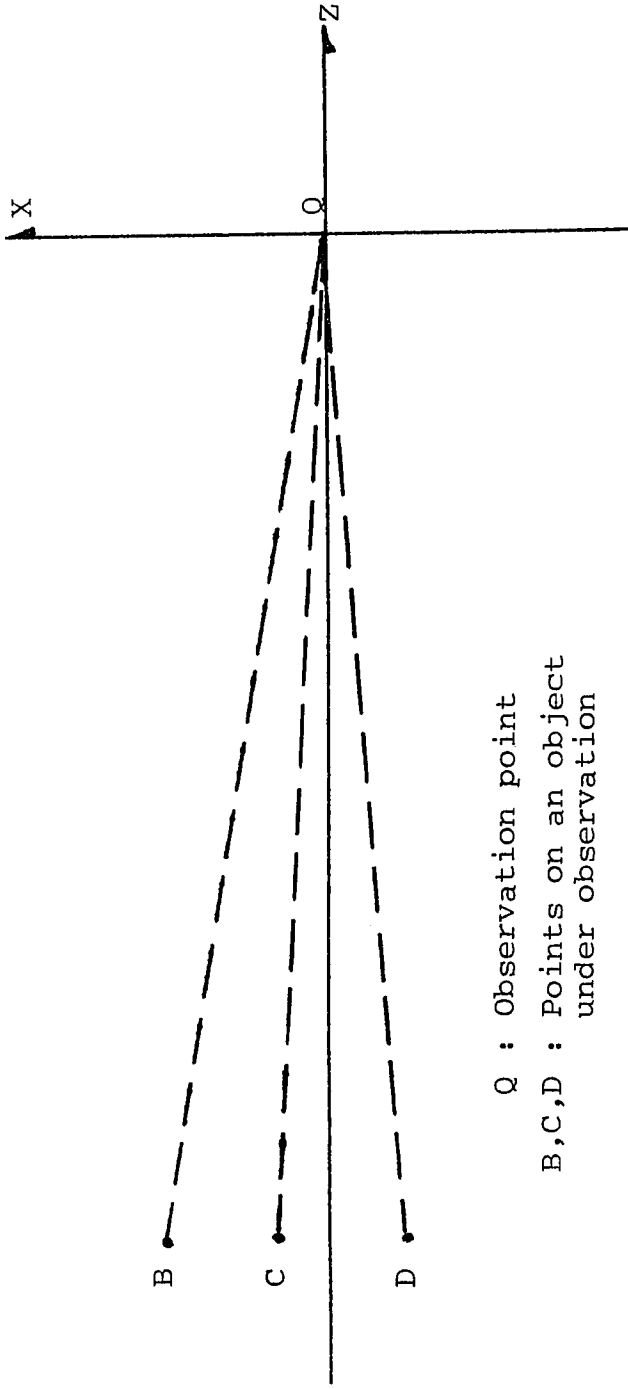
As indicated the most important and inconvenient source of error in precision surveying is turbulence. We shall therefore briefly summarize some characteristics of this disturbance.

Identification of the parameters of turbulence, developing techniques for their measurement, and identifying the effects of turbulence on the transfer characteristics of gas and liquid media, has been the pursuit of researchers for some time. The specific area of concern here is atmospheric turbulence and its effect on the propagation of light, i.e., the investigation of the effects of such parameters as temperature gradients, density variations, presence of moisture, etc., which introduce an uncertainty as to the true location

of an optically observed object.

To obtain some insight into the nature and extent of this uncertainty, and to develop a basis upon which to examine its cause, the conditions in Figure I-1 will be considered. Here is shown an observation point Q, and three randomly selected points B, C, and D, on the object being observed. In the ideal case, where the region between the object and the observation point is a homogeneous and isotropic medium, with an index of refraction = N , the optical paths of light rays from points B, C, and D to point Q would be straight lines as shown. In nature, or more specifically the earth's atmosphere, this homogeneous condition never exists over an extended region.

The reasons for this are too numerous to pursue, but as an example, consider the effect of the simple movement of one's hand in the intervening region between the object and the observer. There is a compression of air in front of the hand, a partial vacuum in the wake of the movement, and the original ambient density in the surrounding undisturbed region. The effect is that there are several mediums, at least three, with different indices of refraction now existing in the immediate vicinity of the movement, where perhaps there was only one before. A realistic representation of a region that the light rays might traverse is indicated in Figure I-2. Here the interposing region between object and observer is represented by a series of layers of medium with different indices of refraction = N_1 ,

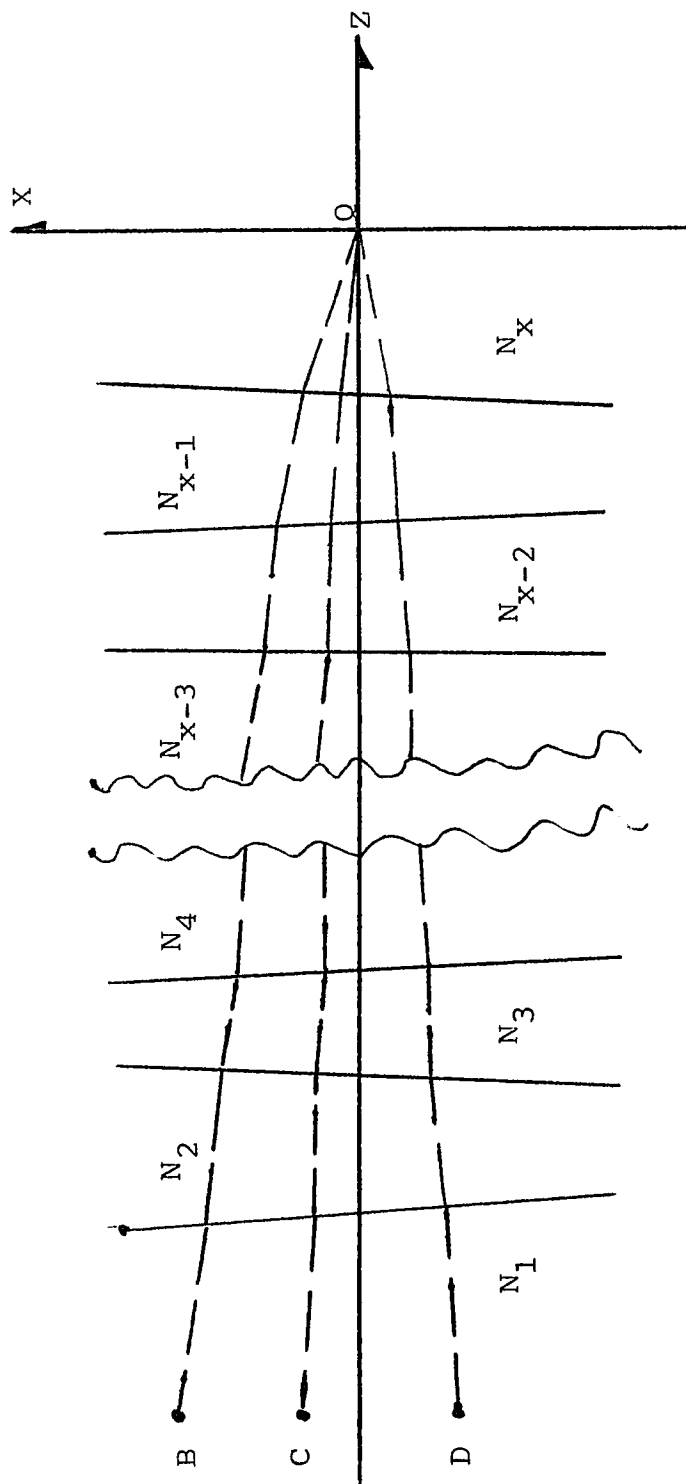


Q : Observation point

B,C,D : Points on an object
under observation

Figure I-1

Optical paths in the absence of turbulence



Q : Observation point
 B,C,D : Points on an object
 under observation
 N_x : Index of refraction
 of a layer of medium

Figure I-2
 Optical paths through a turbulent medium

N_2, \dots, N_x , randomly distributed among them.

This method of representing the influence of turbulence effects on optical paths by assuming homogeneous layers of medium is not new. For several years, thin glass partitions have been successfully used to duplicate the effects of limited regions of atmospheric turbulence both in standard optical imagery applications and in holographic applications.^{2,3} More recently for instance in a holographic application⁴, it was shown that both individual and simultaneous motion of an observed object and a photographic recording medium produce the same effects as a specific quantity of glass partitions on an optical path, the quantities varying in each case with the amount and type of motion.

Based on these findings, it appears reasonable to represent all the possible disturbances that can affect the path a light ray traverses, between object and observer, by a series of homogeneous, isotropic layers of medium, as proposed.

The interfaces between adjacent regions, in Figure I-2, are shown as flat surfaces which intersect the Z axis at random angles. For a single light ray, with zero width

² J.W. Goodman, W.H. Huntley, Jr., D.W. Jackson and M. Lehmann, *Appl. Phys. Letters*, 8, 311 (1966).

³ J.D. Gaskill, *J. Opt. Soc. Am.*, 58, 600 (1968).

⁴ S.I. Feldman, The Effects of Optical Path Perturbation During Recording On A Reconstructed Holograph Image, Doctoral Thesis, New Jersey Institute of Technology, (1976).

dimension, these flat surfaces can be considered as the tangents to the actual turbulence boundaries at the points at which the light ray strikes each boundary. Each of these interfaces is a refractive surface, and as a light ray passes through this stack of refractive surfaces, its path is altered at each surface in accordance with Snell's law of refraction.

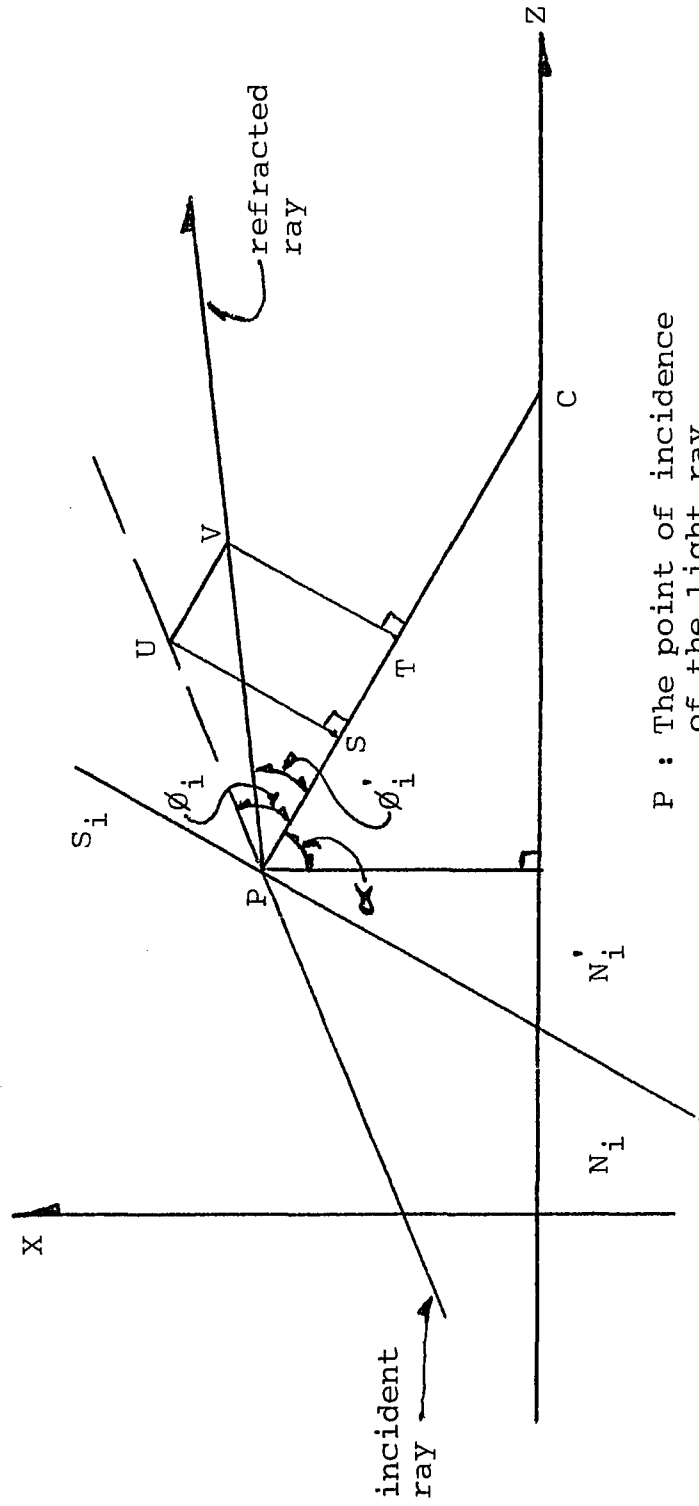
Consider the surface S_i , selected randomly from the stack, shown in Figure I-3. There are two basic operations that control the light ray's path across the region depicted, i.e., Translation across the homogeneous mediums and Refraction at the surface interfacing these adjacent mediums. (Reflection can be considered as negative refraction.)

The methods of geometrical optics provide the means for formulating the point by point bending of the light ray by the use of matrices.⁵ In the development, the following sign conventions will be adhered to:

1. A distance is positive if measured from left to right,
2. A distance is always measured from a refracting surface, and
3. A ray coordinate before and after refraction will be denoted by the same letter, but the one after refraction will be primed.

⁵ E.L. O'Neill, Introduction to Statistical Optics, Chap. 3, Addison Wesley, 1963.

θ'_i : Angle of refraction
 $N(\)$: Index of refraction
 of a layer of medium
 C,S,T,U,V : Geometric construction points



P : The point of incidence
 of the light ray
 S_i : Refractive surface
 θ_i : Angle of incidence
 α : Angle between the Z axis
 and the refractive surface

Figure I-3

The path of a light ray through a refractive surface

The ray strikes the refracting surface S_i , with direction cosines l_i, m_i, n_i , at a point $P(x, y, z)$ and leaves the surface with direction cosines l'_i, m'_i, n'_i . (For simplicity only the XZ plane, with direction cosine l , is considered in this development.) The normal to surface S_i , at point P, intersects the Z axis at point C.

Constructing line segments

$$PU = N_i, \text{ and } PV = N_i \quad (\text{I-1})$$

by the selection of arbitrary units, on the incident and refracted paths, respectively, and dropping perpendiculars from points U and V to line segment PC provides the following:

$$US = N_i \sin \theta_i \quad (\text{I-2})$$

$$VT = N_i \sin \theta_i. \quad (\text{I-3})$$

By Snell's law,

$$US = VT. \quad (\text{I-4})$$

Therefore, UV is proven parallel to PC and both have the same direction cosine

$$\cos (\pi - \alpha) = -\cos \alpha = \frac{0 - x_i}{PC} = \frac{-x_i}{PC}. \quad (\text{I-5})$$

As shown in Figure I-4 the projection of the triangle PVU on the X axis produces:

$$N_i l_i = L_i \text{ and } N'_i l'_i = L'_i, \quad (\text{I-6})$$

and

$$L'_i = L_i - UV \cos \alpha \quad (\text{I-7})$$

or

- $N_{()}$: Index of refraction
- P : The point of incidence of the light ray
- $N_i^l i$: Projection of PU on X axis
- $N_i^l i'$: Projection of PV on X axis

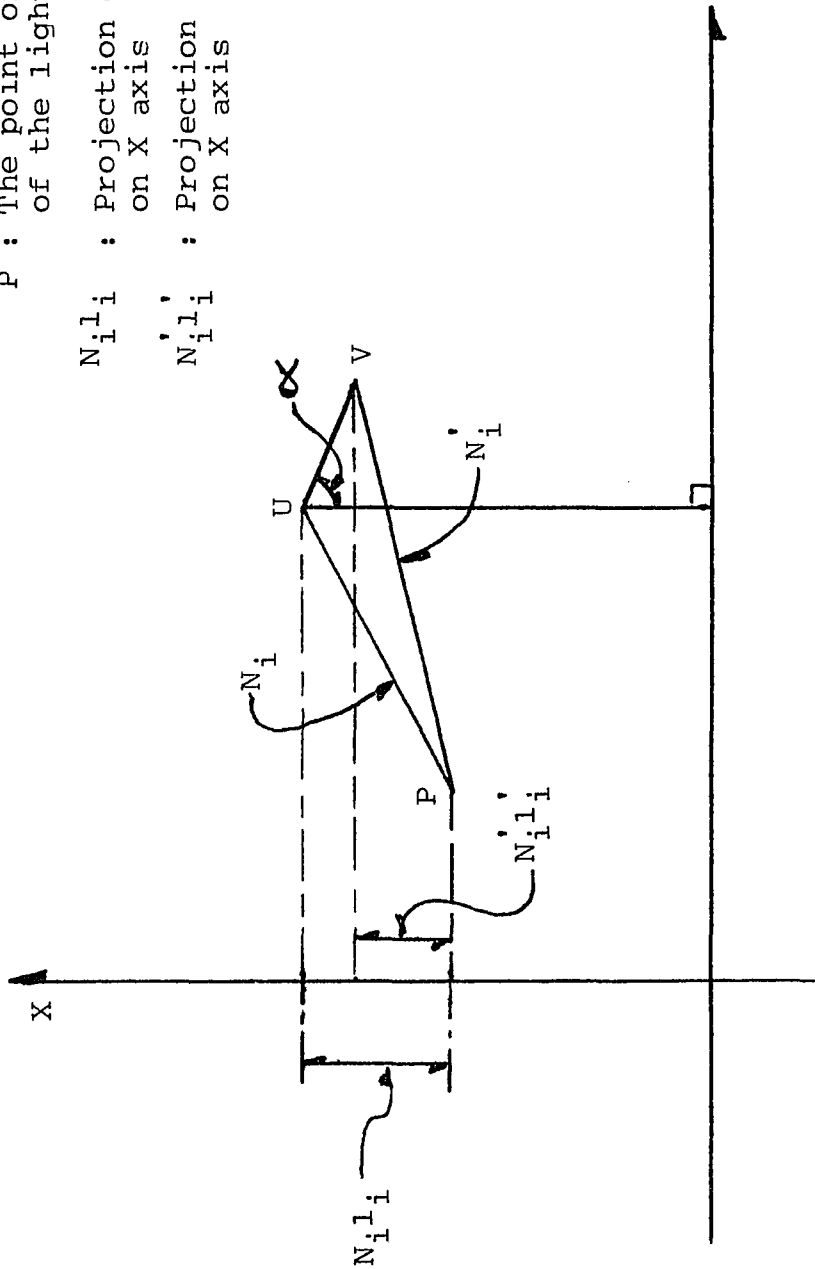


Figure I-4
The projection of triangle PVU on the X axis

$$L_i' = L_i - \frac{UVx_i}{PC} \quad (I-8)$$

But from Figure I-3

$$UV = PT - PS = N_i' \cos \theta_i' - N_i \cos \theta_i, \quad (I-9)$$

therefore,

$$L_i' = L_i - A_i x_i \quad (I-10)$$

where

$$A_i = \frac{N_i' \cos \theta_i' - N_i \cos \theta_i}{PC} \quad (I-11)$$

Then, since $x_i = x_i$, the x coordinate of point P, the Transformation equation for refraction at surface S_i can be written as

$$\begin{bmatrix} L_i' \\ x_i' \end{bmatrix} = \begin{bmatrix} 1 & -A_i \\ 0 & 1 \end{bmatrix} \begin{bmatrix} L_i \\ x_i \end{bmatrix} \quad (I-12)$$

where the refraction matrix is identified as R;

$$R \equiv \begin{bmatrix} 1 & -A_i \\ 0 & 1 \end{bmatrix} \quad (I-13)$$

The light ray now travels along its refracted path through the homogeneous medium, with refraction index = N_i' , until it strikes the next refracting surface, S_{i+1} , (Figure I-5). The ray travels a geometric distance = t_i' , with direction cosine l_i' , and strikes the next refractive surface, S_{i+1} , at x component

$$x_{i+1} = x_i' + PS = x_i' + t_i' l_i'. \quad (I-14)$$

For convenience, if

$$T_i = t_i' / N_i', \quad (I-15)$$

then $T_i L_i' = t_i' l_i', \quad (I-16)$

- N_i : Index of refraction
- S_i : Refractive surface
- t_i : Length of optical path segment
- S : Geometric construction point
- P : Point of incidence of light ray

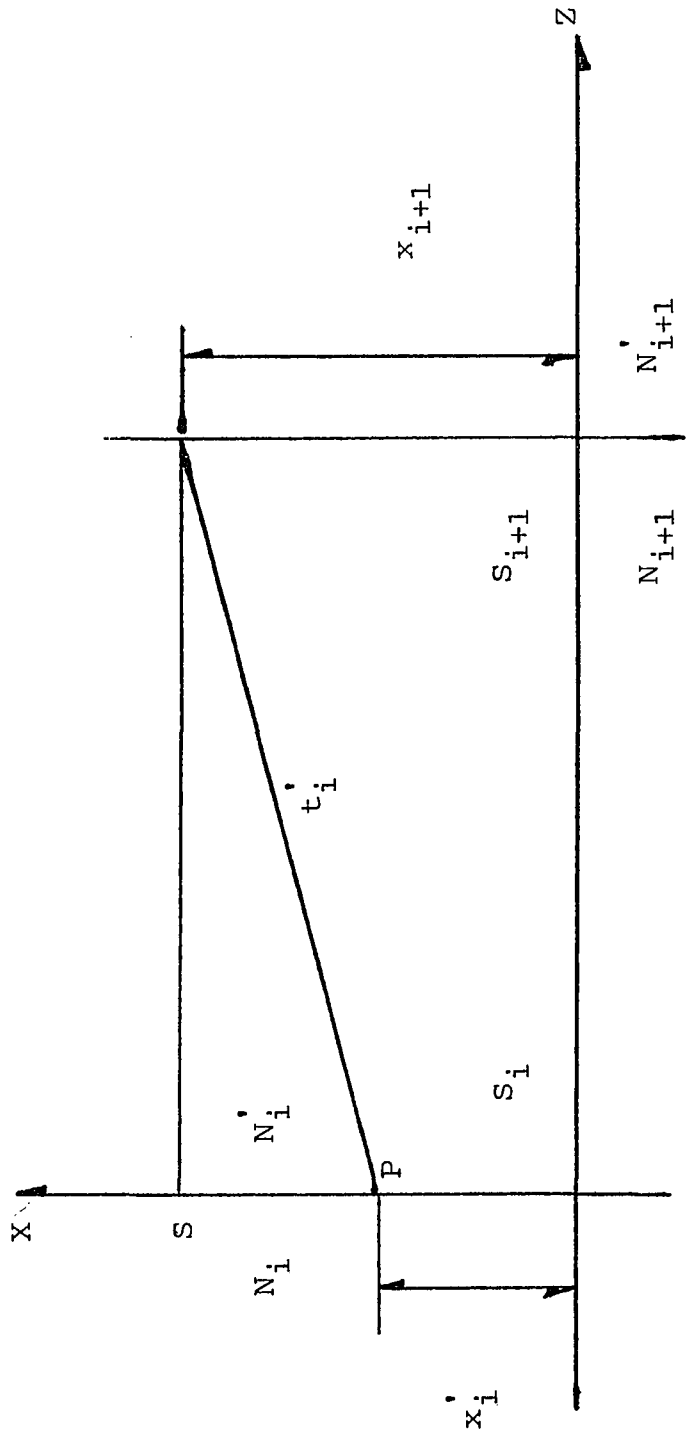


Figure I-5
The path of a light ray
through a homogeneous medium

$$\text{and } x_{i+1} = x_i + T_i L_i = T_i L_i + x_i. \quad (\text{I-17})$$

Also, since

$$N_i' = N_{i+1}, \text{ and } l_i' = l_{i+1} \quad (\text{I-18})$$

then

$$L_i' = L_{i+1}. \quad (\text{I-19})$$

Therefore, the transformation equation for Translation can be written as

$$\begin{bmatrix} L_{i+1} \\ x_{i+1} \end{bmatrix} = \begin{bmatrix} 1 & 0 \\ T_i' & 1 \end{bmatrix} \cdot \begin{bmatrix} L_i \\ x_i \end{bmatrix} \quad (\text{I-20})$$

where the translation matrix is identified as T;

$$T' = \begin{bmatrix} 1 & 0 \\ T_i' & 1 \end{bmatrix}. \quad (\text{I-21})$$

If the two transformation equations are combined, the following results are obtained:

$$\begin{bmatrix} L_{i+1} \\ x_{i+1} \end{bmatrix} = \begin{bmatrix} 1 & 0 \\ T_i' & 1 \end{bmatrix} \cdot \begin{bmatrix} 1 & -A_i \\ 0 & 1 \end{bmatrix} \cdot \begin{bmatrix} L_i \\ x_i \end{bmatrix} \quad (\text{I-22})$$

Performing the matrix operation in this result provides a single transformation matrix

$$\begin{bmatrix} A & B \\ C & D \end{bmatrix} = \begin{bmatrix} 1 & 0 \\ T_i' & 1 \end{bmatrix} \cdot \begin{bmatrix} 1 & -A_i \\ 0 & 1 \end{bmatrix} \quad (\text{I-23})$$

and

$$\begin{pmatrix} L_{i+1} \\ x_{i+1} \end{pmatrix} = \begin{pmatrix} A & B \\ C & D \end{pmatrix} \cdot \begin{pmatrix} L_i \\ x_i \end{pmatrix} \quad (\text{I-24})$$

Extrapolation of this result generates the transformation equation for a light ray traveling from the object to the observation point, through X refracting surfaces and X+1 homogeneous medium regions, as

$$\begin{pmatrix} L_{x+1} \\ x_{x+1} \end{pmatrix} = \begin{pmatrix} A & B \\ C & D \end{pmatrix} \cdot \begin{pmatrix} L_1 \\ x_1 \end{pmatrix} \quad (\text{I-25})$$

The transformation matrix of Equation (I-25) permits determination of the geometrical optics parameters (position and direction of propagation) of the light ray reaching the observer on the basis of the analogous parameters of the light ray leaving each point of the object, after the ray has traversed a turbulent region represented by the model adopted as schematically indicated in Figure I-2. Under the assumptions made, the random time variations of the geometric and optical characteristics of the layers depicted in Figure I-2 evidently dictate that each component of this transformation matrix be a random operator, so that L_{x+1} and x_{x+1} in Equation (I-25) are random, time dependent variables. From the observer's point of view this means that each point of the observed object will appear to move in a random way.

Physically this is due to the variations of the optical characteristics of the traversed medium both from point to point and from instant to instant. In practice, as already noted, these characteristics depend on a large number of different physical parameters such as daily and seasonal temperature variations, atmospheric moisture content, wind conditions, local pressure, variations in radiation and convection characteristics and a host of other causes. In conclusion, the physical system determining the final observation is so complex and varied that the only possible predictions are necessarily statistical in nature.

A study of the statistics of turbulent media has been variously attempted and constitutes, at this writing, an open subject of research. Some important predictions have however been reached, if the model of Figure I-2 and its underlying simplifying assumptions are adopted. In the following we shall mainly refer to the works of Feldman, of Gaskill and of others.^{6,7} Without duplicating here their considerations, the following is a brief synopsis of those conclusions that directly bear on the subject of this thesis. A considerable amount of experimental observations both in conventional optical imagery and holography strongly confirms these conclusions.

⁶ J.D. Gaskill, op. cit.

⁷ S.I. Feldman, op. cit.

For the purpose of our discussion it is expedient to express the pertinent results of these theories in terms of the statistical properties of optical images of objects observed through a turbulent medium of the type depicted in Figure I-2.

Consider an optical system imaging two points A and B into image points A_i and B_i on a plane surface (e.g., a photographic plate). Establishing a reference system in the imaging plane, the position of A_i and B_i can be represented by two position vectors \bar{r}_A and \bar{r}_B , respectively, which will be linear functions of the matrix components of Equation (I-25), and so of the direction and position parameters L_{x+1} and x_{x+1} . Consequently \bar{r}_A and \bar{r}_B are random variables, the statistical characteristics of which are simply related to those of the L and x parameters.

On the basis of the above mentioned theories then the following results have been established by previous investigators:

1. The expected values of \bar{r}_A and \bar{r}_B are slowly time dependent. Consequently the usual assumptions of stationary, or even weakly stationary statistics are invalid.
2. The first increments, however, prove to be stationary.
3. Introducing the vector $\bar{y} = \bar{r}_B - \bar{r}_A$ representing the relative position of B_i with reference to A_i , \bar{y} is in general a random process the

autocorrelation of which, on the basis of observations 1.) and 2.) is easily shown to equal a linear combination of the structure functions of \bar{r}_A and \bar{r}_B .

4. Assuming the model of Figure I-2, the characteristics of such a linear combination can be proven⁸ to result in stationary statistics for \bar{y} , provided the paraxial approximation is valid for the conditions of observation of A and B from the optical imaging system under consideration.
5. The expected value of the difference $\bar{r}_B - \bar{r}_A$ equals the difference of the expected values of \bar{r}_B and \bar{r}_A .

In conclusion: under the above conditions the difference of the expected values of the position vectors is time independent, provided of course statistical averaging operations are extended to a sufficient statistical sample.

Assume now that it is required that the true location of some object is to be determined by observing the object across a field of view that contains turbulence, as in surveying for example. The instantaneous translation and bending, resulting from the turbulence, will cause the object to appear to be moving about in a random fashion. One could attempt to obtain a set of coordinates for the object from a single observation, but there can be no certainty that the results will determine the object's true location.

⁸ S.I. Feldman, op. cit.

A second possible approach, however, is to take a large number of observations over some interval of time, each observation producing a set of coordinates, and make use of time averaging.

The above shows that the expected value of \bar{r}_A and \bar{r}_B cannot be used to determine the absolute position of A and B. However the expected value of \bar{y} will be identical with the analogous value obtained under conditions of absence of turbulence.

Finally therefore: by applying proper statistical averaging to a sufficiently large sample of optical measurements it is possible to determine correctly the relative position of point B with respect to the position of A.

This is very promising, but here again, there is no certainty that this average will identify the object's true location because of the possibility that the coordinates of both A_i and B_i be affected by some error, or fixed translation, associated with the particular region of turbulence involved. Considering the above, it is quite apparent that, even if many observations are statistically averaged, atmospheric turbulence may introduce uncertainty as to the accuracy of surveying results, unless further precautions and techniques are used.

The technique proposed in this thesis combines holographic and standard optical operations to provide a procedure for spot-check or full-scale surveys that

eliminates the need for shutting down the runway, reduces the time and manpower required for a survey and improves the accuracy of the data obtained.

This new survey is performed from a vehicle operated on a path parallel with the runway, at a safe distance from it, and thereby eliminates the need for shutdown. Photographic or computerized recording of the survey data reduces the time and manpower required, and the use of a single continuous true reference along the full length of the runway assures the accuracy of the data obtained.

The three basic tasks in taking a survey are: a. establishing a reference from which to measure, b. taking measurements with adequate instruments, and c. accurately recording the measurement data. Beginning with the task of recording the data, and proceeding in reverse order, the elements of the proposed new method of surveying will be described.

The concept of obtaining a time-averaged set of coordinates for an object observed through atmospheric turbulence was previously set forth, whereby we accurately determine the position of point B with respect to point A. We will then use another device to identify exactly where point A is.

A very effective means of transcribing the data from many observations is by using a photographic recording medium or real time computer analysis. The use of simple

strobing techniques will provide as many observations as desired, over any time period, with all the data captured on one photographic record or in the computer's memory.

In order to accomplish the task of making measurements, the data record must contain a scale with which to determine the relative locations of the observed points. In order for the scale to be useful, it must be free of distortion and be in the focal plane of the observed points. There is an apparent conflict in these requirements in that if the scale were at the location of the observed points, i.e., in the same focal plane, then it would be subject to turbulence and therefore not free of distortion.

Holography provides a way around this obstacle. Two characteristics of holograms, namely the true spatial location of the reconstructed image and the ability to magnify the reconstructed image, make it possible to have a usable scale in the photographic/computer record.

Let a hologram be taken of a given subject; when the developed photographic plate is properly used for holographic reconstruction, the light wave impinging on the viewer's eyes is in all details identical to that received from the original subject, therefore all optically determinable characteristics of the image, including relative spatial location, are identical with those of the original subject. Because of this, the image is said to be reconstructed in space, rather than just reproduced as in other optical techniques. As an example, suppose that the

original subject was located 100' from the hologram recording plate, then if, during observation of the reconstructed image, a telescope is focused for viewing at 100', it will provide an undistorted and properly focused magnification of the original subject, as seen from the observed portion of the hologram, while the telescope is in fact only inches from the plate containing the hologram. This characteristic provides the means for having a scale in the focal plane of the observed points and at the same time have it free from any of the distortion effects of turbulence ⁹.

The second feature of holography to be used is the ability to scale (magnify) the reconstructed image of a hologram. The lateral and depth dimensions of the original hologram subject can be modified during the process of image reconstruction.

This is accomplished by altering the wavelength of the light and/or the radius of curvature (divergence) of the reconstruction light wave from that generated by the reference light source used when recording the hologram. By this means it is possible to magnify the dimensional characteristics of the reproduced image to create a spatial configuration of light distribution identical to that which would have emanated from an original subject of the magnified size and distance from the recording photographic plate.

⁹ R.J. Collier, C.B. Burckhardt, L.H. Lin, Optical Holography, Academic Press, (1971).

It is therefore possible to make a hologram of the desired scale at distances free of turbulence, and to reconstruct the image spatially located at distances at which turbulence most certainly becomes significant.^{10,11}

Having identified a way to insert an undistorted scale into the photographic/computer recording of the turbulence distorted observed points, only one more element is needed to implement the essentials of a survey, namely a reference from which to compute the desired measurements. What is required here is that the true coordinates (location) of one or more of the observed points must be known. Given this condition, then as previously noted, even if the turbulence encountered causes a fixed displacement in the photographic recording, the difference between the true coordinates of the known point and those determined by the time averaged relative measurement can be used to adjust the measured coordinates of all the observed points.

To provide a true reference for use throughout a runway survey, the world's oldest leveling technique will be employed. The solution is the installation of a water pipe around the perimeter of the runway as indicated in Figures I-6 and I-7. At 20' intervals, the pipe will have vertical cylinders, each containing an externally visible float. By

¹⁰ R.W. Meier, Magnification and Third-Order Aberrations in Holography, J. Opt. Soc. Amer. 55, 987 (1965).

¹¹ E.B. Champagne, Nonparaxial Imaging, Magnification and Aberration Properties in Holography, J. Opt. Soc. Amer. 57, 51 (1967).

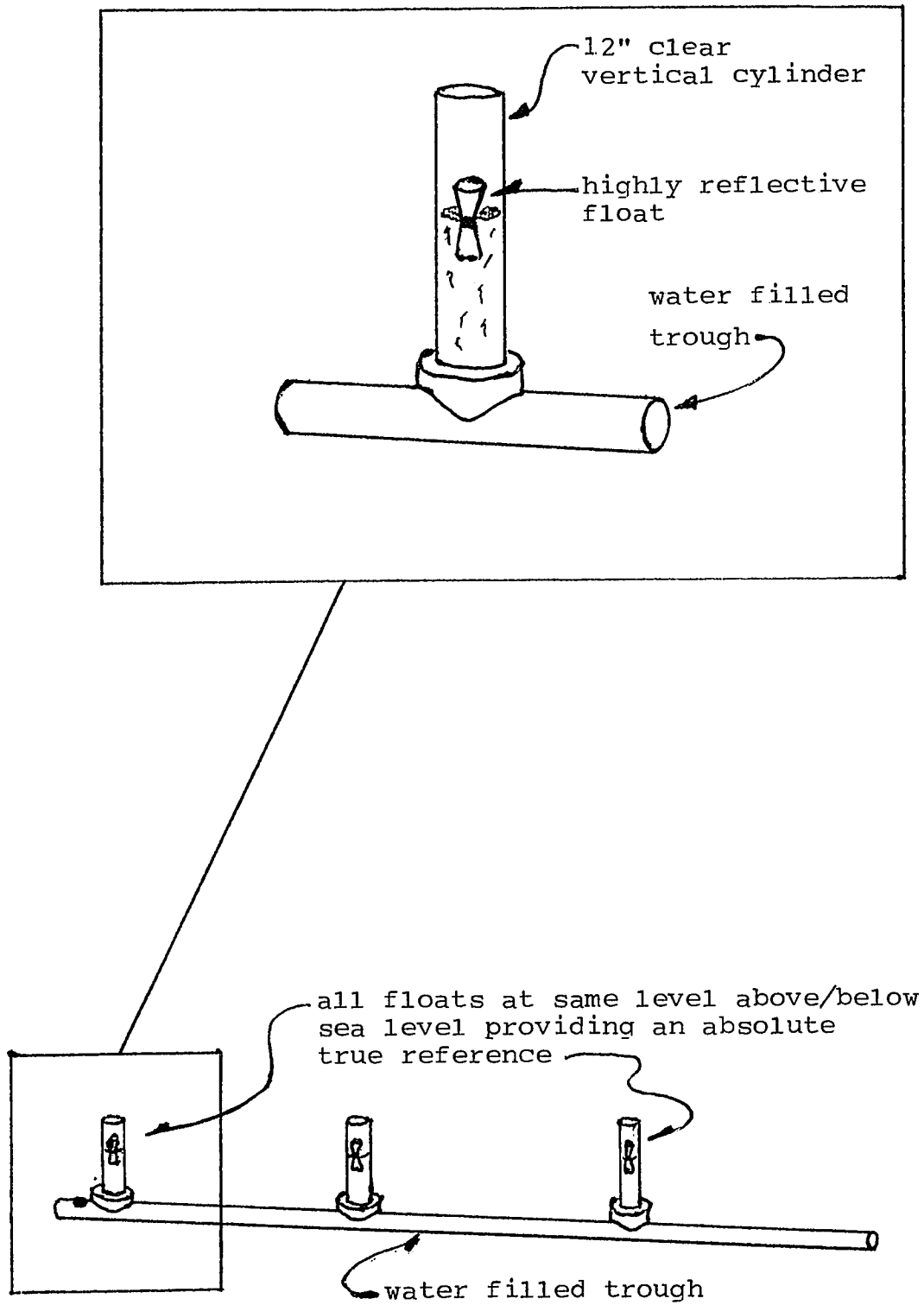


Figure I-6
A water trough method for
providing an absolute reference

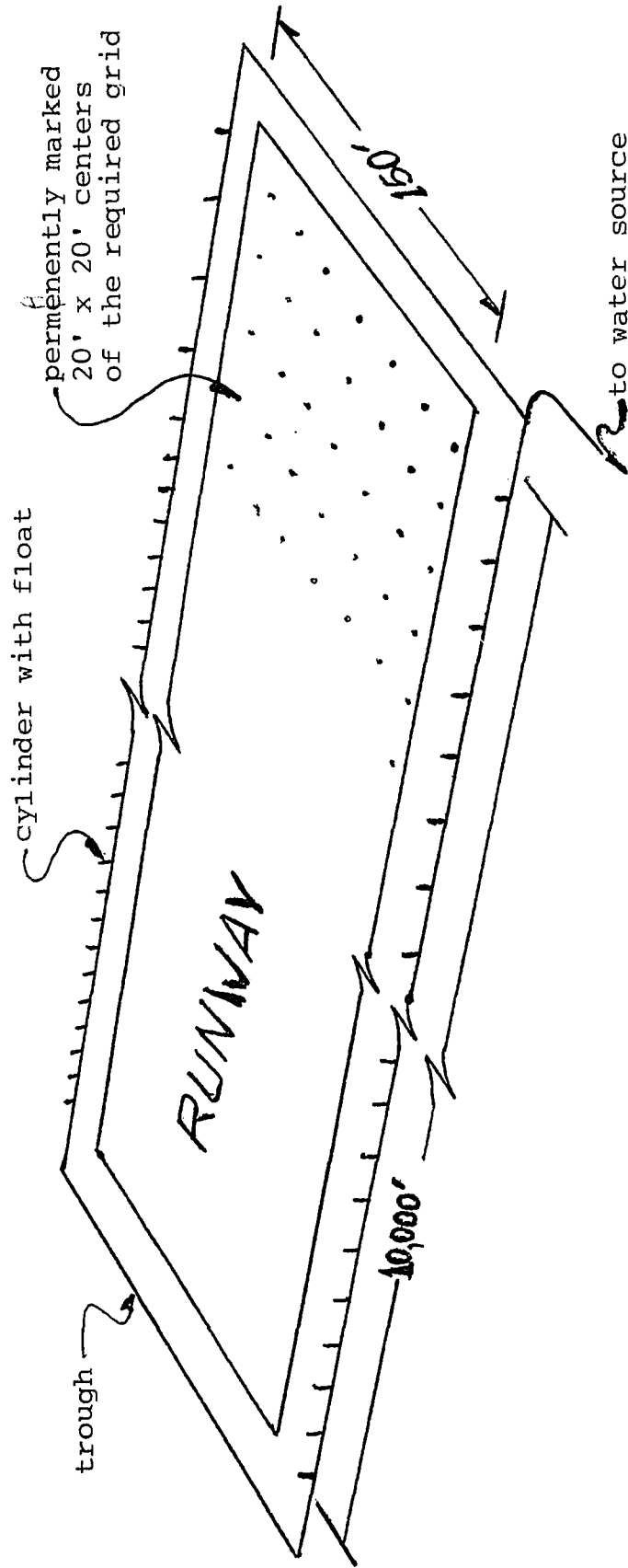


Figure I-7
Airport runway preparation
for the proposed survey process

placing a proper quantity of water in the pipe, all the floats will be afloat in their cylinders and will be at exactly the same elevation relative to sea level. In this situation, a 'straight line' between any two of the floats is a 'true level surface'.

By properly locating the holographic scale between a pair of floats on opposite sides of the runway, as indicated in Figure I-8, all runway surface points in the plane of the scale can subsequently be measured from a suitable data record of the observers' field of view.

Exact alignment of the scale with the turbulence distorted location of the reference floats presents no problem, as spatial positioning of the scale by direct reckoning already provides first order compensation and the second order effects of distortion are removable by statistical observations of the photographic/computer record, to within the desired accuracy, with all other measurements being differentially compensated accordingly.

Also shown in Figure I-8, is a surface preparation for the survey, i.e, the runway should be permanently marked with the 20' x 20' centers of the survey grid. Each row of these 'centers' would be on a line with a float/cylinder on each end. This may appear to be an onerous requirement, but considering that it must only be done once, then periodically maintained thereafter, and that at present such a grid is generated for every survey taken, it actually represents

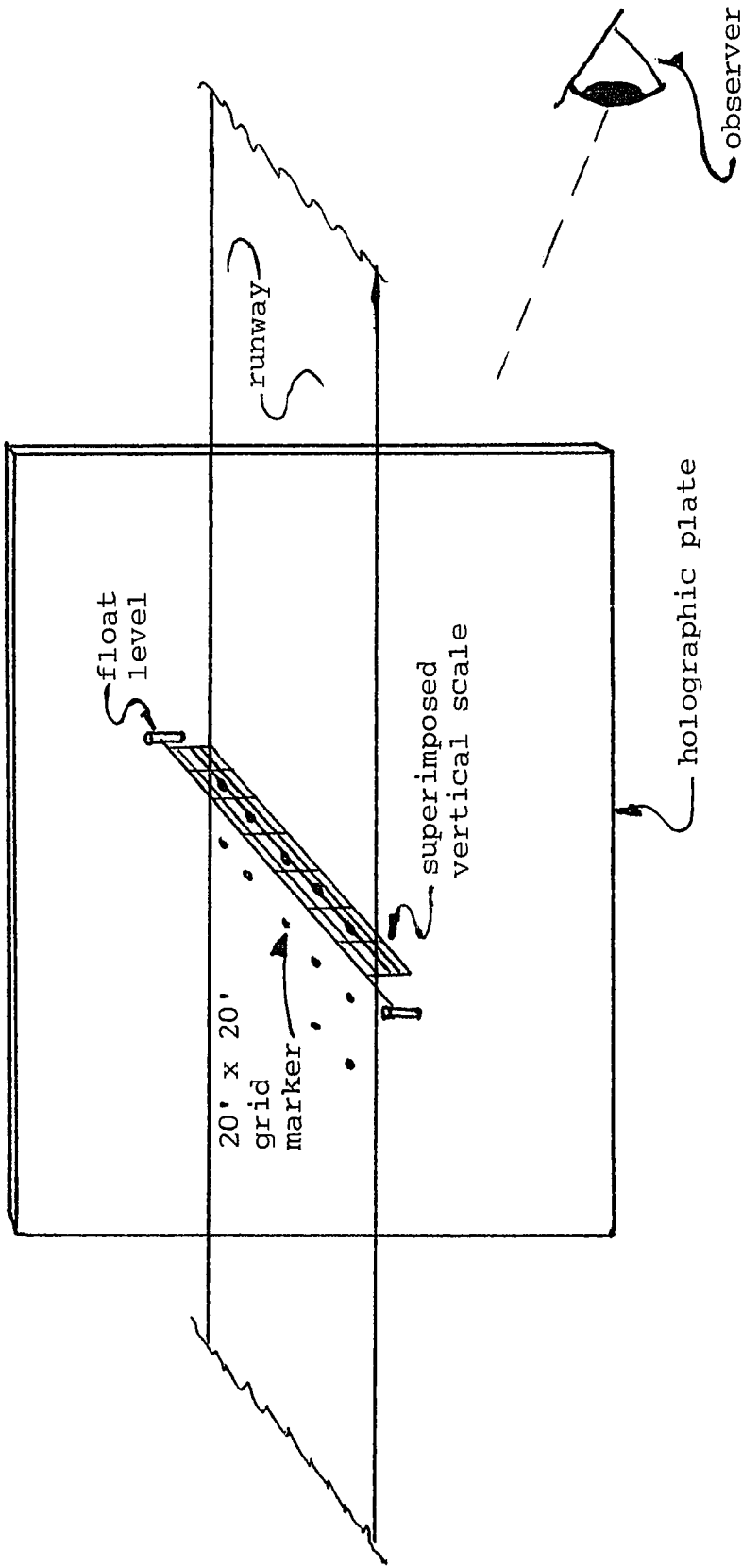


Figure I-8
A holographic image superimposed
on a runway cross section

an improved condition. (The center markings might be paint or reflective metal disks.)

After installation of the water pipe/float cylinders and the 20' x 20' grid centers, the additional devices needed to perform a survey are the holographic plate containing the vertical measuring scale's hologram, a reconstruction light source, and standard photographic or computer and television equipment including telescopic lenses.

The survey is then performed in the following manner. A vehicle, containing the above devices, is positioned at a location convenient for ease of operation, beyond the FAA regulated safe distance from an active runway, (the observer's location in Figure I-9).

By proper adjustment of the hologram's position with respect to the reconstruction light source, a magnified virtual image of the hologram's scale is located in the vertical plane of two selected float cylinders, as shown in Figure I-8. This provides an optical section through the runway's surface and inserts the vertical scale into the plane of this cross-section to within the accuracies of direct reckoning.

The variations in elevation of the grid centers in this plane, relative to the floats' level, can then be observed. Using a telescopic lens, to maximize the accuracy of the obtained data, and adhering to the paraxial approximation restraints by viewing each row at an angle,

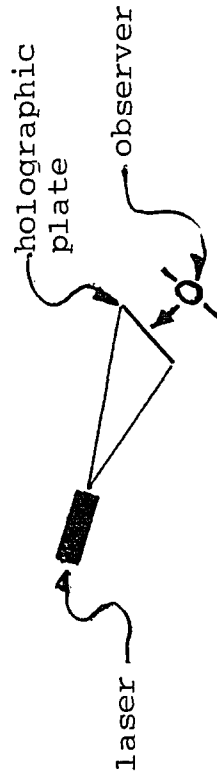
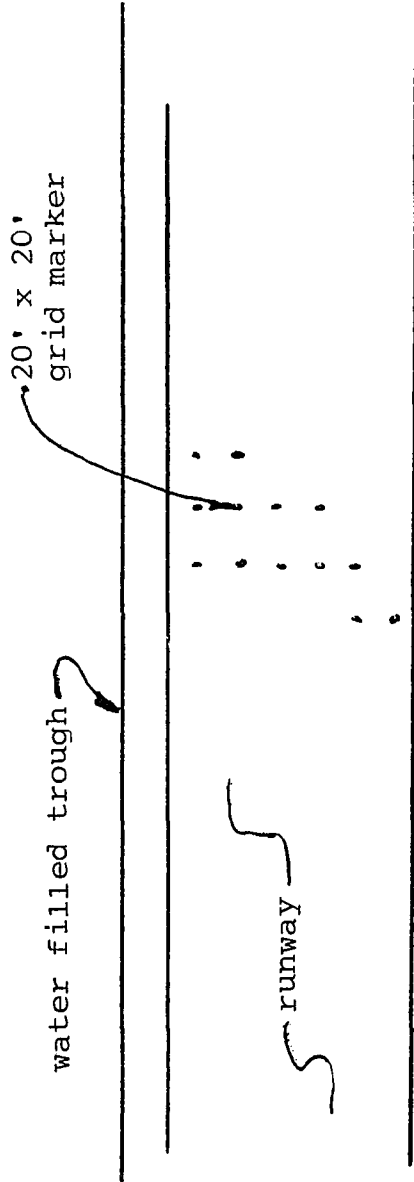


Figure I-9
Plan view of a runway and
hologram image reconstruction equipment

(hence narrowing the width of the viewed field between the floats), multiple observations of these points are then strobed onto one data record.

This process is repeated for the other rows of grid centers until the data for all rows is recorded.

After the photographs are developed, if a camera is used to record the data, the 'mean' coordinates of each point in the record will be visually measured and computed. All the 'mean' coordinate values will then be proportionately adjusted until the values for each grid center's reference floats are zero on the vertical scale. After adjustment, the new mean coordinate values for all grid centers are now directly comparable to each other, and the survey is complete. If a computer is used, then the software will perform all these steps in a real time mode and provide results at the survey site.

In the next chapters the procedure qualitatively described above will be quantitatively analyzed, described in greater detail and finally implemented in a laboratory feasibility study in an effort to prove experimentally the validity of the proposed survey method.

CHAPTER II

DISTORTION AND ACCURACY IN HOLOGRAPHIC IMAGE MAGNIFICATION

The requirement for magnifying the hologram of the vertical measuring scale was stated previously. The reason for this and the methods of magnification will now be considered.

Because of the standard characteristics of airport runways, dimensionally for the envisaged application the vertical scale needed for use with the absolute reference levels must be 150 feet in width and spatially located 520 to 580 feet from the viewer. The question of the possibility of taking a hologram of a full size installation of the required dimensions shall not be belabored, but a few major obstacles to accomplishing such an endeavor will be noted.

1. Producing a 150 foot long object that must be absolutely flat (level).
2. The size of the area (and the preparation of same) needed to obtain the hologram and have it free of any foreground and background images other than the vertical scale. (The scale must "enter" the surface of the runway and extend into its depth.)
3. Acquiring a laser with a power output sufficient to execute the taking of the hologram in a short enough period of time to avoid vibration (motion) problems.

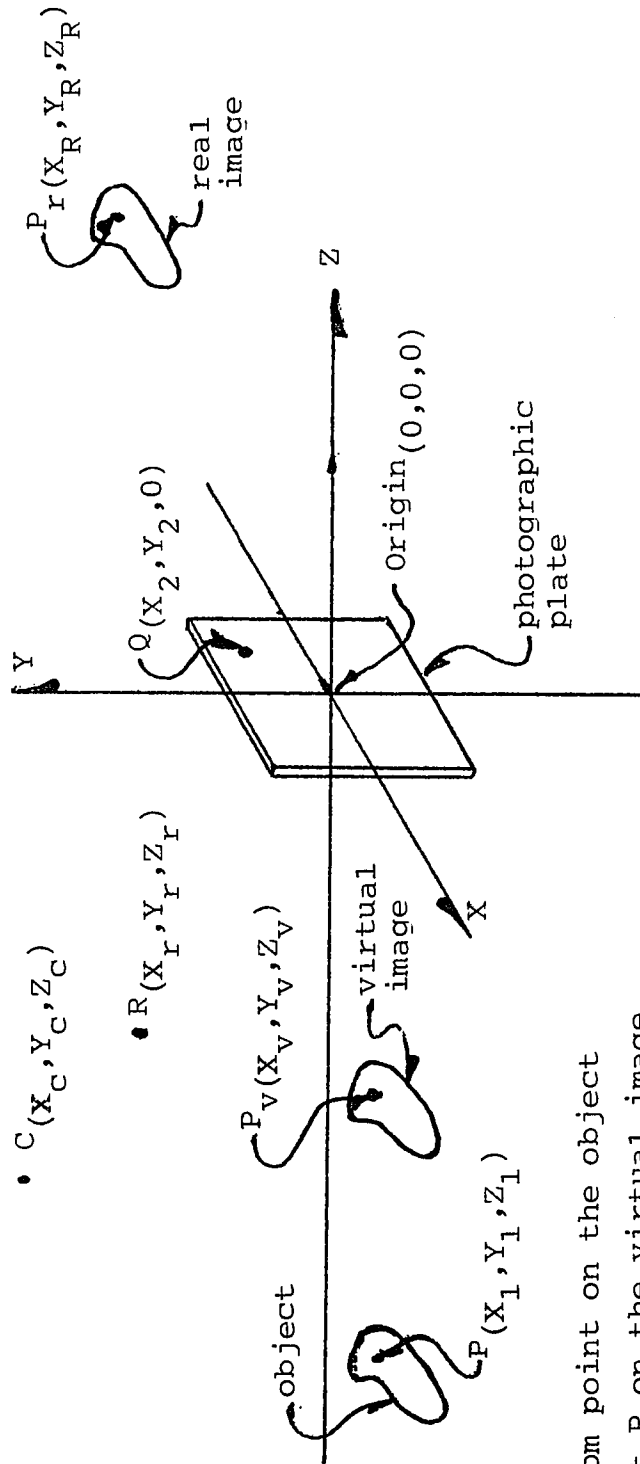
4. The atmospheric turbulence between the object and the holographic plate.

The use of magnification techniques provides the means for avoiding these potential pitfalls of a fullscale undertaking. In addition to providing the obvious advantages of working in a laboratory environment, i.e, isolation from ambient light and uncontrollable vibrations, it also makes possible the machining task needed to produce a vertical measuring scale of achievable proportions with the accuracy required.

The following is an analysis of the operation of magnification in the reconstruction of a hologram's image.

The parameters for magnification which come from the 'classical' development, as originally published by R. W. Meier, are presented. An examination of the 'classic' parameters for magnification will be pursued to identify specific values needed to obtain the required magnification and spatial location characteristics and to identify sources of distortion and methods for avoiding them.

The classic derivation is based on a customary geometric approach to optical imagery. Figure II-1 shows the orientation and position of the elements involved in the making of a hologram and in the reconstruction of the object's image. The concept of the dimensionless point is utilized for identifying each element. Also, the photographic plate is assumed to have 'zero' thickness and to be



- P : Random point on the object
- P_v : Point P on the virtual image
- P_r : Point P on the real image
- Q : Random observation point on plate
- R : Location of reference light source
- C : Location of reconstruction light source

Figure II-1
 Coordinate system for the parameters of
 holographic wave recording and reconstruction

located in the XY plane of a normal three dimensional cartesian coordinate system with its perimeter edges parallel to and equidistant from the X and Y axes. The following definitions identify the elements in Figure II-1.

- A. The object (or subject of the hologram) is designated as point P, with coordinates (X_1, Y_1, Z_1) .
- B. The reference light source is designated as originating at point R, with coordinates (X_R, Y_R, Z_R) .
- C. The reconstruction light source is designated as originating at point C, with coordinates (X_C, Y_C, Z_C) .
- D. The center of the photographic plate is located at the origin of the coordinate system and is designated as point O, with coordinates $(0, 0, 0)$.
- E. An observation point, designated as point Q, is located within the perimeter of the photographic plate with coordinates $(X_2, Y_2, 0)$.

The principles of holographic wave recording and reconstruction will be summarized so that we may point out and discuss some pertinent properties.

The essence of wave reconstruction, or holography as it was named by its inventor, D. Gabor, is contained in

the formulation

$$I = |p + r|^2 = p^2 + r^2 + p^*r + pr^* .$$

"I" represents the intensity of the interference pattern resulting at the intersection of two wave fronts with complex amplitudes $p = p_0 \exp(i\theta_p)$ and $r = r_0 \exp(i\theta_r)$. If these two waves originated from a single coherent light source (of wavelength λ_1), by the use of a beam splitter for example, then a photographic record of their superposition will contain very special properties.

The first two terms in "I", the square of the amplitude of each wave, are of little interest, but the pair of complex conjugate terms contain the entire description of the spatial variations of intensity in the interference fringes at the plane of superposition of the two waves, i.e., the photographic plate.

The meaning of this is that if, for instance, one of the wavefronts was spherical, then future illumination of the processed photographic plate by a coherent light source (of any wavelength λ_2), with a spherical wavefront and complex amplitude $c = c_0 \exp(i\theta_c)$, will effect the reconstruction of the hologram's contents. (The three waves mentioned are taken as emanating from points P, R, and C in Figure II-1.)

The light that emerges from the plate during reconstruction will be proportional to

$$H = c \cdot I = c(p^2 + r^2) + cp^*r + cpr^* .$$

The first term in "H" is related to the amplitude of the transmitted wavefront, which emanated from point C, while the remaining terms represent two additional wavefronts emanating from the hologram, one, H_R , which converges to a real image, and the other, H_V , which diverges from a virtual image (points P_R and P_V , respectively, in Figure II-1), where

$$H_R = cp^*r = c_0p_0r_0 \exp(i\theta_R), \text{ and}$$

$$H_V = cpr^* = c_0p_0r_0 \exp(i\theta_V).$$

The phases of the two generated wavefronts are

$$\theta_R = \theta_C - \theta_P + \theta_r, \text{ and } \theta_V = \theta_C + \theta_P - \theta_r.$$

The phase of θ_V , at the random observation point Q, can be computed relative to its phase at point O by the substitution of cartesian coordinates in this formula, and then invoking the restraints of a paraxial approximation on the distance between points Q and O, relative to the distance to P. This produces the following coordinates for the point P_V , the virtual image of point P;

$$Z_V = \frac{Z_C Z_1 Z_r}{Z_1 Z_r + \mu Z_C Z_r - \mu Z_C Z_1}$$

$$X_V = \frac{X_C Z_1 Z_r + \mu X_1 Z_C Z_r - \mu X_r Z_C Z_1}{Z_1 Z_r + \mu Z_C Z_r - \mu Z_C Z_1},$$

$$\text{and } Y_V = \frac{Y_C Z_1 Z_r + \mu Y_1 Z_C Z_r - \mu Y_r Z_C Z_1}{Z_1 Z_r + \mu Z_C Z_r - \mu Z_C Z_1},$$

where μ equals the wavelength ratio of the reconstruction light source to the reference light source, i.e., $\mu = \lambda_2 / \lambda_1$.

Applying the definitions for magnification to these coordinates for point P_V produces the following parameters;

$$M_V \text{ angular} = d(X_V/Z_V)/d(X_1/Z_1)$$

$$\text{or } M_V \text{ ang} = \nu,$$

$$M_V \text{ lateral} = dX_V/dX_1 = dY_V/dY_1$$

$$\text{or } M_V \text{ lat} = \left[1 + Z_1 \left(\frac{1}{\nu Z_C} - \frac{1}{Z_R} \right) \right]^{-1},$$

$$\text{and } M_V \text{ longitudinal} = dZ_V/dZ_1$$

$$\text{or } M_V \text{ long} = \frac{1}{\nu} \cdot \left[1 + Z_1 \left(\frac{1}{\nu Z_C} - \frac{1}{Z_R} \right) \right]^{-2}$$

$$\text{or } M_V \text{ long} = \frac{1}{\nu} (M_V \text{ lat})^2.$$

Remembering from Figure II-1, that the numerical values of all Z components are negative, a cursory examination of the above parameters shows that

$$M_V \text{ lat} = 1, \text{ for } Z_C = Z_R,$$

$$M_V \text{ lat} > 1, \text{ for } Z_C > Z_R,$$

$$\text{and } M_V \text{ lat} < 1, \text{ for } Z_C < Z_R.$$

Second, that angular magnification is independent of geometric considerations. Therefore, given a fixed set of parameters, the ratio of the wavelengths of the reference and reconstruction light sources can be varied to alter the

relationship between lateral and longitudinal magnification. The effect of such an adjustment is that for $\mu < 1$, longitudinal magnification is reduced less than lateral, and for $\mu > 1$, longitudinal magnification is increased less than lateral. Finally, it is obviously seen that lateral magnification is not equal to longitudinal.

This is a serious distortion which will be discussed in some detail in Chapter V, but one which need have no effect on the hologram of the vertical measuring scale used in our application. Indeed, since the scale is to be used in a two dimensional plane, proper orientation of the real scale with reference to the photographic plate, during the making of the hologram, can avoid any effects of longitudinal distortion, i.e., if the planes of the scale and the plate are parallel then Z_1 is a constant.

Though the hologram can be made free of longitudinal distortion, this is not true for lateral distortion. Under the restraints of a paraxial approximation, the coordinates for point P_Y were obtained assuming that observation of P_Y occurred through an infinitesimal area of the photographic plate around its center, i.e., that point $Q \approx (0,0,0)$. Consequently, in the derived formulas, the coordinates of P_Y do not explicitly show dependence on the observation point Q .

Independence from Q would be a very desirable feature in that it would allow viewing of the hologram's contents through any portion of the photographic plate

without lateral distortion. The coordinates of P_V , however, are not independent of Q . Consider Z_V and X_V rewritten in the form

$$Z_V = \frac{Z_1}{\nu} \cdot M_V \text{ lat, and}$$

$$X_V = \left[X_1 + \frac{Z_1}{\nu} \cdot \left[\frac{X_C}{Z_C} - \frac{\nu X_R}{Z_R} \right] \right] \cdot M_V \text{ lat} \cdot$$

(Y_V has the same form as X_V).

Here it can be seen that while Z_V/Z_1 is equal to a constant, X_V/X_1 is not constant as the observer traverses the photographic plate. This becomes obvious if the conditions stated above are rephrased to identify the fact that the observation point is the center of the coordinate system. Therefore, as Q moves there is a corresponding translation of the axes, and the values of the X and Y components change proportionately with this movement.

Variations of X_V/X_1 with horizontal displacement of the observation point are due to the addend

$$\frac{Z_1}{\nu} \cdot \left[\frac{X_C}{Z_C} - \frac{\nu X_R}{Z_R} \right] \cdot$$

During observation of the processed hologram, under conditions of specified magnification, none of the components in this factor can be varied with the exception of X_C . If, as point Q is shifted, and X_R consequently varies, the

position of the reconstruction source were simultaneously manipulated to keep

$$X_C = \mu Z_C \cdot \frac{X_R}{Z_R}$$

then the above mentioned addend would be always identically equal to zero. Assuming this relationship between X_C and X_R is maintained, then

$$Z_V/Z_1 = \frac{1}{\mu} \cdot M_V \text{ lat, and}$$

$$X_V/X_1 = M_V \text{ lat.}$$

(The effect of angular magnification, μ , is well identified in these results.)

Under this condition, the spatial location of the reconstructed object point, P_V , is kept constant, independent of the observation point. (Similar considerations are valid regarding the Y_C coordinates of the reconstruction light source.)

There are two simple methods by which to properly control the value of X_C . Consider the configuration in Figure II-2. If the observation point, Q , moves to the right from $x = 0$, to $x = 3$, the value of X_R goes from 6 to 3. If, simultaneously, C moves to the left a distance of 6 units, then the restraint on X_C is satisfied. Therefore one method is to have the location of the reconstruction

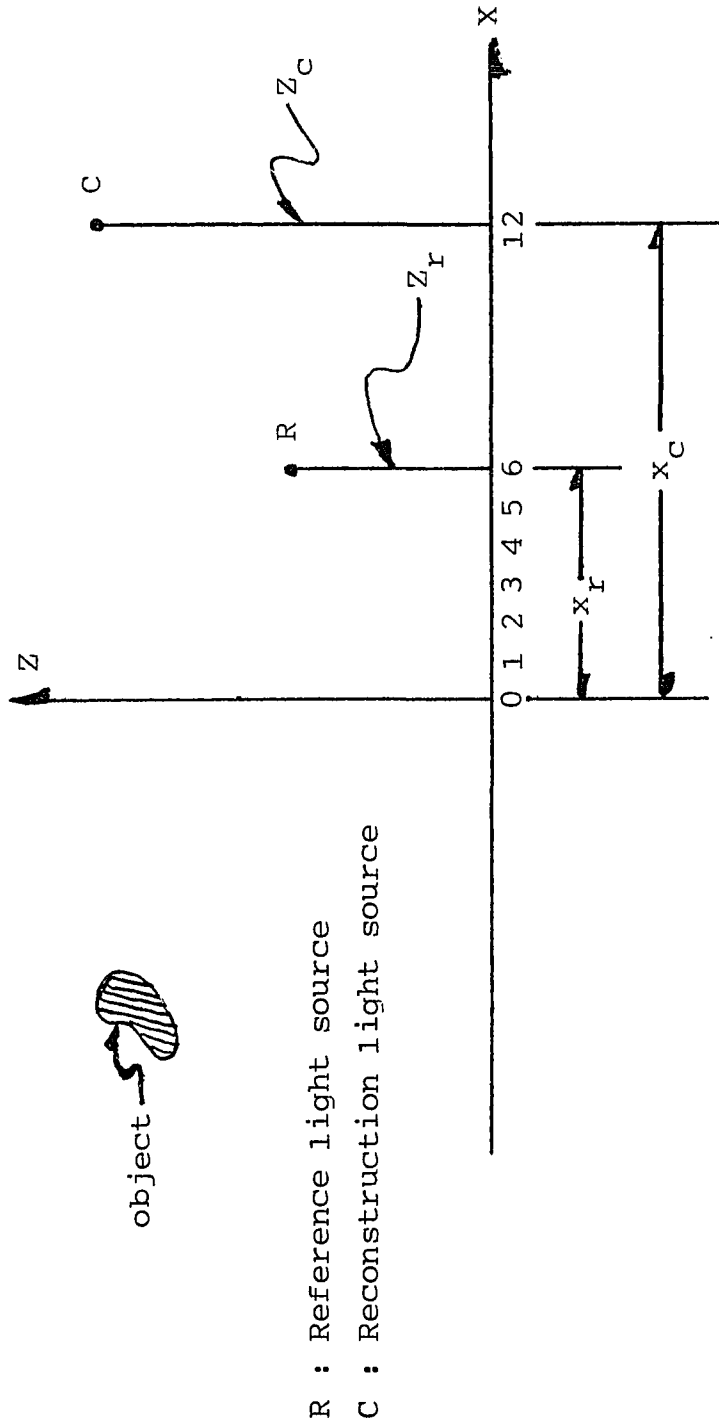


Figure II-2
Plan view of the locations of the
reference and reconstruction light sources

source in the XY plane change by the ratio $-X_C/X_R$ times the change in the observation point. The second method permits keeping the reconstruction source at a fixed location provided the holographic plate is moved in response to changes in the observation point. Moving the plate has the effect of moving the reference source location, after the fact, and offers a distinct advantage over the first method.

Consider again Figure II-2. Let Q move 4 units to the right, X_C is now equal to 8. With this geometry, if the plate moves 2 units to the right, the X_R equals 4 and again the relationship of X_C to X_R is maintained. The added advantage in this method is that moving the plate a distance $= +Z_R/Z_C$ times the change in Q is in practice equivalent to increasing the effective size of the holographic plate by a factor of $+Z_C/Z_R$, i.e., a 10 unit plate in Figure II-2 would provide 20 units of lateral viewing distance by this method, for the geometry shown.

The interrelationship of the variables in the magnification parameters, and their control of the spatial location of the magnified image, will be examined next.

The spatial location of the reconstructed image and its enlargement relative to the scale's original location and dimensions can be fully described by the functions X_V/X_1 , Y_V/Y_1 , and Z_V/Z_1 . These are the ratios of the coordinates relative to the origin. Ideally, individual control of these functions, independently of each other, would be desirable. But this is simply not possible since

these functions are dependent results of a single geometric variable, i.e., the location of the reconstruction light source. Given this restriction, the least troublesome relationship would be that these ratios be equal to each other at all times. In this case, an adjustment in one dimension would produce exactly the same effect in the other two.

To this end, it has been shown that it is possible to insure that

$$X_V/X_1 = Y_V/Y_1 = Z_V/Z_1 = M_V \lambda_t.$$

Using either of the two methods for controlling the relation between X_C and X_R , and setting λ equal to 1, (by using the same wavelength of coherent light in the recording and reconstruction of the hologram), provides this feature.

Adopting these conditions, the only variables available to control the value of $M_V \lambda_t$ are the distances of the object and reference light source from the photographic plate and that of the reconstruction light source from the processed plate, i.e., Z_1 , Z_R , and Z_C , respectively.

Certain criteria of value in examining these variables are

1. The reconstruction light source must be near to the holographic plate to avoid too unwieldy a physical setup for field applications and to avoid excessive laser output power requirements.

2. If the reconstruction light source's distance from the holographic plate is less than, equal to, or greater than that of the reference light source, then the resulting magnification will be less than, equal to, or greater than one (1), respectively.

Based on the need for a scaling greater than 1, the above criteria and the geometric requirements for making a hologram, the following is proposed for the initial investigation

$$z_r < z_c \leq z_1.$$

The sensitivities of the spatial location and size of the virtual image of the hologram with respect to z_1 , z_r , and z_c , individually, must be determined in order to identify the most convenient variable for manipulation. To this end, the following functions are examined:

$$z_v/z_1 = M_V \text{ lat}, \quad dz_v/dz_1 = M_V^2 \text{ lat}, \\ dz_v/dz_r, \quad dz_v/dz_c, \quad \& \quad dz_c/dz_r.$$

$$z_v/z_1 = M_V \text{ lat} = \left[1 + z_1 \left(\frac{1}{z_c} - \frac{1}{z_r} \right) \right]^{-1},$$

$$dz_v/dz_1 = M_V^2 \text{ lat}$$

$$\frac{dz_v}{dz_r} = - \left[\frac{z_1 z_c}{z_1 z_r + z_c z_r - z_c z_1} \right]^2$$

$$\frac{dz_v}{dz_c} = \left[\frac{z_1 z_c}{z_1 z_r + z_c z_r - z_c z_1} \right]^2$$

and from
$$\frac{\frac{dz_V}{dz_R}}{\frac{dz_V}{dz_C}} = \frac{dz_C}{dz_R}, \quad \frac{dz_C}{dz_R} = -\left(\frac{z_C}{z_R}\right)^2$$

It is apparent from a cursory examination of the derivative functions that the only maximum or minimum points are the trivial ones, i.e., $dz_{()} / dz_{()}$ equals zero only if one or more of the $z_{()}$ components are equal to zero. Little can be expected from further probing of these functions. Some useful results are obtained, however, from a detailed investigation of the remaining function, z_V/z_1 .

This function, and its equivalents in the X and Y planes, are of primary importance in that they identify the actual positioning of the reconstructed image. Plots of

$$z_V/z_1 \text{ as a function of } z_R, z_C, \text{ and } z_1,$$

(coupled with the aforementioned criteria), clearly establish the relative dependence of these variables and the range of values of each that will produce the desired values of magnification.

The graphs in Figures II-3 and II-4 appear to be inverted duplicates of each other, but a comparison of the discontinuities in each points out a distinct difference. In the graph of Figure II-3 the discontinuity occurs at

$$z_R = z_C \cdot z_1 / (z_C + z_1) ,$$

The plot of positive values of Z_r is not shown. Since Z_1 was chosen as negative, positive values of Z_r place the reference light source on the opposite side of the photographic plate from the object. Useful reconstruction of the resultant hologram would produce an inverted image and is not of interest here.

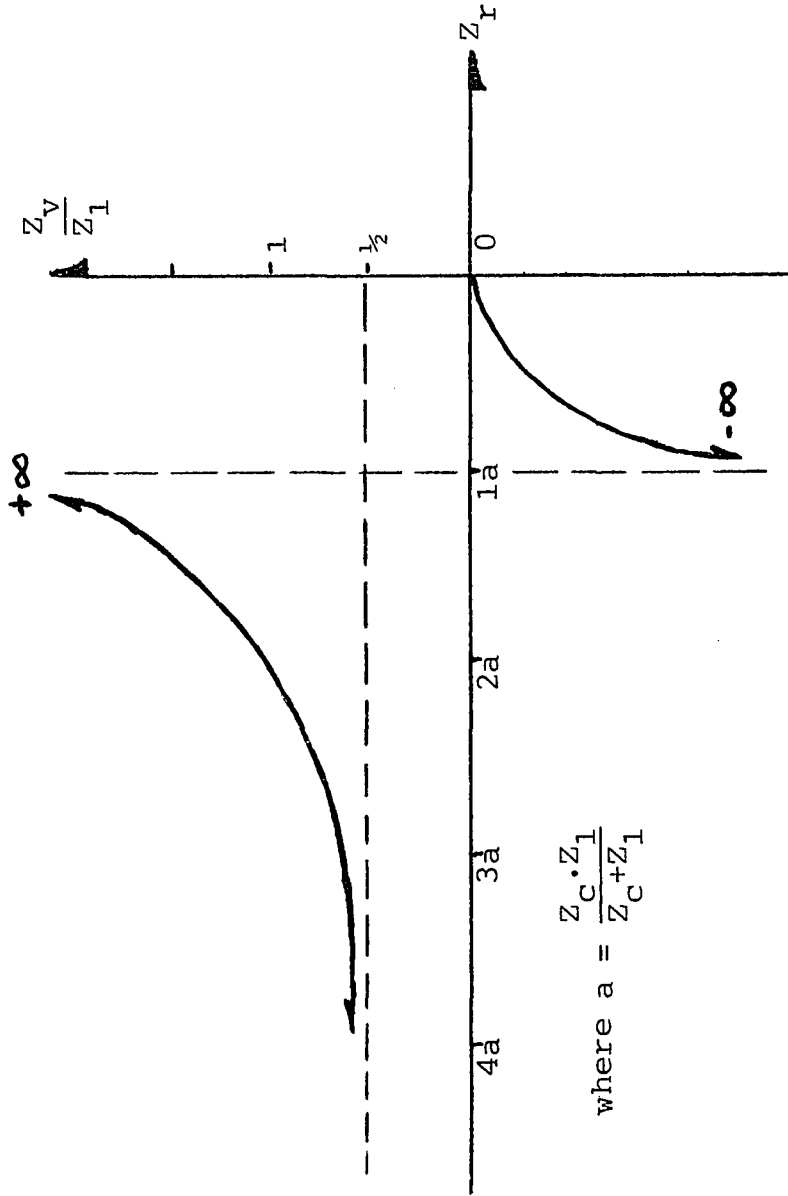


Figure II-3
 Plot of the values of image displacement
 (magnification) as a function of Z_r

The plot of positive values of Z_C is not shown, for the same reason given in figure II-3.

$$\text{where } b = \frac{-Z_r Z_1}{Z_r - Z_1}$$

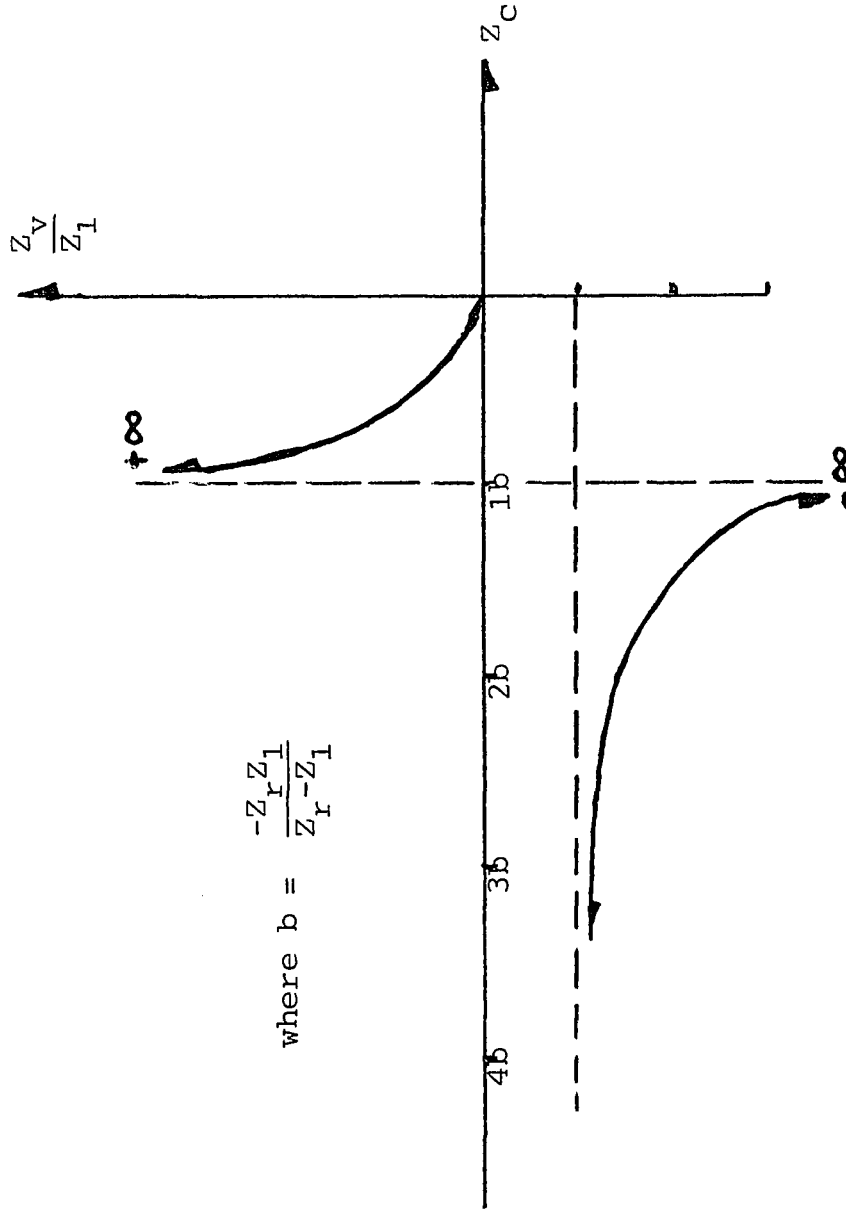


Figure II-4
 Plot of the values of image displacement (magnification) as a function of Z_C

while the plot of Z_V/Z_1 vs Z_C in Figure II-4 produces its discontinuity at

$$Z_C = -Z_R Z_1 / (Z_R - Z_1)$$

In this latter function, if Z_R is allowed to approach the value of Z_1 , the magnitude of Z_C approaches infinity. In the absence of other considerations, it would be most desirable to have such a variable control the magnitude of Z_V/Z_1 . With a continuum of values, from zero to minus infinity, infinitesimal vernier control would be possible. But the distance restraint placed on the reconstruction source's location prevents taking advantage of this characteristic. The value of Z_C must be of reasonably small absolute magnitude.

The discontinuity in Z_V/Z_1 vs Z_1 (see Figure II-5) occurs at

$$Z_1 = Z_C Z_R / (Z_C - Z_R).$$

This establishes the limitations on the value of Z_1 for given values of Z_C and Z_R . If the object's location is such that its Z_1 value is less than the critical value then its magnification will be predictable, for those Z_1 values near the critical value lateral magnification will approach infinity, and for all Z_1 values larger than the critical one, the virtual image will be inverted and located on the wrong side of the holographic plate.

The plot of positive values of Z_1 is not shown since it places the object on the wrong side of the photographic plate.

$$\text{where } c = \frac{Z_C Z_I}{Z_C - Z_I}$$

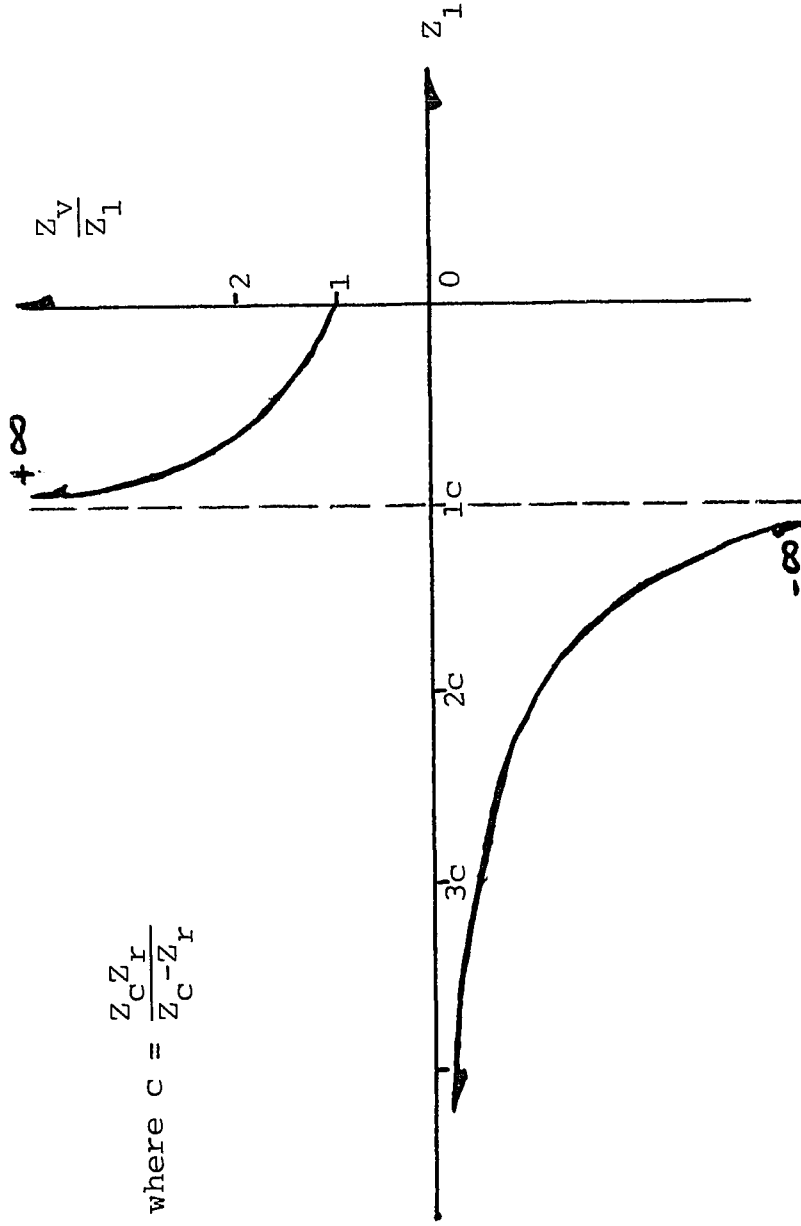


Figure II-5
Plot of the values of image displacement
(magnification) as a function of Z_1

The graph in Figure II-3 clearly indicates the range of Z_r values for which positive lateral magnifications greater than 1 are achieved, i.e.,

$$\left| \frac{2Z_c Z_1}{Z_c + Z_1} \right| > |Z_r| > \left| \frac{Z_c Z_1}{Z_c + Z_r} \right| .$$

Insertion of test values for the variables and calculation of the resulting Z_r values is the next step. Recognizing the symmetrical relationship of Z_c and Z_1 , nothing is lost in fixing one of these variables, say $Z_1 = -1$, and varying the other to establish the limits of Z_r within the given range. The following is a tabulation of these values.

Z_1	Z_c	$>Z_r>$	
-1.0	-0.00	-0.00	-0.00
-1.0	-0.25	-0.20	-0.40
-1.0	-0.50	-0.33	-0.66
-1.0	-0.75	-0.43	-0.86
-1.0	-1.00	-0.50	-1.00
-1.0	-1.50	-0.60	-1.20
-1.0	-2.00	-0.66	-1.32
-1.0	-2.50	-0.71	-1.42
-1.0	-3.00	-0.75	-1.50

The above range of values cannot be applied literally, however, because of the two relative variable restraints previously established. The first of these requires the absolute magnitude of Z_c to be greater than that of Z_r in order to obtain lateral magnifications larger than 1. The second is the requirement for the absolute magnitude of Z_r to be less than that of Z_1 . If this is not so, then the maximum attainable value of lateral magnification approaches $Z_r/(Z_r - Z_1)$, asymptotically, as Z_c goes to infinity. (This in contrast to the case

where Z_r is less than Z_1 , then the value of magnification goes to infinity as Z_c approaches the value of $(-Z_r)/(Z_r - Z_1)$. If these restraints are applied to the tabulated ranges for Z_r , the results are as follows.

Z_1	Z_c	$\langle Z_r \rangle$	
-1.0	-0.00	-0.00	-0.00
-1.0	-0.25	-0.20	-0.25
-1.0	-0.50	-0.33	-0.50
-1.0	-0.75	-0.43	-0.75
-1.0	-1.00	-0.50	-1.00
-1.0	-1.50	-0.60	-1.00
-1.0	-2.00	-0.66	-1.00
-1.0	-2.50	-0.71	-1.00
-1.0	-3.00	-0.75	-1.00

All the above parameter ranges are valid for the application at hand, and in the absence of other considerations, the largest Z_r range would provide the maximum vernier control, i.e.,

$$Z_1 = Z_c = -1, \quad -0.50 \quad Z_r \quad -1.00 .$$

Proceeding with the unit value approach, the parameters for specific values of lateral magnification will be computed. Substituting $Z_c = Z_1 = -1$ in the formula for Z_V/Z_1 , and setting the result equal to M_z produces

$$M_z = \frac{Z_r}{2Z_r + 1} .$$

The following is a tabulation of Z_r values for certain integer values of M_z .

M_z	Z_r
1	-1.0000
2	-0.6666
3	-0.6000
4	-0.5714
5	-0.5555
6	-0.5454
7	-0.5385
8	-0.5333
9	-0.5294
10	-0.5263

The relationship between the image's magnified size and the image's spatial location was also identified, i.e.,

$$M_x = M_y = M_z = M_{lat},$$

where $M_{lat} = (1 + Z_1 (1/X_c - 1/Z_r))^{-1}$

This relationship between the image's size and spatial location can be simply stated for the case where the image is of an object that originally existed only in a plane parallel to the plane occupied by the photographic plate, i.e., the object had no depth and Z_1 has the same value for every point on the object. In this specific case, the factor of magnification is always equal to the factor of displacement. Therefore, if the image of the object is made 5 times larger, then the spatial position of this image will be 5 times farther away from the holographic plate (along a straight line through the viewing point on the holographic plate and the viewed point on the object's enlarged image).

Limiting the orientation of the object and the photographic plate to parallel planes is extremely useful for surveying applications. Choosing the factor of magnification

for a specific measuring grid and survey application is a relative judgment. It identifies an area, rather than an exact point, where the image reconstruction equipment can be located during the survey.

We cannot assume that existing terrain conditions will allow us to select an exact location from which to operate for all the observations required during the survey. The ability to spatially locate the reconstructed image at an exact point, regardless of the location of reconstruction equipment, is the important feature that the holographic techniques provide, which relieves us of the almost impossible restriction of having to be physically located at a specific point for each observation.

The phenomenon of parallax provides the tool for exactly locating the reconstructed image. After the holographic plate and reconstruction light source have been set up, the spatial location of the reconstructed image is altered by changing the distance between the plate and the source. Viewing the subject of the survey through the holographic plate with a telescope or a camera's lens, one has merely to focus on the subject. Then by moving one's head slightly from side to side, one of the following conditions will be observed through the eyepiece.

1. The holographic image will move in the opposite direction to the motion of your head. This means that the image is in front of the subject and the light source must be moved farther from the

holographic plate.

2. The holographic image will move in the same direction as the motion of your head. This means that the image is behind the subject and the light source must be moved closer to the holographic plate.
3. There is no motion of the holographic image relative to the subject as your head is moved from side to side. In this case the reconstructed image is spatially located in the same plane as the subject.

This procedure for locating the image at an exact point is easily accomplished in a matter of minutes, with extreme accuracy.

The factor of magnification is not exactly known, however, after completing the preceding application for spatially locating the hologram's reconstructed image, since the location of the reconstruction light source was altered to accomplish the positioning of the image.

The means by which the size of the magnified image can be determined with sufficient accuracy is by measurement of the new Z coordinate of the light source. This value for Z_r is then used in the formula for M_{lat} and the new factor of magnification is computed.

Given the above, the final step in the survey process is to make the photographic/computer records of the

survey data, i.e., a data record of the scale's spatially located image with each set of survey points, where each set contains at least one (1) reference point. The coordinates of the survey points relative to the reference points will then be determined from the properly developed and printed photographs or in real time analysis by the computer.

Statistical operations are required in both of these methods and for this, a way must be devised for predicting the size of a sufficient sample for the prevailing conditions.

CHAPTER III

EXPERIMENTAL ARRANGEMENT FOR A FEASIBILITY STUDY

In Chapter I it was suggested that holography can provide the basis of a new method for surveying an airport runway. This new method is not an improvement on or a modification to standard surveying practices, but rather an entirely different approach to performing the same tasks. As such, this method employs new techniques which have unique requirements for their implementation.

These requirements are three:

1. that there be one absolute reference point for the entire subject of the survey, (a means of providing this for a runway was presented);
2. that the hologram image of a suitable measurement scale be spatially located in the plane occupied by the survey subject;
3. that a data record be made which contains the measurement scale and a statistical sample of the apparent positions of the reference point(s) and the survey points on the subject, relative to each other and to the scale.

In Chapter II, the principles of hologram image magnification were reviewed, and the causes of the lateral and longitudinal distortion inherent in magnification were investigated. The parameters operative in image magnification were analyzed on the basis of the requirements of the

applications selected for this thesis. The optimum characteristics for the relative positions of the equipment during the recording and reconstruction of the hologram image were identified. Also in Chapter I the method for spatially positioning the reconstructed image at an exact location was described.

While an actual survey cannot be conducted in a laboratory environment, it will be possible to perform a feasibility study to verify:

1. the ability to magnify a reconstructed image to a preselected exact size;
2. the ability to spatially locate the reconstructed image exactly at a preselected location;
3. the ability to record survey data;
4. the effectiveness and validity of performing time-averaging statistics on these data.

The methodology required for items 1.) and 2.) has been stated above. We will now discuss the criteria for recording the survey data and for performing time-averaging statistics on these data.

Chapter I presented the random characteristics of turbulence and the use of time-averaging techniques for compensating for the distortions and displacement that generally are introduced by turbulence.

This is based on the fact that¹² the random difference vector, \bar{y} , displays stationary statistics, so that its average position over a sufficiently large statistical sample is time independent. Furthermore the type of statistics is such that the expected value of the difference value equals the difference vector of the expected position of the extremes.

In such a case, the position of one point relative to a second point can be identified with certainty, and if that second point is our absolute reference point, then the true locations of both points can be identified.

As this is true for all conditions of turbulence, it is obviously true for the condition of no turbulence. In this case the data from a single observation would correctly identify the true relative positions of the survey points.

In the absence of turbulence, photography would be the most expedient medium for recording the survey data. A single photograph would accurately record all the data and the relative locations of all points can be measured from a print of the developed negative.

With turbulence present, or anticipated, time-averaging must be used in recording the survey data. A single observation cannot be relied upon to identify the true relative locations of the survey points. At least two methods are available for obtaining a time-averaged record of

12 S.I. Feldman, op. cit.

the survey data.

One method again uses photography and can be employed if the degree of turbulence is mild. Here the strobing of multiple exposures on a single photographic frame is utilized to acquire a sufficient amount of random data to identify the time-averaged locations of the survey points. Then the developed photograph is analyzed, and the expected value of the position vectors for the points of interest is determined. This is readily accomplished by enlarging the photograph, having it screened by standard offset printing methods, and then superimposing a 1/16th inch grid on the results. After undergoing this process, the photograph is ready for analysis using a magnifying glass. Each grid element contains an 8 x 8 matrix of weighted dots from which one computes the weighting factor for that element. These grid element values are then used to identify the center of gravity for the points of interest.

Determination of minimum sample size required to achieve stationarity of the statistics of \bar{y} must, for the time being, be done by empirically measuring convergence of the standard deviation of the expected value of \bar{y} over variable samples. Assuming equispaced strobing instants, the strobing period required to achieve a desired accuracy will depend on the nature of the turbulence present, i.e., on the variance in the "observed" locations of the survey points. Future work must be done to establish bench marks for the

minimum strobing periods for given atmospheric conditions.

The second method uses computerized electronic techniques to perform data acquisition and statistical averaging at the same time. In this case a TV camera or some other electronic optical analyzer, can be employed to provide input to a computer. A software program will then statistically process the survey data contained in each frame. This processing will continue until the software determines that it has identified the time-averaged locations of the survey points to within the accuracy desired, thereby automatically controlling the sample size.

The use of the electronic medium is perhaps the most desirable surveying method under all conditions, i.e., with or without turbulence. In one operation, the computer will determine for the user what minimum observation period is required, based on the actual atmospheric conditions during that period, by recomputing the mean deviation of the statistical sample, on a real time basis, until the deviation is reduced to an acceptable value by additional observations. At the same time, the computer will identify the coordinates of the relative positions of all the survey points.

In contrast, the use of the photographic method carries with it the inherent uncertainty of whether the observation (strobing) period was of sufficient duration; a question which cannot be answered until the film is developed and the prints analyzed.

For the laboratory feasibility study to be under-

taken here, photographic records will be used to acquire the data relative to the simulated survey points.

Figure III-1a shows the usual geometric parameters involved in hologram recording, and Figure III-1b shows the analogous parameters of holographic image reconstruction.

For this study a distance of 15 feet was selected as the distance between the hologram's image and the holographic plate in Figure III-1b.

The selection of 15 feet was dictated by available photographic equipment and laboratory space. The telephoto lens used to record the measurement data had a minimum focusing length of 12 feet, therefore a distance greater than that had to be used. Then the physical constraints of the laboratory in which this work was performed provided the upper boundary on this distance.

After allowing for the placement of the camera (and room to operate it) and the holographic plate and reconstruction light-source at one end of the lab, and locating the survey points and a light-source for their illumination at the opposite end of the lab, the unobstructed viewing distance available was 15 feet.

It would, of course, have been possible to increase the effective viewing distance by the appropriate use of mirrors and this was done in some preliminary experiments, but the added experimental complexities and discomfort proved to be disproportionate to the minimal value of the increased distance to the purposes of the study. The selection of the

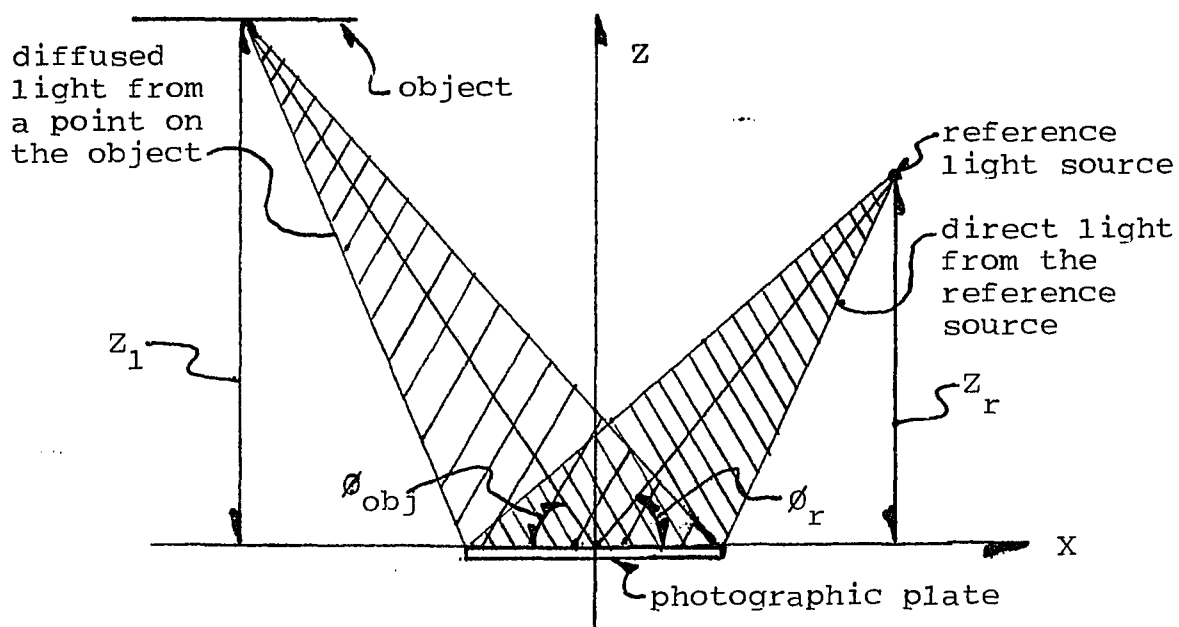


Figure III-1a
Elements for recording a
hologram

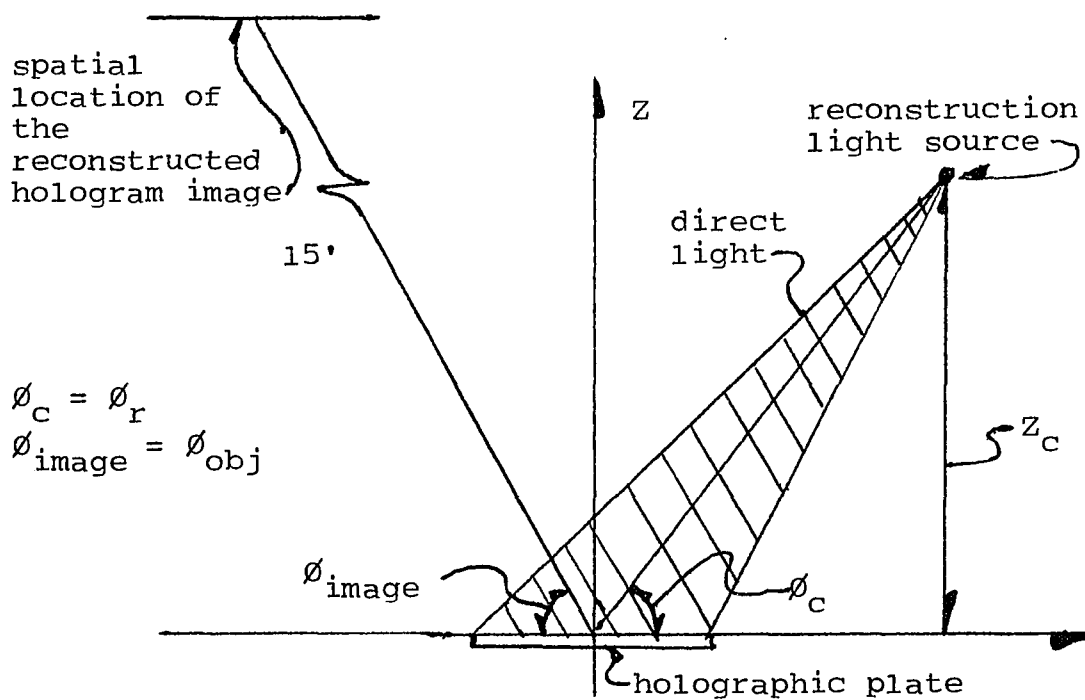


Figure III-1b
Elements for reconstruction of hologram image

parameters for the remaining elements in Figures III-1a and III-1b was based on more technical consideration.

One goal in this undertaking was to put to a practical test the accuracy obtainable in applying the holographic technique for magnification of a hologram's reconstructed image, in this case the vertical scale. Magnification by a factor of 5 was selected as being fully representative of this dramatic capability. Therefore, the vertical scale must be 3 feet from the photographic plate if we are to attain the selected measurement distance of 15 feet.

The locations of the miniature scale model and the reconstructed hologram image were chosen to lie on the same line when observed through the photographic plate.

This viewing angle, which is shown in Figure III-2 as θ_1 , is the angle between the axis of the camera's lens and the perpendicular to the plane of the holographic plate during observation of the reconstructed image and is dictated by the physical conditions under which the survey is to be conducted. In the case set forth in Chapter I, a survey of a runway from a position alongside the runway was mandated at a viewing angle of approximately 30° .

The orientation of the reference light source and the photographic plate, during the making of the hologram, is determined by the viewing angle selected, and a second factor which involves preventing the camera's lens from gathering direct light from the reconstruction light source.

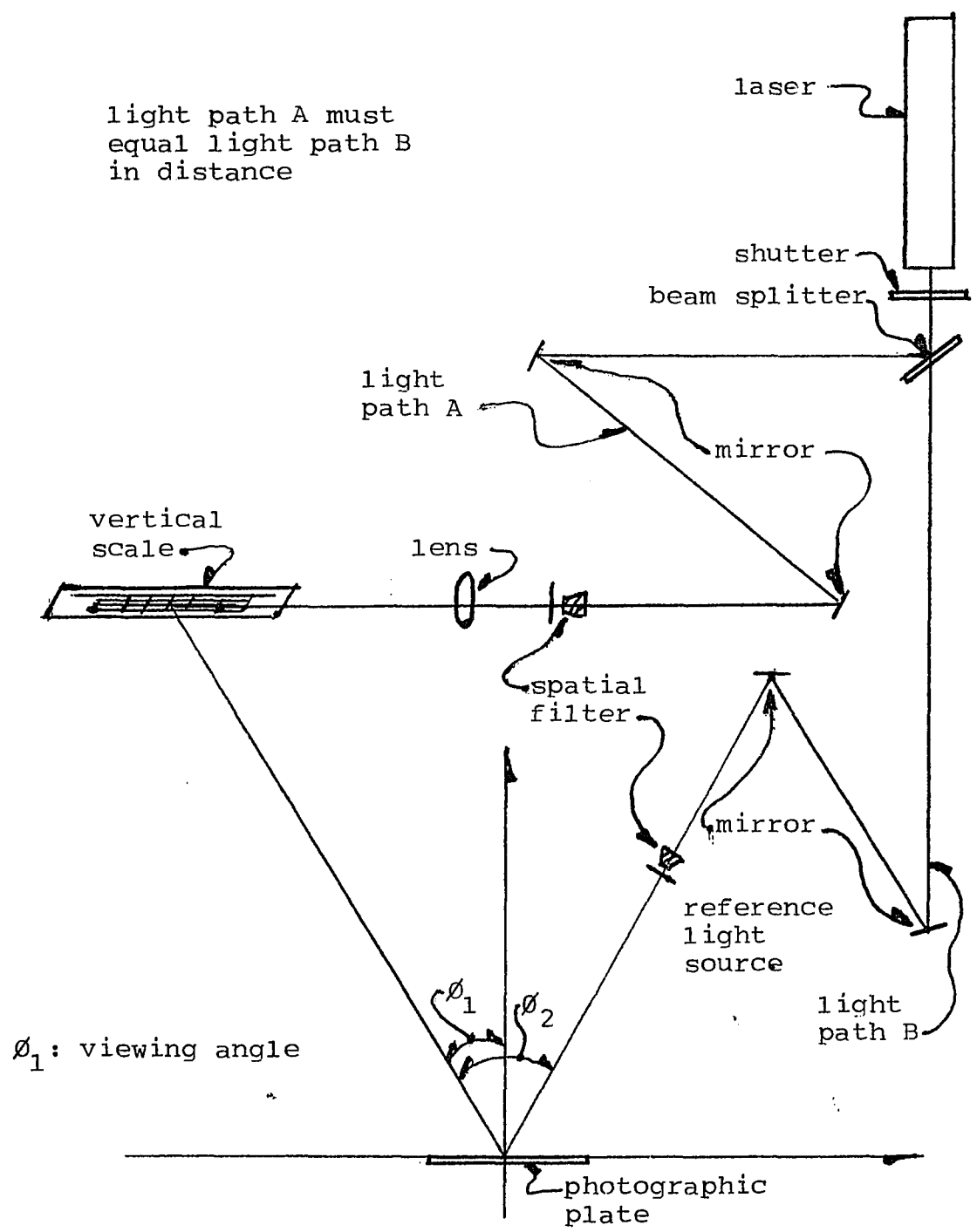


Figure III-2
Equipment arrangement for recording
hologram of vertical scale

Since the axis of the reconstruction light source must intersect the plane of the holographic plate at the same angle as did the reference light source's (to avoid the distortion associated with image magnification identified in Chapter II), the selection of the reference light source's position is influenced by the obvious requirement that the reconstruction light source not be "seen" by the camera during observation of the reconstructed image. For the vertical scale's hologram, approximately 53° was selected as the value for this angle.

In Chapter II the photographic plate was located in the XY plane, at the center of our hologram's coordinate system. In this chapter considerations were outlined for selecting the viewing distance of the reconstructed hologram image, and its orientation and magnification factor. This determined the location of the vertical scale's model, from which the orientation of the reference (and reconstruction) light source was selected.

The distance from the photographic plate to the reference light source is determined from the location of the scale model and the formulations developed in Chapter II (this is also true of the location of the reconstruction light source). As the formulations in Chapter II were developed on a unit value basis, only elementary scaling techniques are required to apply them to any situation.

Finally, there remains the orientation and illumination of the vertical scale model. For the runway

application at hand and the requirements of the scale, it was decided that the planes of the photographic plate and the scale model be parallel in order to avoid having to compensate for the distortions associated with magnification along the Z axis. The illumination source for the scale model was located so as to avoid any direct reflection of light from the object, i.e., non-diffused light, from impinging on the photographic plate.

Figure III-2 shows a lens in the path of the light illuminating the object. This lens was used in conjunction with a 10 power (low power) objective to form a beam spreader. The narrow beam of light from the laser passes through the objective which brings it to a focus. Past the focal point the light emerges as a diverging beam which in turn passes through the lens and is re-collimated. The ratio of the focal lengths of the objective and the lens is the ratio of the diameters of the beam before the objective and after the lens. The desirable feature of a collimated beam is that, if proper spatial filtering is used, the intensity of the light is essentially uniform throughout the volume of the beam, as opposed to the condition in a diverging beam, where intensity decreases in proportion to the square of the distance traveled. The use of the lens therefore provided even intensity of illumination across the width of the vertical scale.

The collimated light from the lens under the above stated conditions contained too many fringes, therefore a 5μ

pinhole was placed after the objective and was used successfully to spatially filter the beam. Color aberrations were of no concern since only a monochromatic record was sought. The minor 3rd order and spherical aberrations that were present in the object illuminating beam were of no concern since the only portion of this light reaching the photographic plate is diffused by the object which completely disperses the beam.

Figure III-3 depicts the vertical scale used in making the hologram. The scale's vertical dimensions were selected for the proposed observation of the laboratory survey points, after magnification by a factor of 5, within the constraints of the construction methods available. The scale's horizontal dimensions were chosen to facilitate verifying the amount of magnification. The selection of materials and method for construction of the scale's model was dictated by the following criteria for the magnified hologram image.

1. The grid lines of the scale's image must be sharply defined and highly visible.

Magnification of the model's image by a factor of 5 will also accentuate any imperfections in the model by the same amount. This eliminated the possibility of any type of artistic (hand) rendering for the model's construction. (Usually employed methods for producing good artwork involve hand construction of an oversized object, followed by photographic reduction to the desired size. This diminished

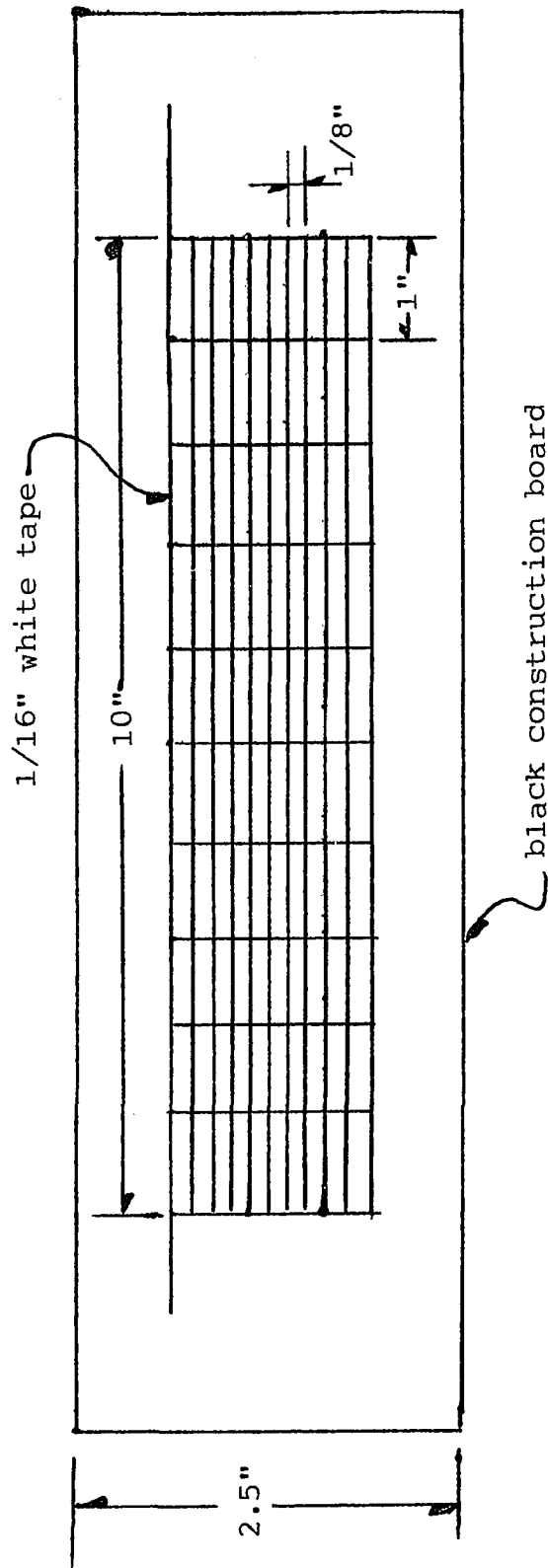


Figure III-3
Dimensions of vertical scale used for
recording hologram

any imperfections, and is the opposite procedure of ours.) The use of materials with machine-made tolerances was essential for grid lines of the scale.

Test holograms were made of both red and white materials to establish maximum visibility. Although the laser to be used for illumination provided a red light output, the whiter material was found to produce the largest quantity of re-diffused light.

2. The grid background must appear "invisible" in the magnified reconstructed image.

The background surface of the scale model, therefore, must be a light absorbing material. This will prevent the background from being recorded, photographically, in the hologram, so that it will not be visible in the reconstructed hologram image. As in acoustics, the most absorbent surfaces are made of multi-directional scattering materials. The "blackest" man-made materials all have a pile or velveteen-like surface. This proved totally unsuitable for supporting the grid lines of the scale within the close tolerances required. A material with less desirable light absorbing characteristics, but with a structural surface adequate for supporting the scale's grid lines, had to be selected.

Black mat cardboard was used for the background with 1/16 inch white tape adhered to it for the grid lines with good results. The use of the tape provided equal line widths and uniform light reflection characteristics, as well as a convenient medium for construction of the vertical

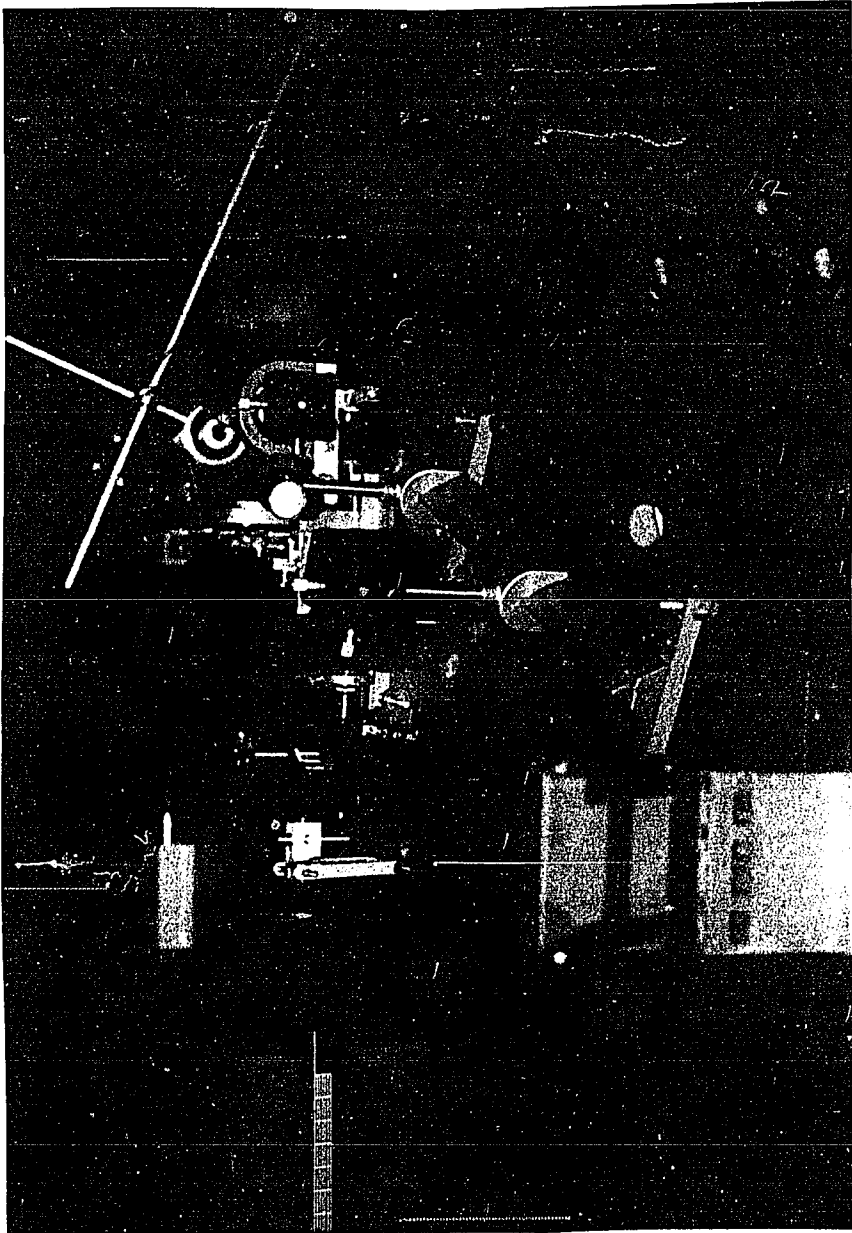
scale model.

A hologram was then made of the constructed vertical scale model. Photographs III-1 and III-2 are of the actual laboratory equipment arrangement used in making the hologram, taken from different sides of the optical table. The individual components in these figures can be identified by comparison with Figure III-2.

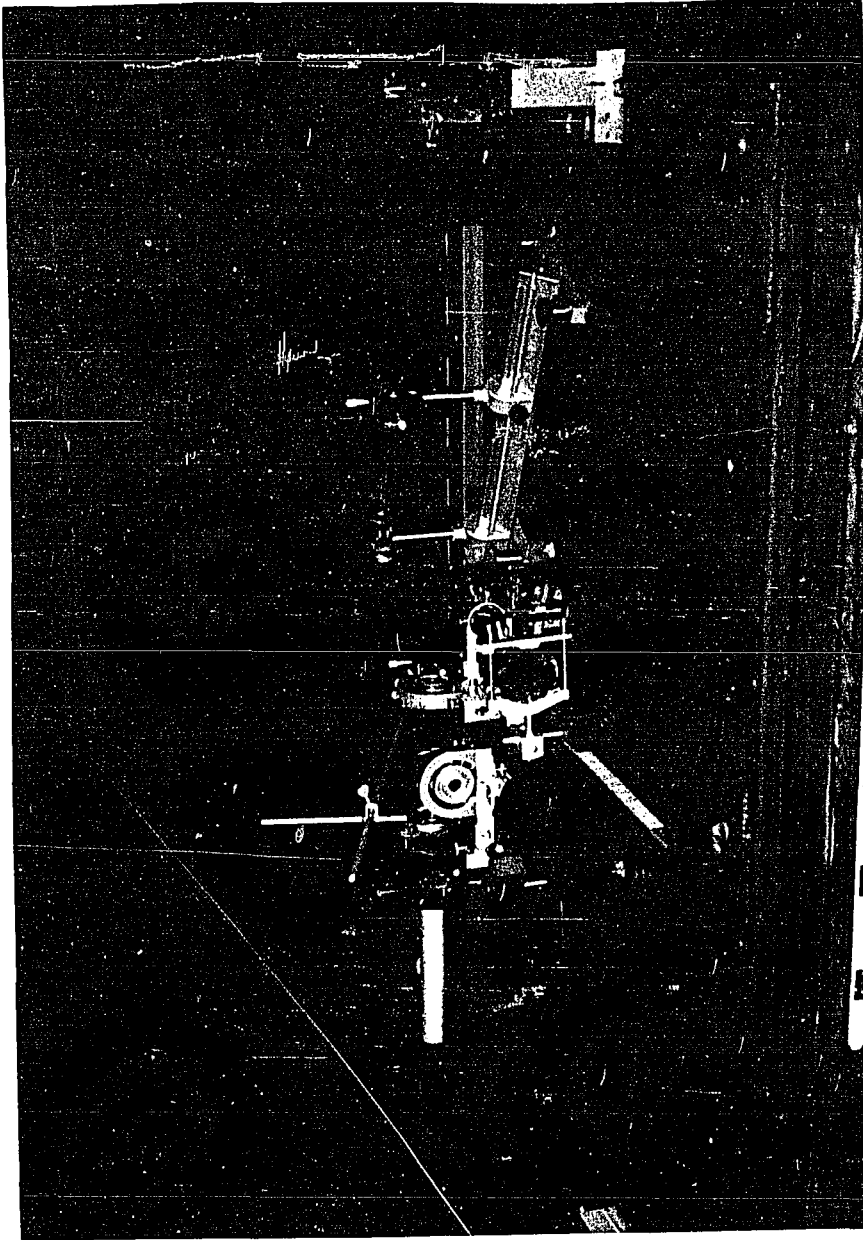
The processed holographic plate was used to reconstruct the image of the vertical scale model. In Photograph III-3 the scale's reconstructed image is spatially located in the same plane as that originally occupied by the scale model, and is reconstructed in the same size as the scale model. The scale model remains in its original position and a 12 inch ruler has been introduced and is supported atop the scale model. As shown in Photograph III-3 no difficulty is encountered in obtaining high precision spatial location of the image and in reproducing its exact size. The ruler indicates the original size of the scale model and of the reconstructed image.

Photograph III-4 shows the full holographic plate in its holder and the spatially located plate image seen in Photograph III-3.

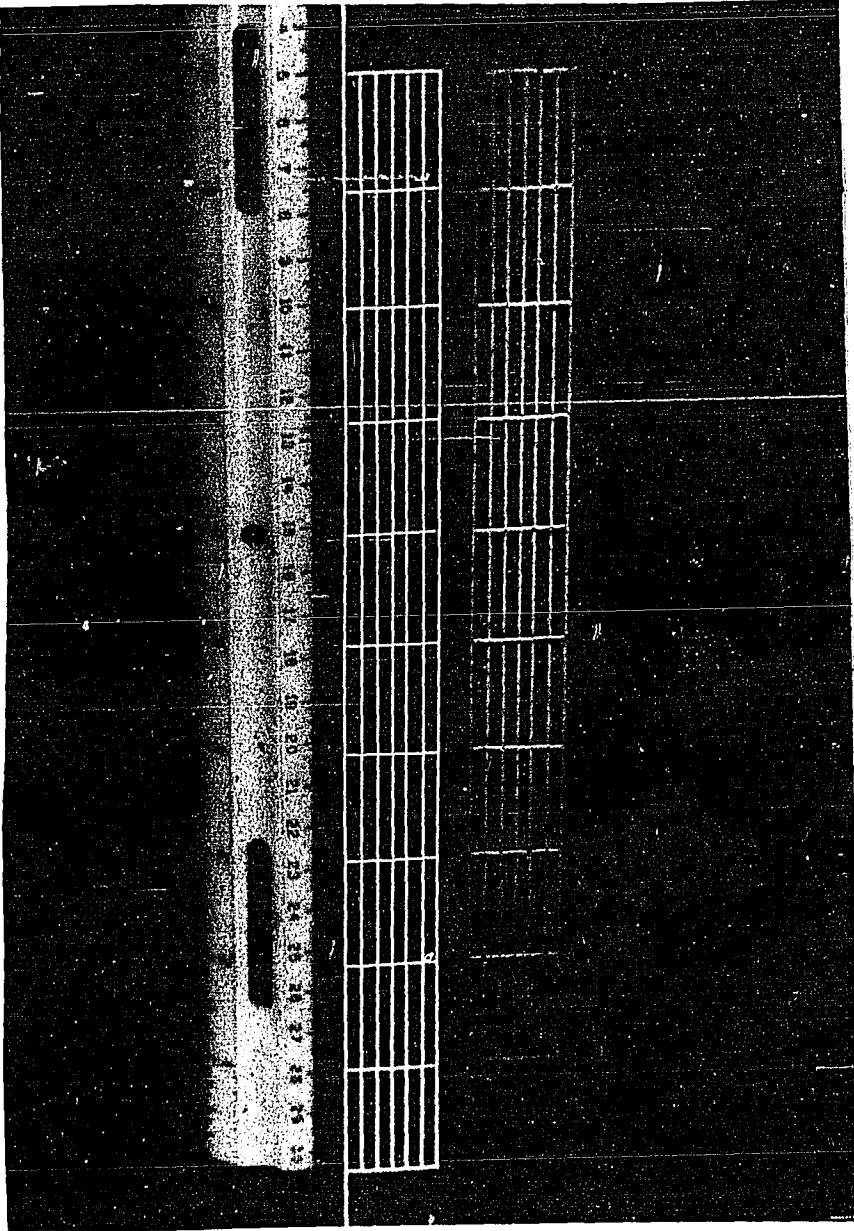
Next a piece of wire was bent into an irregular shape and this function of position was measured using the reconstructed scale's image. This wire was placed in the approximate location originally occupied by the scale model. Then the reconstructed hologram image was spatially located



Photograph III-1
Equipment arrangement for recording hologram



Photograph III-2
Equipment arrangement for recording hologram



Photograph III-3
Reconstructed image juxtaposed to hologram model



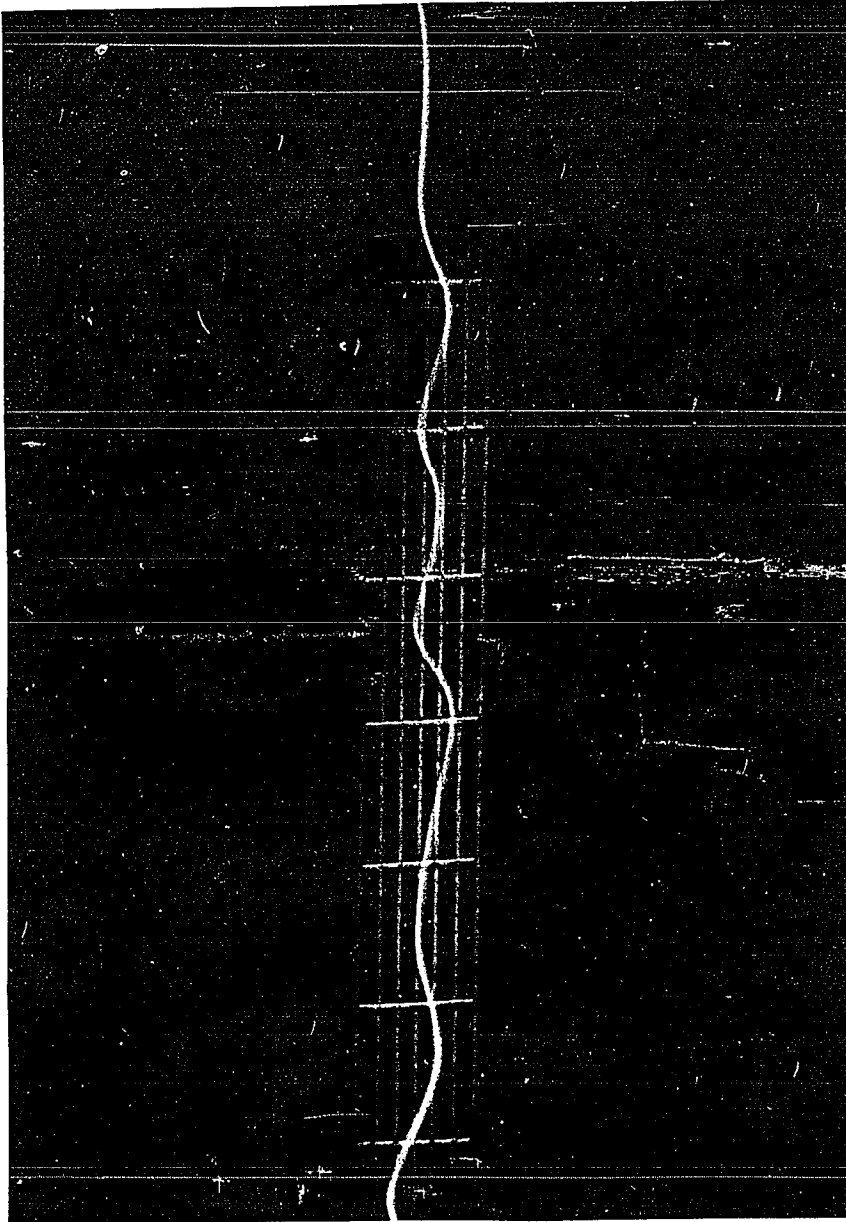
Photograph III-4
Equipment arrangement for reconstruction of hologram image

in the plane of the wire and Photograph III-5 was taken. In an actual survey condition, points would have been marked on the wire at known equidistant intervals. This would provide bench marks for precise measurement of the contour of the wire.

Photograph III-6 shows the reconstructed image superimposed on a cross-section of a sheet of construction paper. There are three pieces of tape adhered to the paper. The image is superimposed in the plane of the center piece of tape. Note that the nearest and furthest pieces of tape are out of focus (blurred) while the center piece of tape and scale image are in sharp focus. The same comments that were made above for Photograph III-5 concerning the use of the scale's image for measurements are applicable here.

The location of the reconstruction light source, relative to the holographic plate, controls the size and spatial location of the reconstructed image of the vertical scale model. Figure III-4 identifies the difference between the location of the reference light source during hologram recording and the location of the reconstruction light source during observation required to attain magnification of the hologram's image by a factor of five. (Cfr. Chapter II)

After changing the laboratory equipment arrangement, Photograph III-7 was taken of the magnified image of the scale model. The same ruler shown in Photograph III-3 is used here again, to verify the factor of magnification. As shown in Photograph III-3, the vertical grid lines in the



Photograph III-5

Reconstructed image used as measurement scale



Photograph III-6
Reconstructed image superimposed in cross section

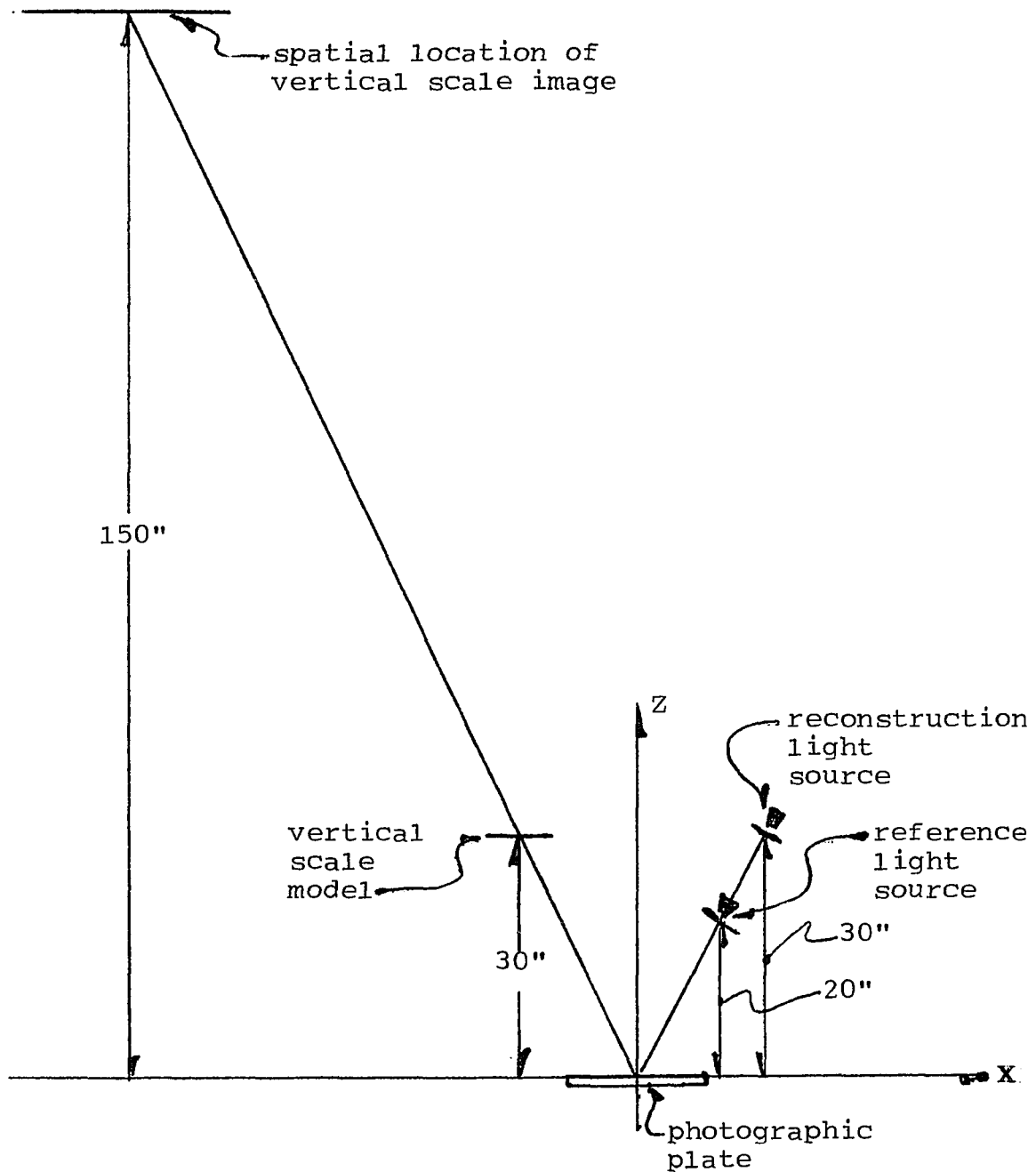
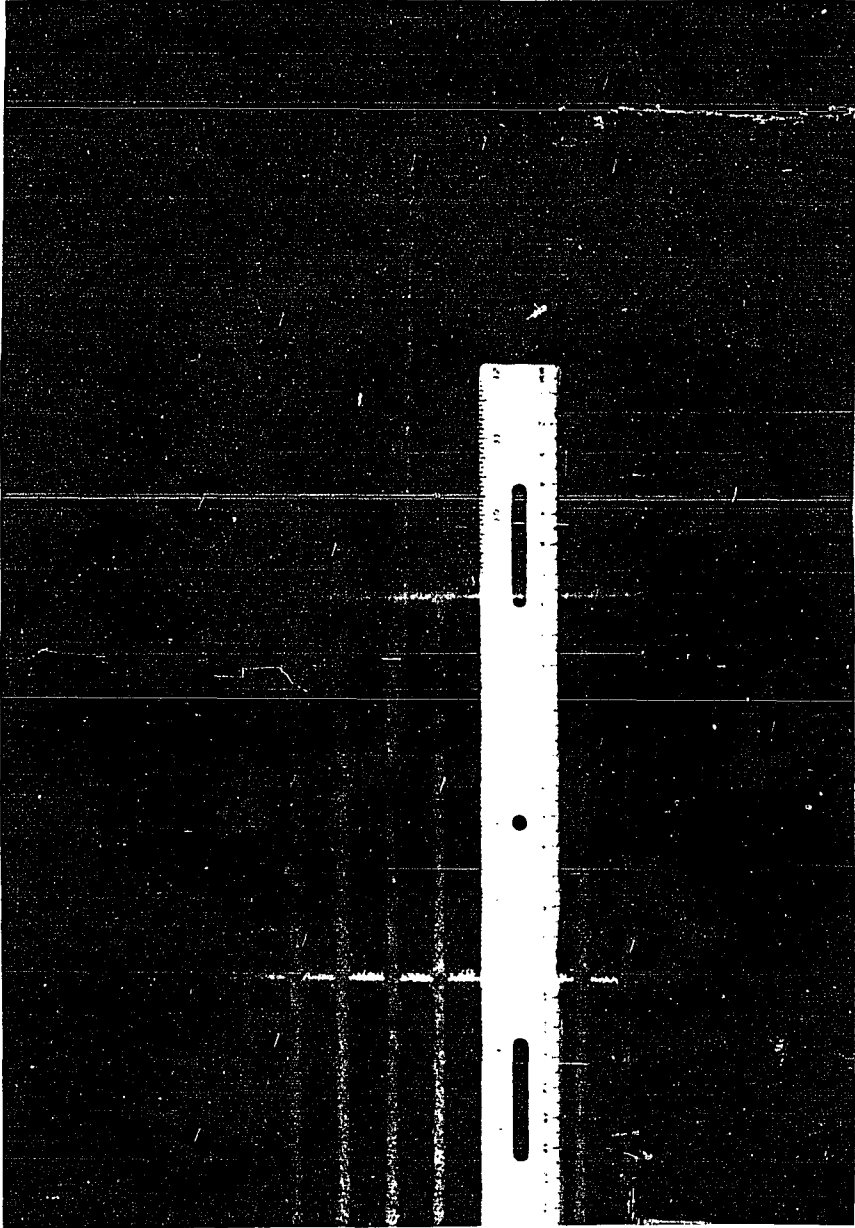
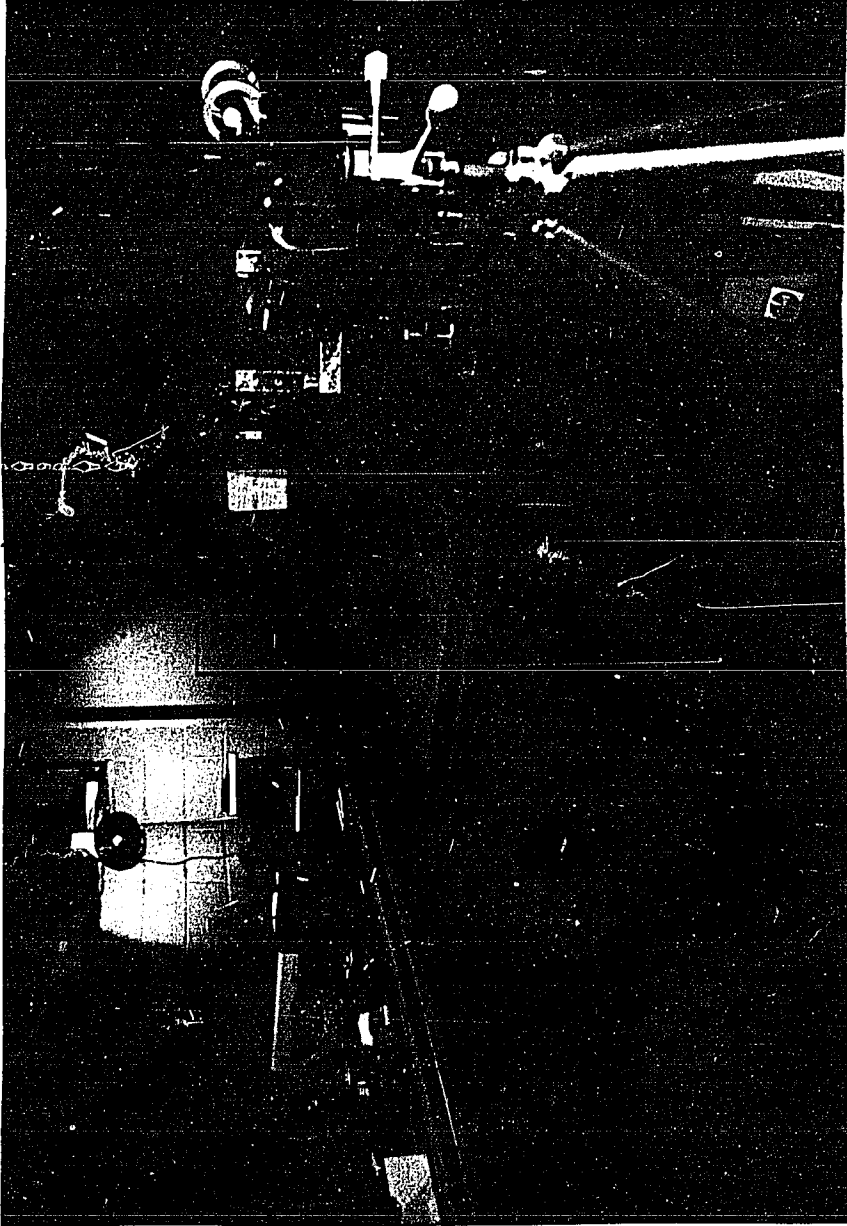


Figure III-4
Locations of principle elements
in recording and reconstruction
of hologram image



Photograph III-7
Reconstructed image magnified by a factor of five (5)



Photograph III-8
Equipment arrangement for magnification of hologram image

scale model are equispaced one inch (1") apart. It is readily verified in Photograph III-7 that the vertical grid lines in the magnified scale image are five inches (5") apart. Photograph III-8 shows the physical locations of the ruler seen in Photograph III-8 relative to the holographic plate. They are in fact 15 feet apart.

With regard to the spatial location of a hologram's image, as shown in Chapter II the X, Y, and Z components of the image's position, relative to the center of the hologram coordinate system (i.e., the center of the holographic plate) are controlled by the position of the reconstruction light source relative to the holographic plate. These two pieces of equipment, i.e., the light source and the plate, are the only devices used in the reconstruction process and they are normally both mounted on a single optical bench. This rigid system, i.e., the bench, light source, and plate, may be moved anywhere, physically, and may be placed in any position, and such translation and/or rotation will result in exactly the same amount of translation and/or rotation of the hologram's reconstructed image. This is indicated in Figure III-5 and represents the final tool for precisely spatially locating the hologram image.

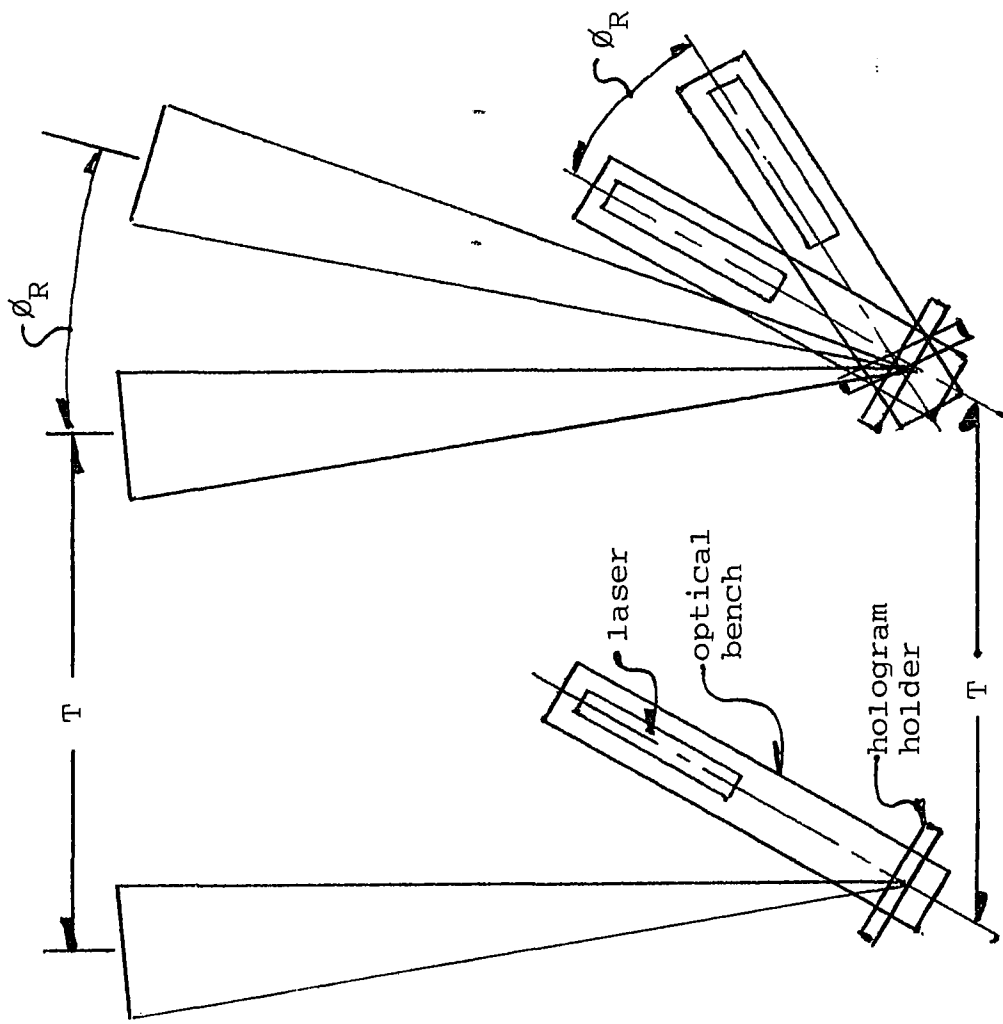


Figure III-5

Translation and rotation of reconstructed image

CHAPTER IV

EXPERIMENTAL SIMULATION OF TURBULENCE CONDITIONS

With the arrangement presented in Chapter III, the final steps in the laboratory feasibility study are the simulation of turbulence conditions and the time-averaging of data observed through the turbulent medium.

Experimental verification of the validity of the assumptions adopted on the basis of the theory of Chapter I, and of the effectiveness of the proposed surveying technique in obviating image distortion and errors in data acquisition due to atmospheric turbulence is of fundamental importance to this feasibility study.

To this end, several methods of generating turbulence in different mediums under laboratory constraints were investigated. For the purpose of acquiring data, two models were prepared to serve as the subjects under observation.

The first model consisted of two object points and is depicted in Figure IV-1a. The second model consisted of a reference point and two object points as depicted in Figure IV-1b. The intended use of the two point subject was to provide experimental verification of the theory that if a sufficient statistical sample is taken, then the difference vector, y , displays stationary statistics (as defined in Chapter I, y represents the position of one point relative to the other point).

The three point arrangement was used to demonstrate

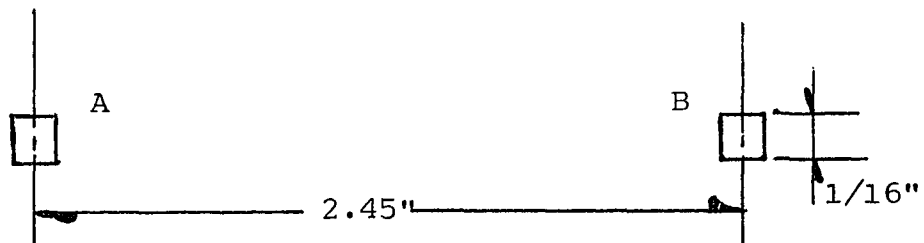


Figure IV-1a
Two point arrangement for survey subject

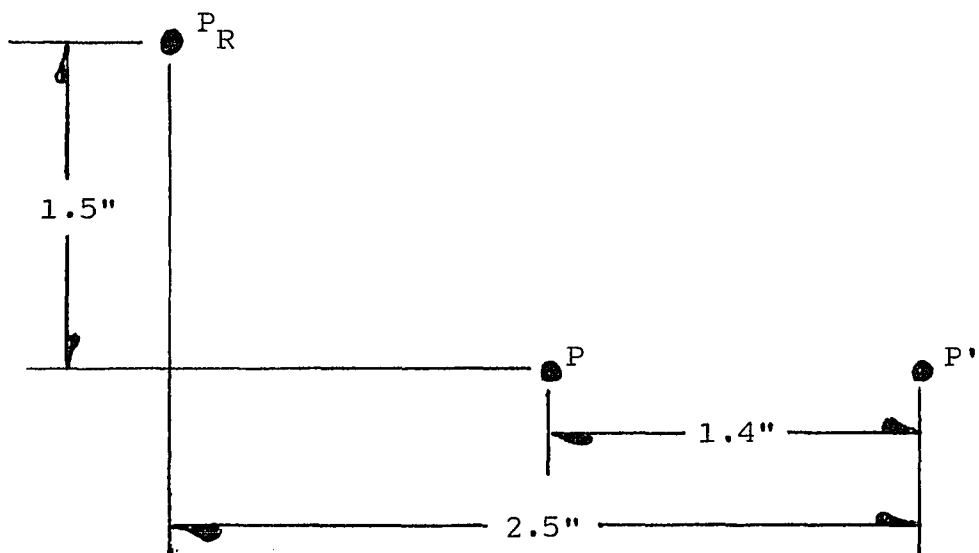


Figure IV-1b
Three point arrangement for survey subject

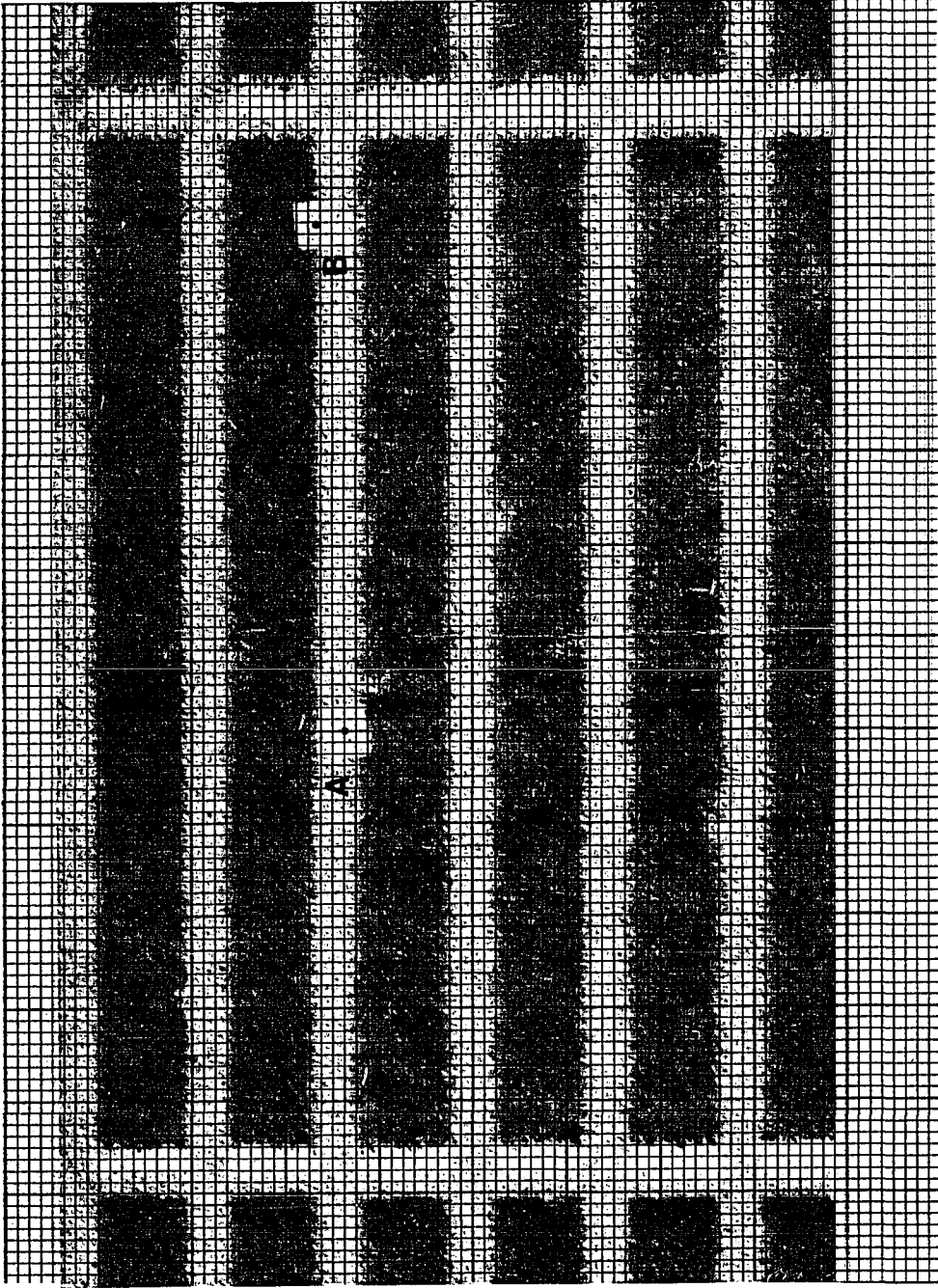
the role of the absolute reference point in the proposed surveying technique. As stated in Chapter I, time domain statistical averaging of a sufficient sample yields the accurate positions of several points relative to each other. Then, if the true position of one of these points is known, the true position of all the other points may be easily obtained (see Chapters I and III).

The three point arrangement was constructed by sticking straight pins in a backdrop board covered with velveteen. The straight pins had a mat plastic head effectively diffusing the light and required no covering. For the two-point arrangement, two squares of typing correction tape were adhered to the velveteen. This type of tape has a very good mat (light diffusing) surface.

The two point survey subject was then placed at a distance of approximately 15 feet from the holographic plate. The scale image was spatially located on the subject by the method described in Chapters II and III, and Photograph IV-1 was taken in the absence of turbulence and exposed for 1/2 second at a lens opening of $f 11$.

This reference picture therefore represents the true locations of the points relative to the image of the scale and relative to each other.

From the dimensions of the subject array and measurements from the photograph, the factor of magnification for this spatial location of the image was computed to be 5.13 times the image's original size. As shown in Figure



Photograph IV-1

Two point survey subject with scale in the absence of turbulence

IV-1, the coordinates of the points relative to an arbitrary cartesian reference superimposed on the picture after processing are

$$\text{for Point A, } X_A = -5.2/16", Y_A = 22.8/16"$$

$$\text{for Point B, } X_B = 38.4/16", Y_B = 25.2/16"$$

so that the components of the difference vector are

$$\text{for Vector AB, } Y_x = 43.6/16", Y_y = 2.4/16"$$

The next item to be analyzed was the geometrical distortion and displacements introduced into the photographic records, due to atmospheric turbulence. To this end, several methods of generating distortion in different mediums under laboratory constraints were investigated.

As a first approach turbulent hot air currents were generated both by resistive electric heating elements and by open flame. In both cases, the hot air generator was placed immediately beneath the line of sight between the observation point and the object. The selected hot air source was also placed as close as possible to the observation point. The reason for this, as is shown in Figure IV-2, is that the magnitude of the apparent displacement of an observed point, due to a refraction surface between the point and the observer, depends on the ratio between the distance from the observed point to the refraction surface and the distance from the refraction surface to the observation point. The greater this ratio,

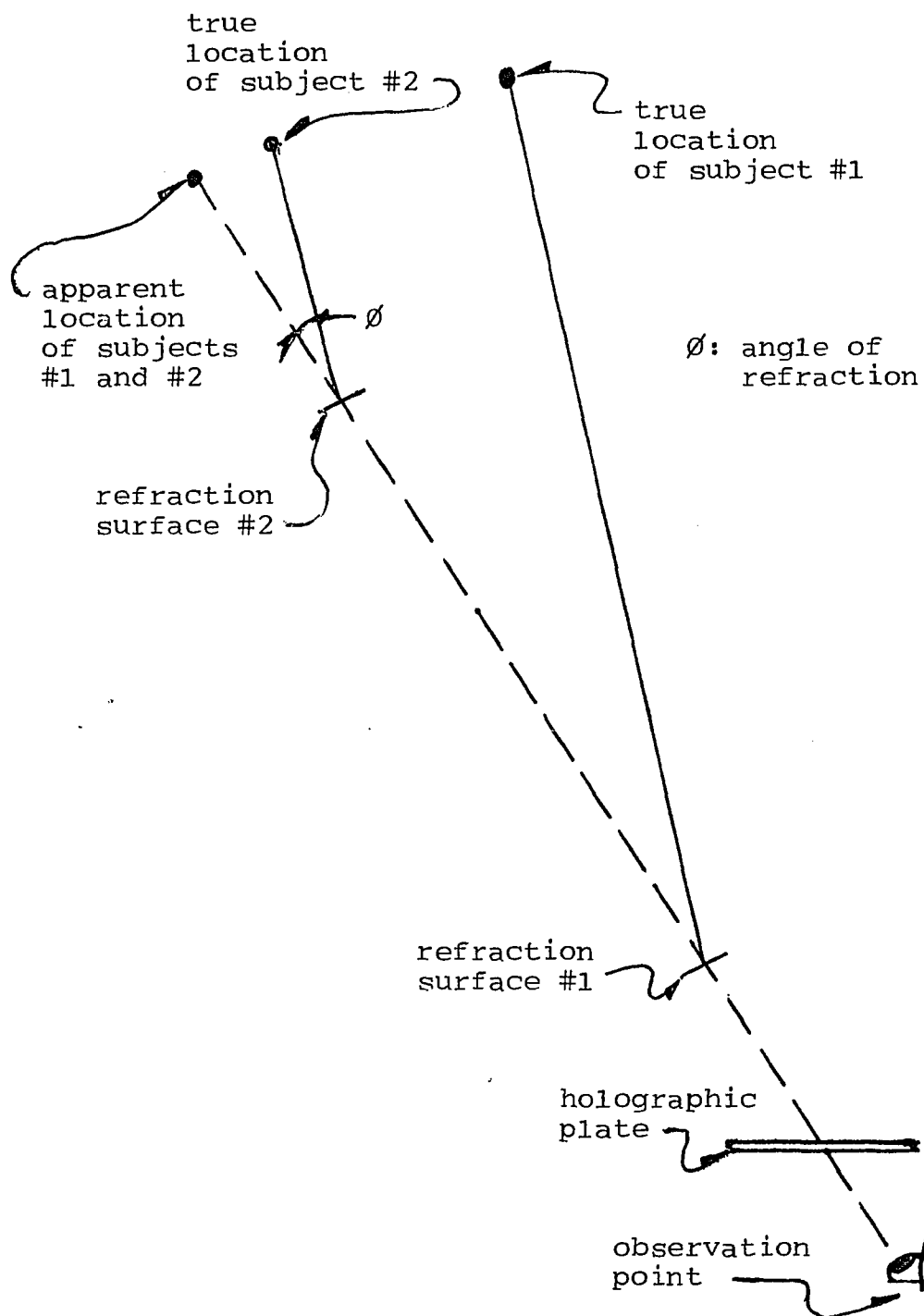
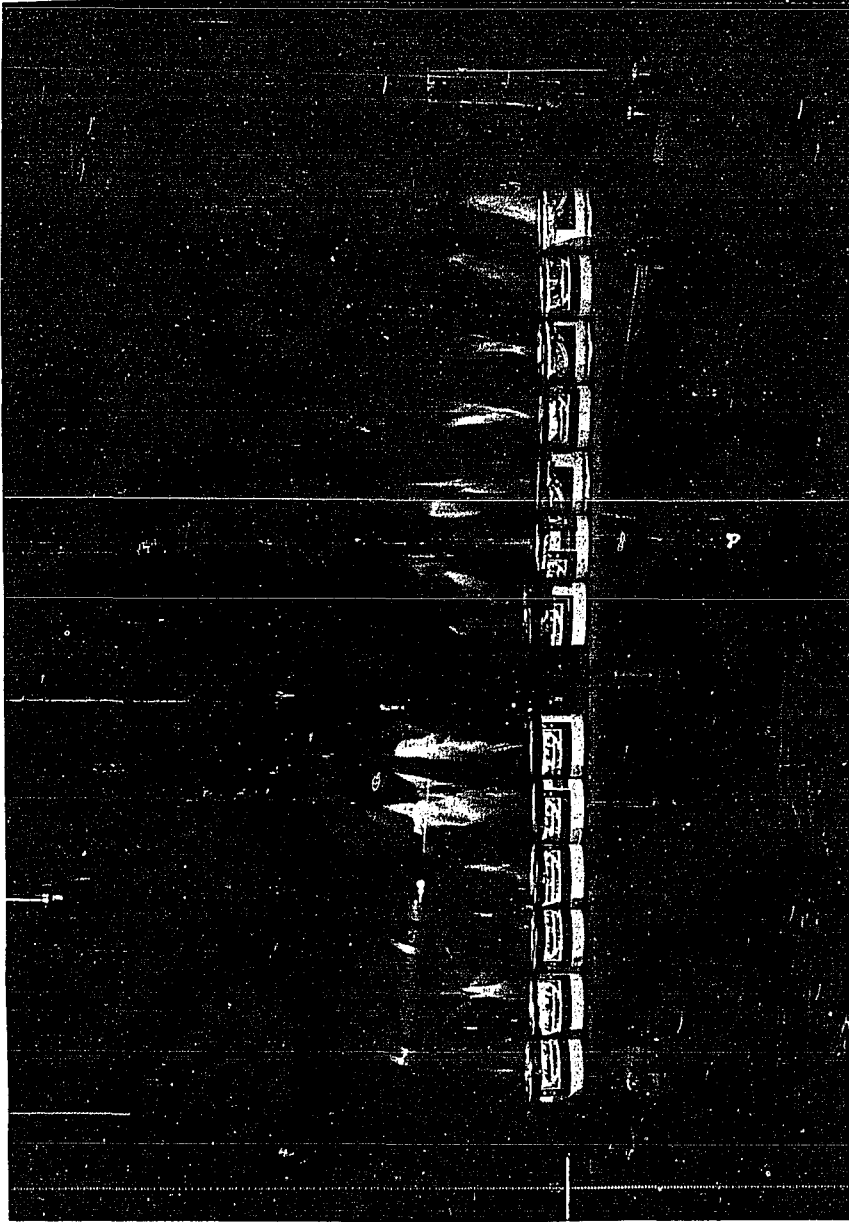


Figure IV-2
Distortion as a function of
the location of turbulence

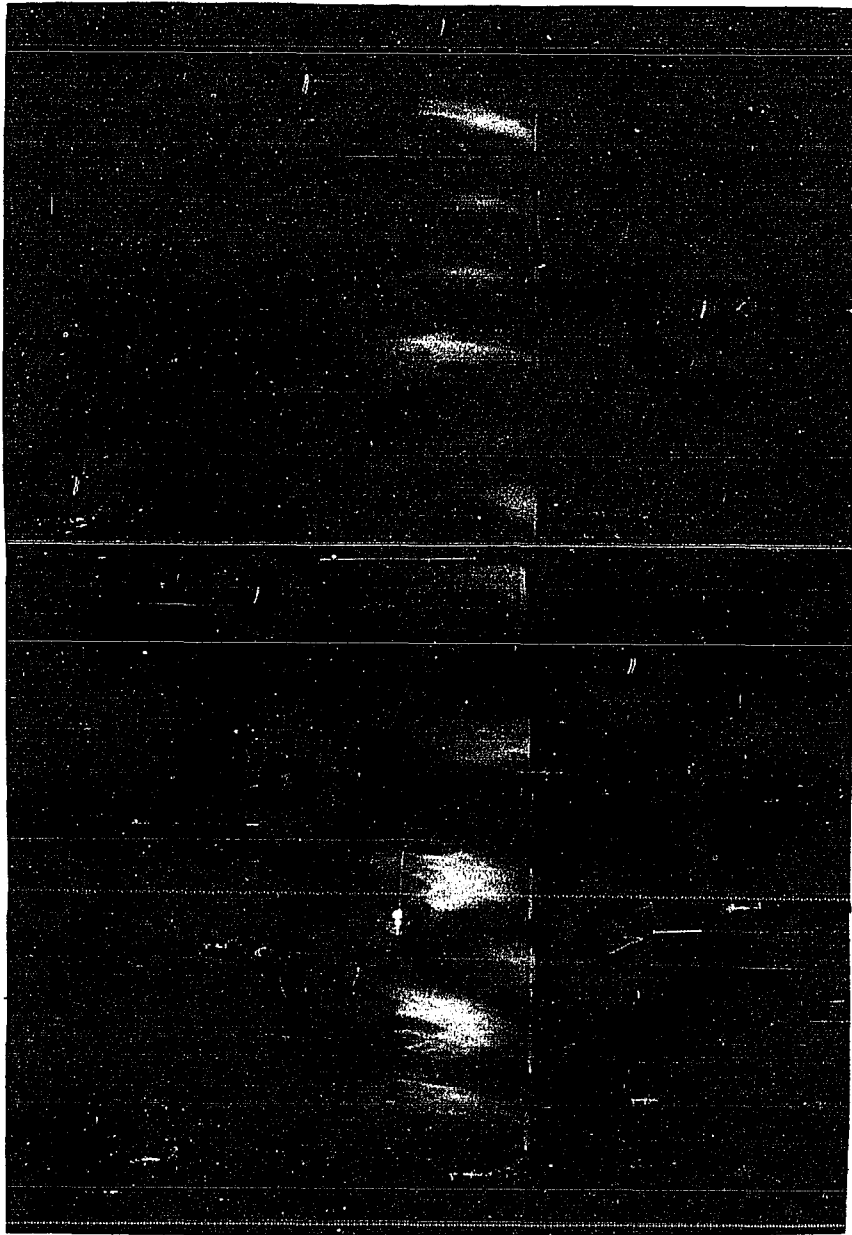
the greater the apparent displacement of the observed point from its true location. (For a more detailed and rigorous analysis, cfr 6.)

The quantity of hot air generated by the electric heater was not sufficient to produce a discernible amount of distortion. This was also the case when steam was used. The use of open flame however produced the desired results. Ignited cannisters of sterno were employed for this purpose. As shown in Photograph IV-2a and IV-2b, 13 cannisters were attached to a board in a single file, and the board was then supported immediately beneath the optical path between the survey subject and the holographic plate.

Several different geometrical arrangements for the ignited cannisters were used and a large number of experimental observations were made and photographically recorded both with stationary cannisters and with random motion of the cannister array during exposure. Random movement of the board and cannisters from side to side during observation greatly enhanced the magnitude of the apparent displacements of the observed objects. With turbulence generated in this manner, stroboscopic exposures of a photographic plate were used to obtain several data points on a single photograph. Many pictures were taken and the sample size was widely varied. It was very difficult to obtain individually identifiable sample points in these multiple exposure photographic records.



Photograph IV-2a
Equipment arrangement for generating turbulence with open flame



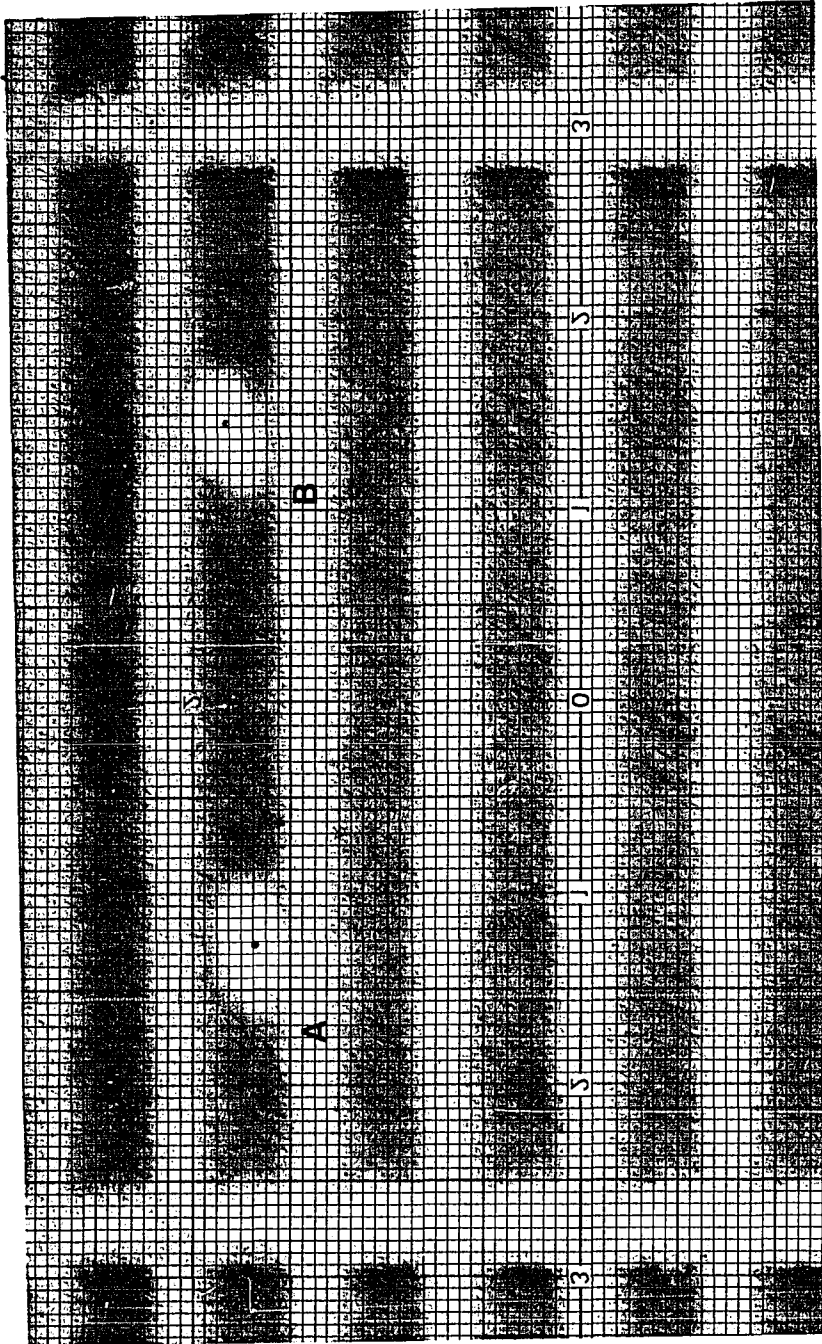
Photograph IV-2b
Turbulent medium

In an attempt to increase the magnitude of the apparent displacement of the observed objects, a mirror was used to multiply the observation distance by several factors. Operating with magnifications of 10 and more on the reconstructed image it was found that object point displacement, due to turbulence, was not sufficiently increased to add significantly to the cogency of the tests. Therefore this complexity was abandoned.

Photograph IV-3 was taken using random motion of the ignited cannisters. It is the result of multiple exposures on a single negative. A rotating disk provided the strobing action in 14 exposures at an equivalent of a 1/60th of a second shutter speed. The camera's lens opening was set at f 4.5.

Photograph IV-3 shows the main features of the effect of turbulence in the optical propagation medium on the photographic image.

The square survey targets are not discernible any more and a pair of blurred oval patterns, due to the superposition of their displaced images, take their place. The 14 individual positions of the targets in the 14 superimposed exposures are not distinguishable in this photograph, because the standard deviation of the random motion is less than the lateral dimensions of the target. In this experiment, however, we shall follow the position of the center of gravity of the target, as shown in Photograph IV-1 so that the randomness introduced in the image position by the



Photograph IV-3
Statistical stationary sample through a turbulent medium

artificially generated turbulence is quite sufficient to simulate the phenomenon in a validly measurable amount.

The effectiveness of the method used to introduce the turbulence (open flame) is also proven by the very sizeable apparent displacements of the centers of gravity of the oval images (which represent the expected values of the positions of the centers of gravity of the two targets) with respect to the actual target position as shown in Figure IV-1. A detailed analysis of the measurements and statistical results obtained follow.

Photographs IV-1 and IV-3 are enlargements produced to better identify the positions of the survey points in each. In order to facilitate the statistical computations, the print of Photograph IV-3 was screened by the usual offsetting techniques and a 1/16 inch grid was burned into both prints to provide corresponding precision cartesian coordinates for ease of position measurements.

Each of the 1/16 inch square inside of this grid was considered as a "picture element" in the computation of the center of gravity of the picture. It was treated as a two-dimensional object element and an equivalent "mass" was attributed to it. Evaluation of this mass was obtained by computing the mean photographic density of the element.

For this computation the dots produced by the screening process and clearly visible in the picture only under magnification by a medium sized enlarging lens, provided an easy means of digitalization. The tedious

process here performed "by hand", can, of course, easily be mechanized if standard appropriate equipment were available. It was estimated that sufficient accuracy could be achieved by assigning to each picture element a digitalized weighting coefficient of 1 to 10 easily computed on the basis of the above observations. Notice that, with the type and size of screen used in this photograph, the precision of the weighting process could very easily be raised to 256 weighting levels or more.

The positions of the centers of gravity of the two oval regions were then computed, considering each picture element as a mass point located at the center of the element and having a weight of 1 to 10 computed as previously described in arbitrary units.

The results of this computation are indicated by the black dots in Figure IV-3. Within the precision of the computations, their coordinates turn out to be

$$\text{for Point A, } X_A = -20.3/16", Y_A = 26.8/16"$$

$$\text{for Point B, } X_B = 23.3/16", Y_B = 29.2/16",$$

the resulting components of the relative position vector AB are therefore

$$Y_x = 43.6/16" \text{ and } Y_y = 2.4/16".$$

Comparing these values with the ones given in page 88 for the

target positions observed in the absence of turbulence we notice that, although the target coordinates have been noticeably displaced by the effect of turbulence, the relative position vectors are indeed identical within the limits of precision of the measurements in excellent agreement with the predictions of the theory.

From the above it can be concluded that, for the conditions of turbulence prevailing during this experiment, the small sample of 14 observations constituted a sufficient statistical sample for our computations.

Also of interest toward experimental corroboration of the theory is the gathering of laboratory observations for insufficient statistical samples. For such conditions the theory predicts no correlation between the observed expected value of the relative position vector and the actual relative positions of the chosen target elements.

For a very small statistical sample it is important to be able to distinguish the individual observed positions. This requires that the individual random displacements be larger than the target dimension.

Accordingly an effort was made to produce smaller targets and larger displacements. This resulted in the previously described arrangement of Figure IV-1b and in the selection of a different method of simulating turbulence of the optical propagation medium in the laboratory.

To this end it was decided to use water as a propagation medium for the light over a portion of the

optical path. This provided a greater difference between the indices of refraction of the two mediums through which the subject would be viewed and consequently permitted recording of distinct multiple object points.

The insertion of the water medium in the optical path was accomplished by the following arrangement of apparatus. A container was filled with water and a mirror was placed on the bottom of the container. The intent of this arrangement was to have the viewed light from the subject deflected onto the mirror at the bottom of the water which in turn would reflect the light up out of the container along a second path. The light emerging from the water surface would then be directed to the observation point. Two additional mirrors were positioned above the water container to properly establish the line of sight as shown in Figure IV-3.

Front surface mirrors were used for interfacing with the ambient air to avoid additional reflection surfaces. A rear surface mirror was used at the bottom of the water container with a waterproof covering over the silvered surface. This was done to prevent the potential damage to the mirror from the water. The problem of additional reflection surfaces was not encountered here since the indices of refraction for water and glass are almost equal.

This arrangement provided extremely high gradients of the refraction index at two randomly varying surfaces, i.e., the interface between the air and water at the points

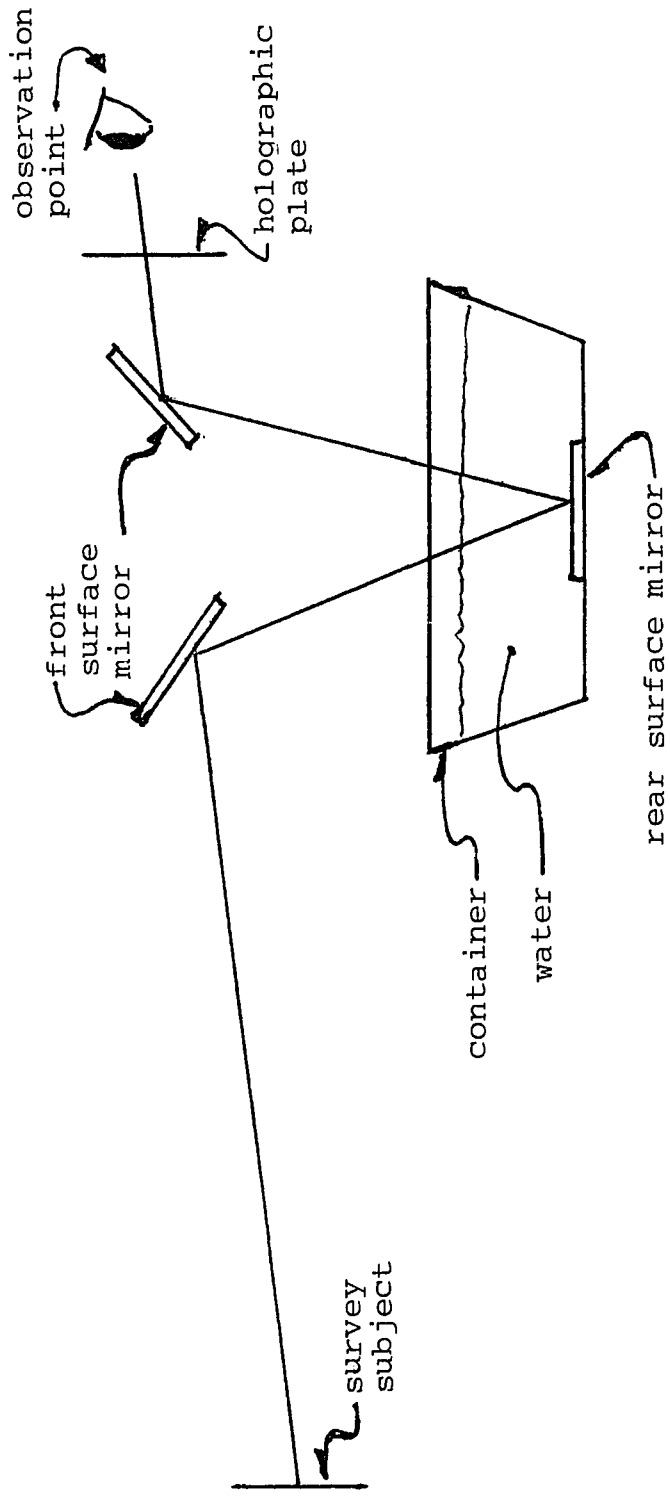


Figure IV-3
Equipment arrangement for optical path thru water

of entry and exit.

The next task was to simulate the effects of random turbulence at these refractive surfaces. The water container selected had an irregularly serrated side wall surface, which therefore, reduced the probability of the generation of regular standing waves in any wave motion.

Three DC motors were employed to agitate the water. Long shafts were attached to the motors using a silicone rubber adhesive so that the motors could be supported above the container. This also allowed for flexing of the drive shaft while rotating and dampening off the vibrations that would be transmitted by the motors. Rectangular paddles were then attached to the ends of the shafts.

Each shaft was attached to its paddle at a different point on the paddle, and none were attached at the center of the paddle. This was done so that each motor would be rotating under unbalanced conditions, different from one motor to the other.

The three motors were then attached to a strut suspended over the water container. Each motor was supported at a slightly different angle to the water's surface and held to the strut by elastic bands to enhance the vibration generated by the motion of the center of gravity of the system.

Finally, a potentiometer was placed across the battery that powered the motors to control their speed. The arrangement is shown schematically in Figure IV-4.

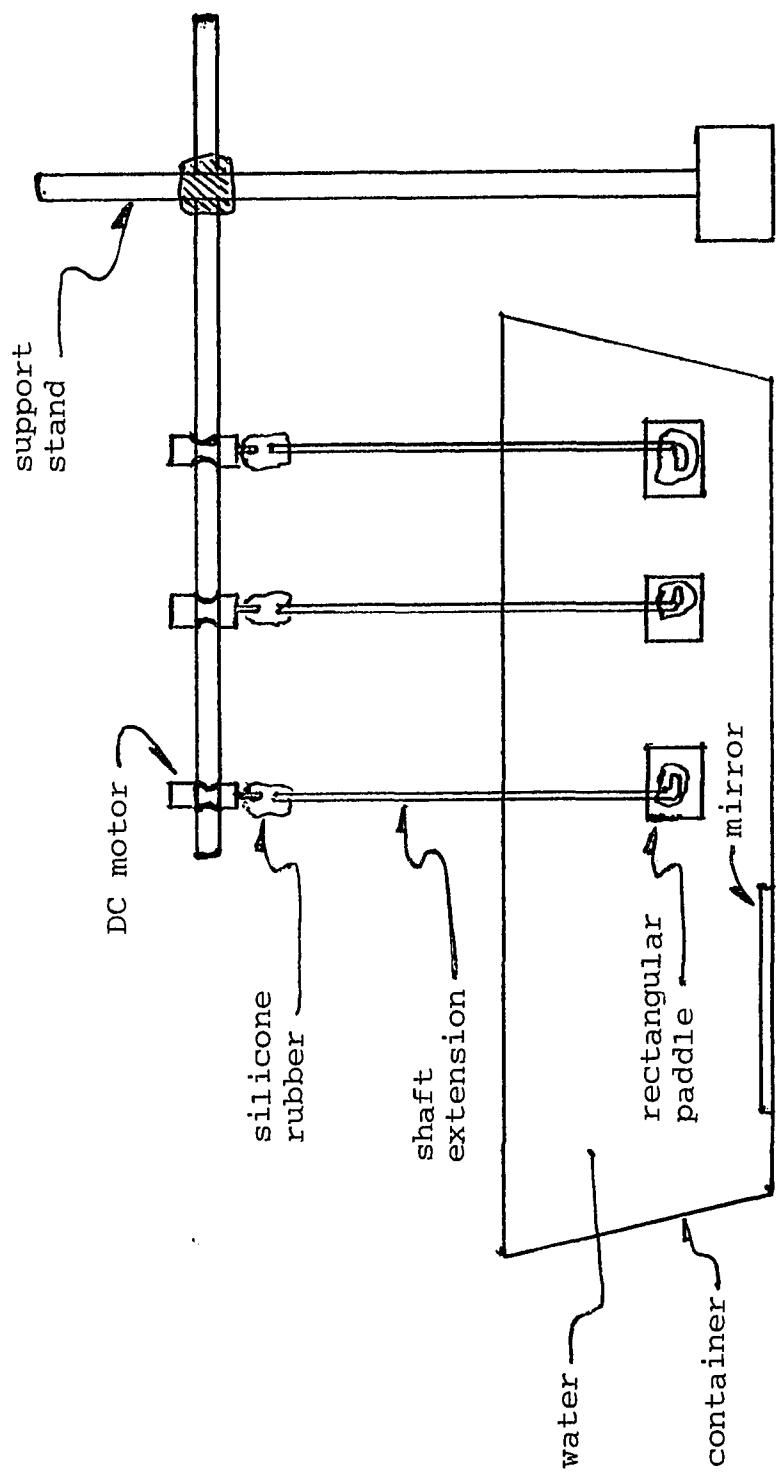


Figure IV-4
Equipment arrangement for generating turbulence in water

Photograph IV-4 shows the actual laboratory implementation.

Photograph IV-5 was taken of the three point survey subject observed through the water medium, as described above, in the absence of turbulence with a lens opening of f 4.5 and a shutter speed of $1/30$ th of a second. Photograph IV-6 of course identifies the true locations of the survey points. Their coordinates are

for Point P_R , $x = 6/16"$, $y = 18.5/16"$

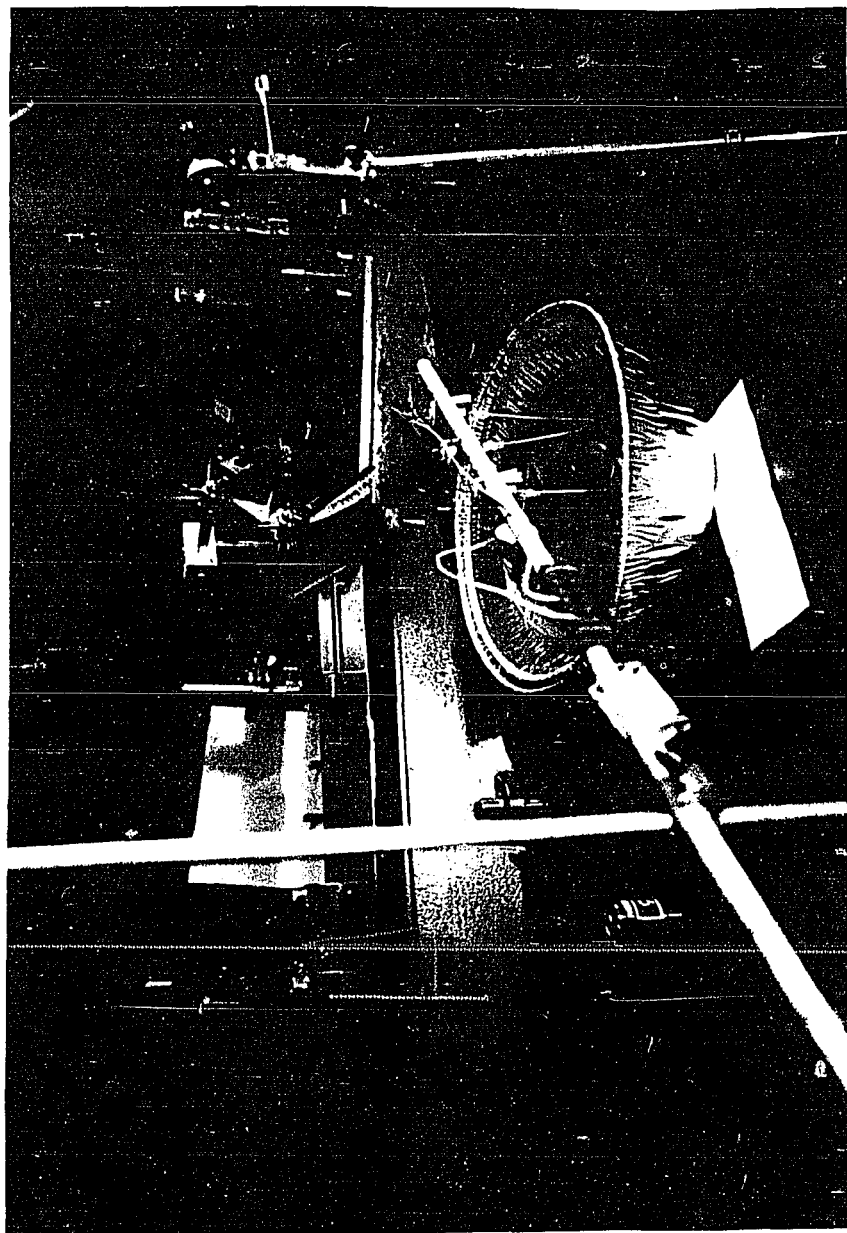
for Point P , $x = 12.8/16"$, $y = 7.5/16"$

for Point P' , $x = 22.5/16"$, $y = 7.5/16"$.

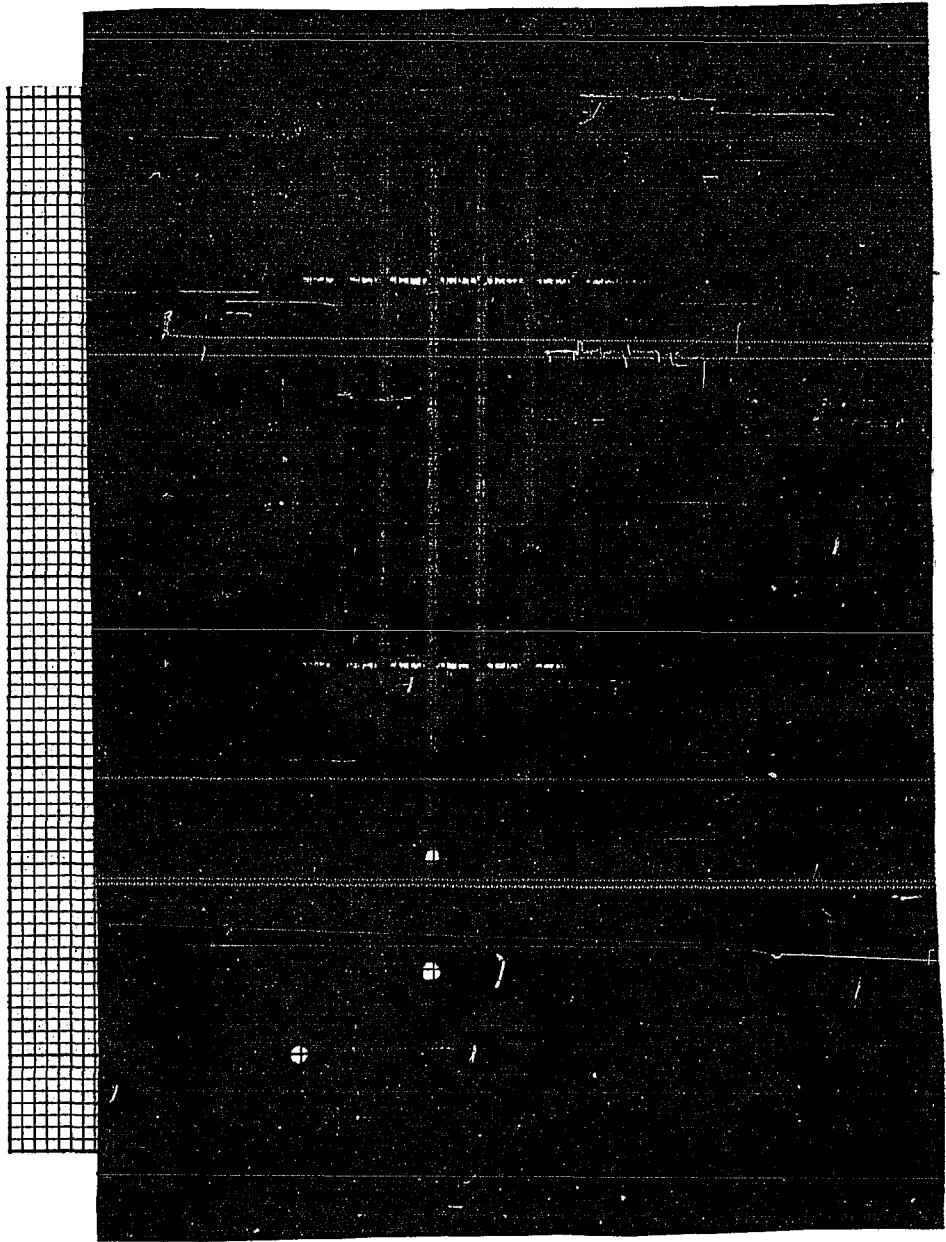
Photograph IV-6 was taken under conditions of random motion of the water surface with a lens opening of f 4.5 and a shutter speed of $1/125$ th of a second. Four exposures were strobed onto a single negative at these settings. As can be seen, their arrangement permitted the recording of identifiable separate positions of the observed points at 4 different instances in time.

In Photograph IV-6 the 4 corresponding positions are indicated by the numbers 1 through 4 and the 3 different points by priming and by the subscript R for the reference point.

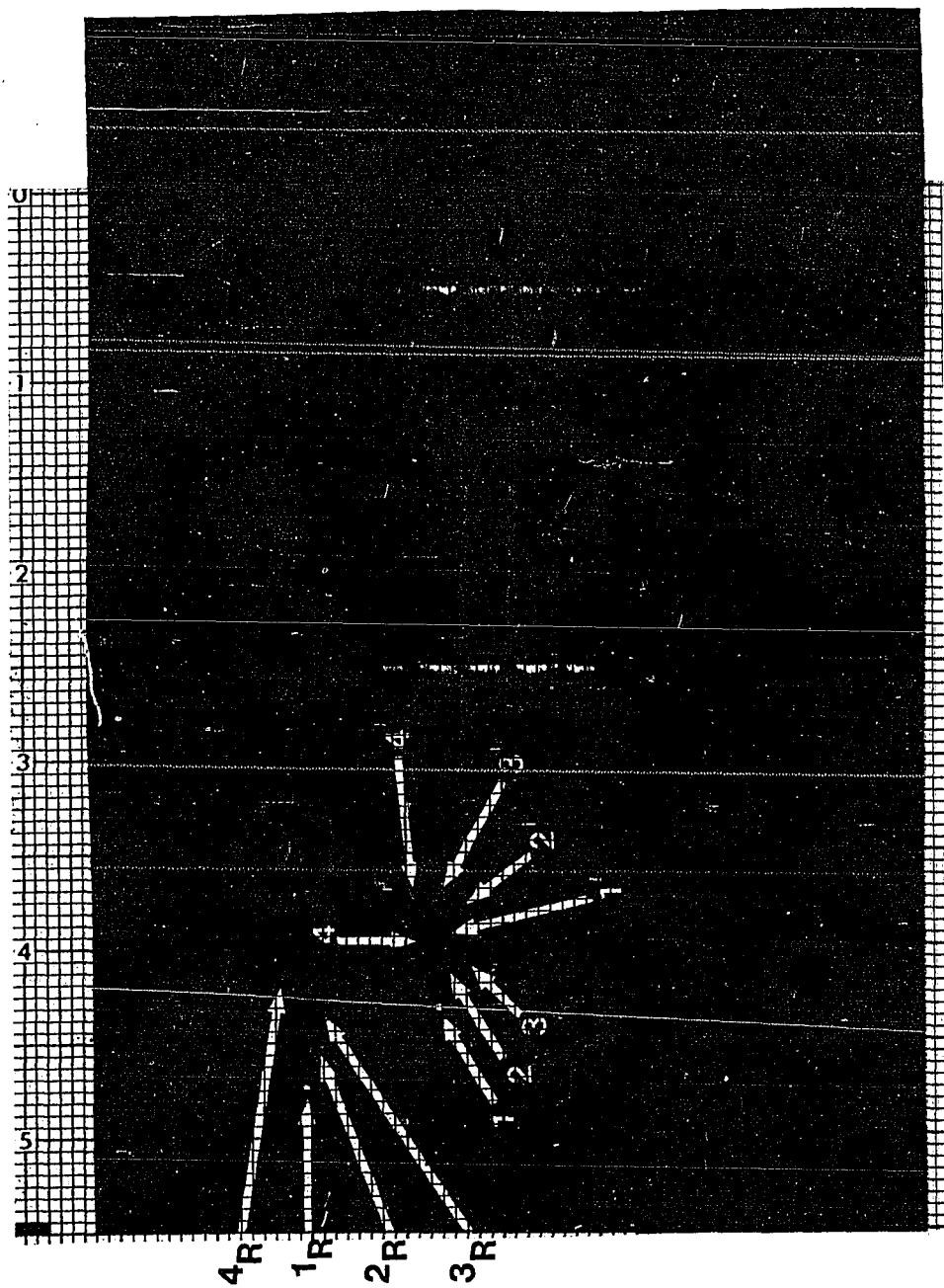
Determination of the expected values of the three random positions is now extremely simple as no determination of intensity is required. (The different brightness of two of the dots in Photograph IV-6 is attributable to a reflection from the very small target. Indeed the



Photograph IV-4
Equipment arrangement for generating turbulence in water



Photograph IV-5
Three point survey subject with scale observed through a water medium



Photograph IV-6
Multiple exposures of precise point positions thru turbulent water

possibility of such selective reflection was the reason that prompted the selection of larger targets for the previous experiments of Photographs IV-1 and IV-3).

Following is a tabulation of the coordinates of the expected values (centers of gravity of the positon observations for the 3 dots and of the components of the relative position vectors.

x/16"	P _R	P	P'	y/16"	P _R	P	P'
1	2.5	9	15.2	1	16.5	5.5	5
2	6	12.7	17.5	2	16	5	3.7
3	9	13	19	3	15.5	3.3	5.3
4	11.7	15	18.5	4	18.8	7.5	7.8

the expected values are therefore,

for Point P_R, $x = 7.3/16"$, $y = 16.7/16"$

for Point P, $x = 12.425/16"$, $y = 5.325/16"$

for Point P', $x = 17.55/16"$, $y = 5.45/16"$

and the difference vectors are

vector P_RP, $x = 5.125/16"$, $y = -11.375/16"$

vector P_RP', $x = 10.25/16"$, $y = -11.25/16"$.

From the coordinates of Photograph IV-5 on page 102 we have

vector P_RP, $x = 6.8/16"$, $y = -11/16"$

vector P_RP', $x = 16.5/16"$, $y = -11/16"$,

therefore the difference vectors of Photograph IV-6 have neither the magnitude or the direction of the reference vectors.

As predicted, for insufficient sample size, no correlation with the unperturbed positons or relative positions is apparent, confirming that only statistical

averaging of the observations over a valid statistical sample can result in correct computation of the true relative positions. This assumption, suggested by the previous theory (Chapter I) of course, constitutes the core of the proposed surveying method.

Some observations about the magnitude of the apparent motion of the observed optical images are in order. Field experience in conventional surveying as compared with the averaging methods discussed herein and summarized by the photographic data gathering method described, bring into evidence an interesting phenomenon.

Real time observation of an object through a turbulent medium, appears to yield much more considerable distortion than indicated in these pictures. In reality the effect is psychologically magnified by the simultaneous observation of points close to each other being displaced in opposite directions. This destroys the connected image as the lines defining the object as perceived in our mental image are randomly distorted. The actual magnitude of the maximum displacements on a time integrated basis proves to be much less than surmised.

As was often pointed out in the course of this investigation, one prominent characteristic of the effect of turbulence in the optical propagation medium and clearly duplicated by open flame turbulence generation is that it is accompanied by a translation of the expected value of the image point positions in the XY plane, i.e., there is a DC

component to the displacement of the observed points with respect to the stationary grid. This translation usually consists of a small displacement in the upward vertical direction and a generally more substantial shift in the apparent positions of the points in the horizontal direction.

This DC translation has been clearly evidenced in the previous comparison of the results of Photograph IV-1 and Photograph IV-3. The magnitude of this displacement has been computed as .944 inches to the left horizontal and .25 inches vertically.

This "DC component" is actually a slowly time varying random variable, so that no "a priori" prediction can be made about it. This is the reason for the requirement of an absolute reference.

A much faster random "vibration" is the feature most prominently noticed in conventional surveying. In time integrated data records such as the photographs shown, this results in a blurred enlargement of the object points. The success of the reported experiments rests on the fact that computing the center of gravity for this blurred image did identify a statistically stationary average which correctly determined the relative positions of the points.

Some practical observations about some experimental occurrences may prove useful to future experimenters in this field.

The turbulence generated in the water medium

results in much slower "vibration" components than those exhibited by the flames. As a result, the observed apparent translation of the object points was not only larger, but the apparent displacement of each point took a much longer period of time to occur. This enabled us to obtain distinguishable instantaneous positions for each object point on the time integrated data records, as shown in Photograph IV-6.

This slowness of movement was independent of the intensity of the turbulence introduced in the water. When the paddle motors were run at full speed, the object points appeared to move more quickly, and the magnitude of the translation increased proportionately. The experimental arrangement shown made it possible to move the focused position of the points far enough for them to leave the field of view.

The increased magnitude of focused point displacement has a serious effect on the sample time. While we had previously been able to strobe multiple exposures onto the data record in a reasonable length of time, 10 to 30 seconds, in turbulent air, and obtain a stationary statistical sample, the nature of turbulent water lengthened this exposure period to beyond a minute, which introduced a problem.

The photographic records contain the hologram image and the object points. When the hologram was strobed onto the negative for a long period of time, it over exposed the film and tended to wash out the data points. There are two solutions to this problem. One is accomplished by having the

measuring scale model built professionally with the width of the grid lines kept very narrow. In spite of the usual photographic image spread the area affected by this phenomenon is much more limited. The second solution is to have a reconstruction laser with a variable power output. With such a unit, one would reduce the light output proportionately with the increased exposure time and avoid burning in the grid on the negative. Neither of these methods were available for this feasibility study.

As previously stated the problem of theoretical determination of the minimum valid sample size is, as yet, unsolved. Several empirical methods are available. For the case of electronic data acquisition, the same computer performing the statistical average can keep track of the deviations and automatically determine when convergence is achieved within any chosen specification.

It should be remembered that this parameter depends on the characteristics of the turbulence during observation. A theoretical criterion would much simplify the practice of surveying and is a highly desirable result to be achieved. It is hoped that future research will be done in this direction.

CHAPTER V

MINIATURE AND SPECIAL EFFECTS (AN APPLICATION TO MOTION PICTURE TECHNIQUES)¹

This chapter presents an application of the previously analyzed holographic techniques to the solution of some problems relative to the practice of miniature shooting, often used in the motion picture industry. The method suggested herein utilizes the characteristics of a truly three dimensional holographic virtual image, namely the ability to spatially position this image at will, and simple techniques for magnifying this image, to provide distinct advantages over the inherent limitations of the standard miniature method presently used.

Miniature techniques are used in the motion picture industry to reduce the capital expense of set construction by building a portion of a required set at a dramatically reduced scale. Utilizing this technique, the portion of a set needed to be built at full scale is limited to the region actually occupied by the performers, as seen thru the camera's lens, and allows the remainder of the set to be built in miniature scale. By correctly selecting the

¹ This application was presented together with a ten minute demonstration film at the XIV Congress UNIA TEC in Varna, Bulgaria - Sept. - Oct., 1980, cfr. Actes du XIV Congress UNIA TEC, Oct. 1980 (and translated into Italian in "Note di Tecnica Cinematografica", Dec. 1980). A brief summation in English was the subject of a presentation at the 1981 Congress of the SMPTE, New York.

dimensions of this miniature set and positioning it at precisely the right location between the camera and the full scale portion of the set, then by perspective projection, the miniature set will appear to be the same size as and an integral extension of the full scale set, within the camera's field of view.

With this technique, however, the illusion relies completely on the relative positions of the camera, the miniature and full scale sets. Any variations of camera location or orientation destroy this illusion and are therefore not allowed. Shooting is restricted to fixed camera conditions, as indicated in Figure V-1, where trucking or panning are not permitted, and only limited zooming is possible.

The method for miniature techniques described herein circumvents these disadvantages. After proper positioning of the photographic plate (containing a hologram of the miniature set) and of the reconstruction light source, relative to each other and to the full scale portion of the set, the conditions depicted in Figure V-2 are produced. Here the magnification of the hologram provides a three dimensional virtual image of the miniature set that is full scale and spatially located at the exact position that would be occupied by the missing portion of the actual set. Consequently, as long as the set is viewed through the holographic plate, the camera can pan, truck and zoom, and can selectively focus on any part of the set without experiencing distortion or loss of the illusion that a

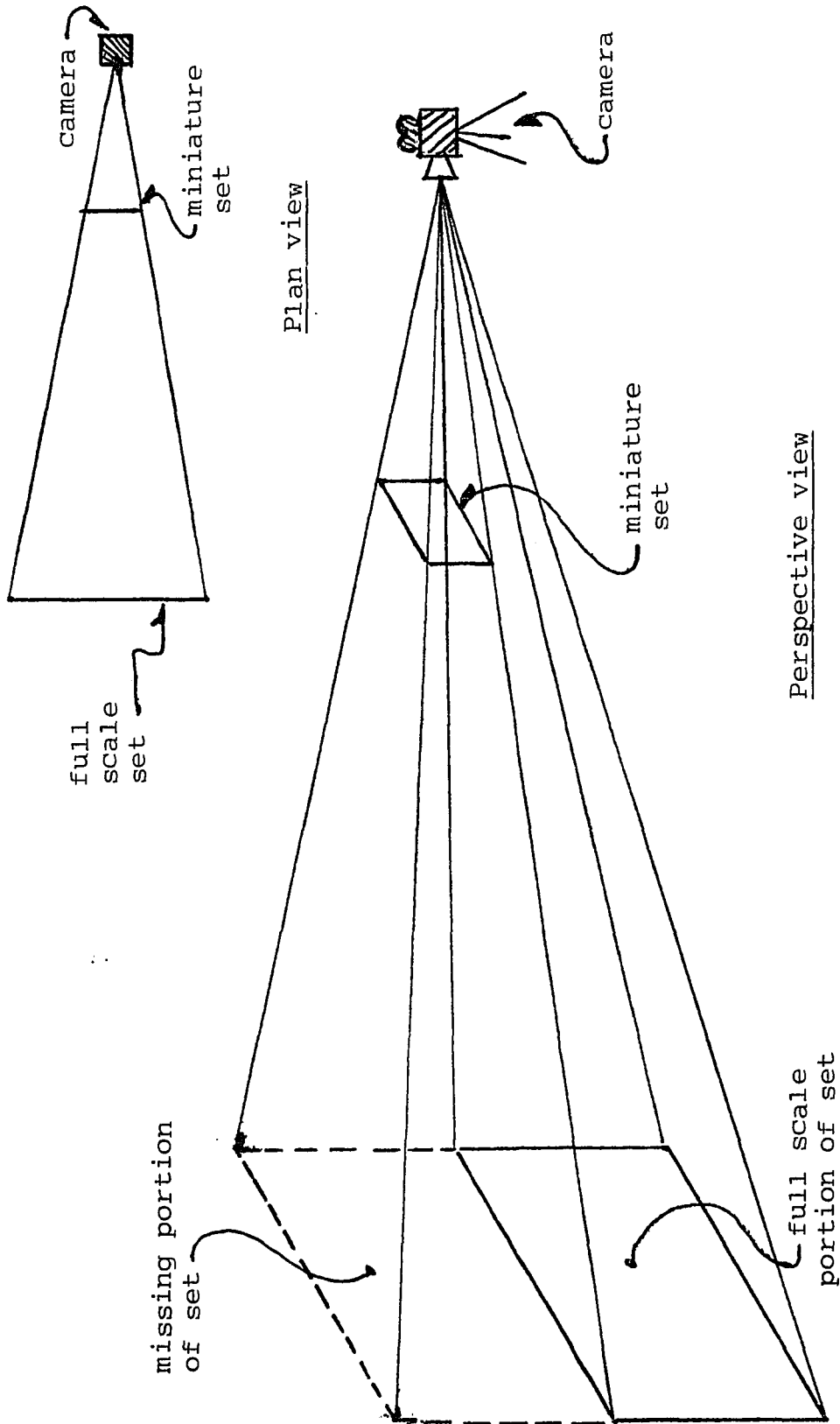
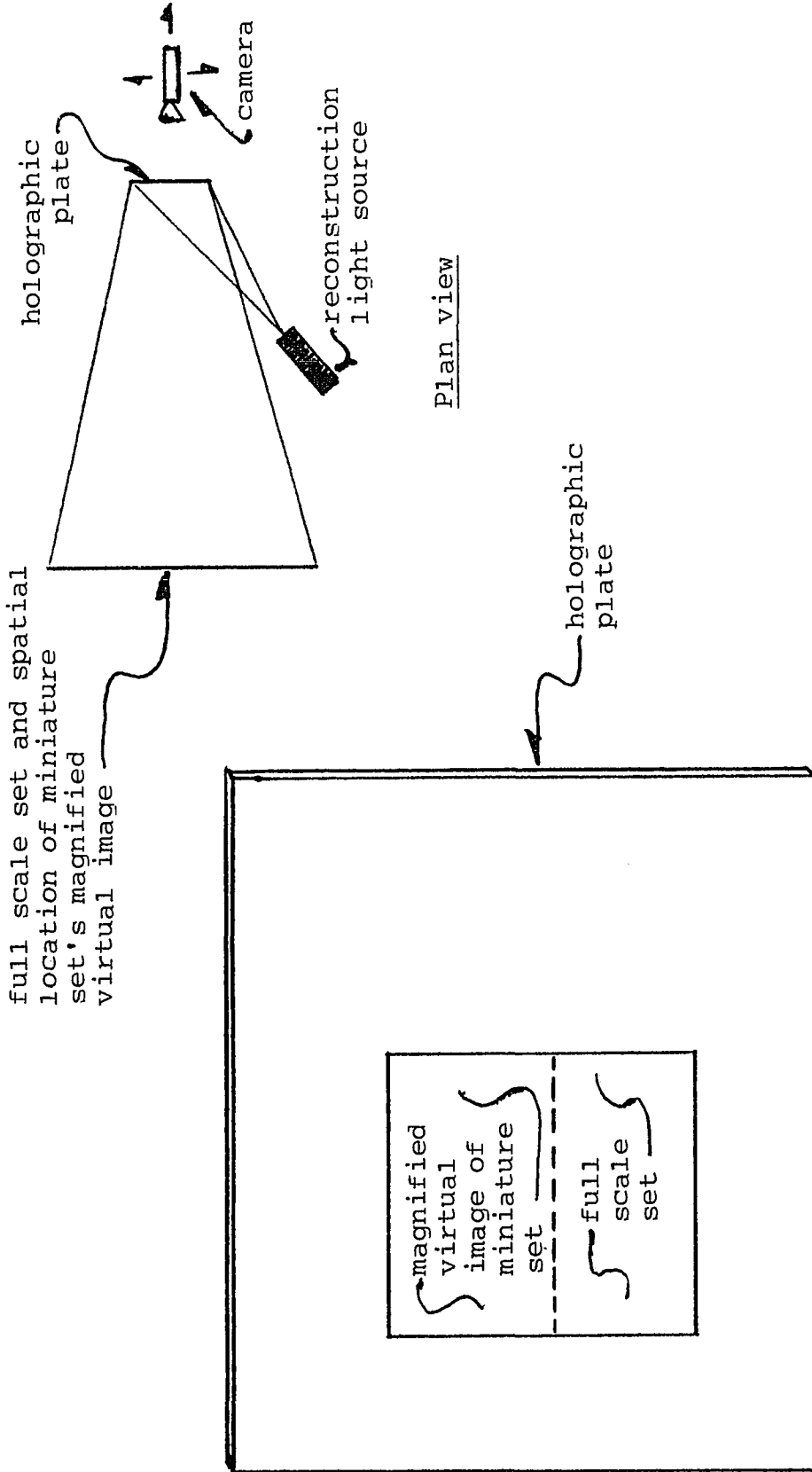


Figure V-1
Miniature shooting using standard techniques



Camera's view
(through any portion of hologram)

Figure V-2
Miniature shooting using holographic techniques

complete full scale set is being photographed.

The process begins with producing a hologram of the miniature set. The elements involved in this are the same as described in Chapter II and depicted in Figure II-1 (reproduced here as Figure V-3 for convenience).

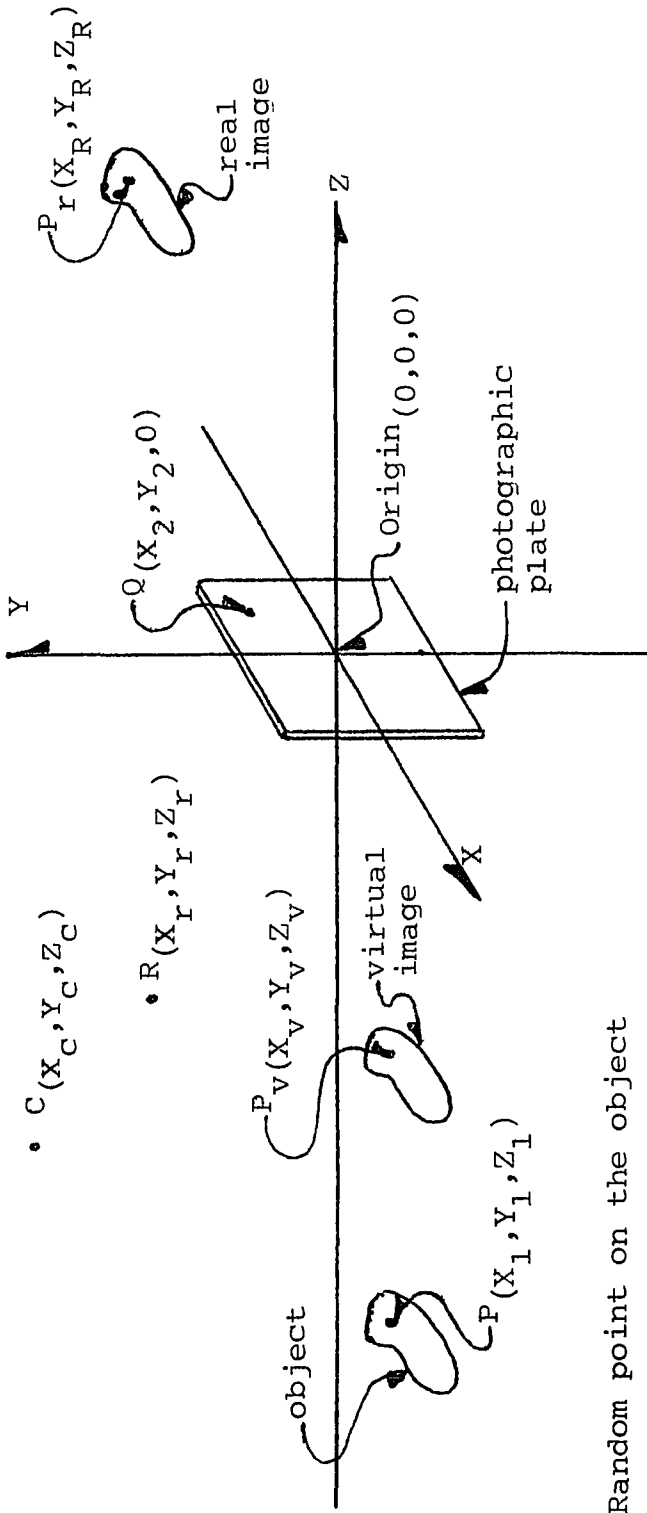
Anticipation of the desired value of magnification of the hologram during reconstruction, and the expected orientation of the camera and of the full scale set during filming, dictates the relative locations of the miniature set, the photographic plate, and the reference and reconstruction light sources. Therefore with the locations of the principal elements involved in the making and reconstruction of the hologram fixed by these predetermined conditions, the only factors remaining of major concern are those related to distortion.

In Chapter II it was indicated that lateral distortion can be avoided by moving either the reconstruction light source or the holographic plate simultaneously with, and in proportion to, changes in the location of the observation point Q (the camera).

It was shown that if this dependent movement was such that it maintained the condition $X_C = X_R \cdot Z_C/Z_R$ at all times, then the coordinates of point P_V (the virtual image of point F in the miniature set)

$$Z_V = \frac{Z_C Z_1 Z_R}{Z_1 Z_R + \mu Z_C Z_R - \mu Z_C Z_1} ,$$

$$X_V = \frac{X_C Z_1 Z_R + \mu X_1 Z_C Z_R - \mu X_R Z_C Z_1}{Z_1 Z_R + \mu Z_C Z_R - \mu Z_C Z_1}$$



- P : Random point on the object
- P_v : Point P on the virtual image
- P_r : Point P on the real image
- Q : Random observation point on plate
- R : Location of reference light source
- C : Location of reconstruction light source

Figure V-3
 Coordinate system for the parameters of
 holographic wave recording and reconstruction

and
$$Y_V = \frac{Y_C Z_1 Z_R + \mu Y_1 Z_C Z_R - \mu Y_R Z_C Z_1}{Z_1 Z_R + \mu Z_C Z_R - \mu Z_C Z_1}$$

reduce to
$$Z_V = \frac{1}{\mu} Z_1 \cdot M_V \text{ lat},$$

$$X_V = X_1 \cdot M_V \text{ lat},$$

and
$$Y_V = Y_1 \cdot M_V \text{ lat}.$$

Therefore adherence to this constraint eliminates distortion that would otherwise occur due to panning and trucking.

The relationship of M_V lateral and

M_V longitudinal, i.e.,

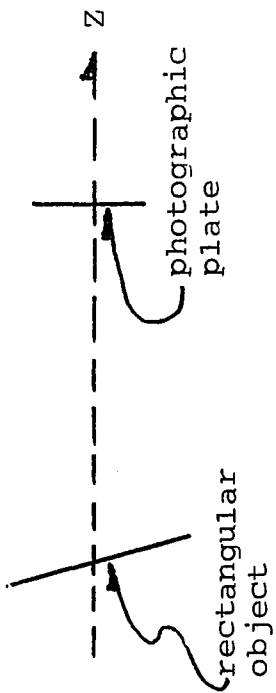
$$M_V \text{ lat} = \left[1 + Z_1 \left(\frac{1}{\mu Z_C} - \frac{1}{Z_R} \right) \right]^{-1}$$

$$M_V \text{ long} = \frac{1}{\mu} \cdot (M_V \text{ lat})^2,$$

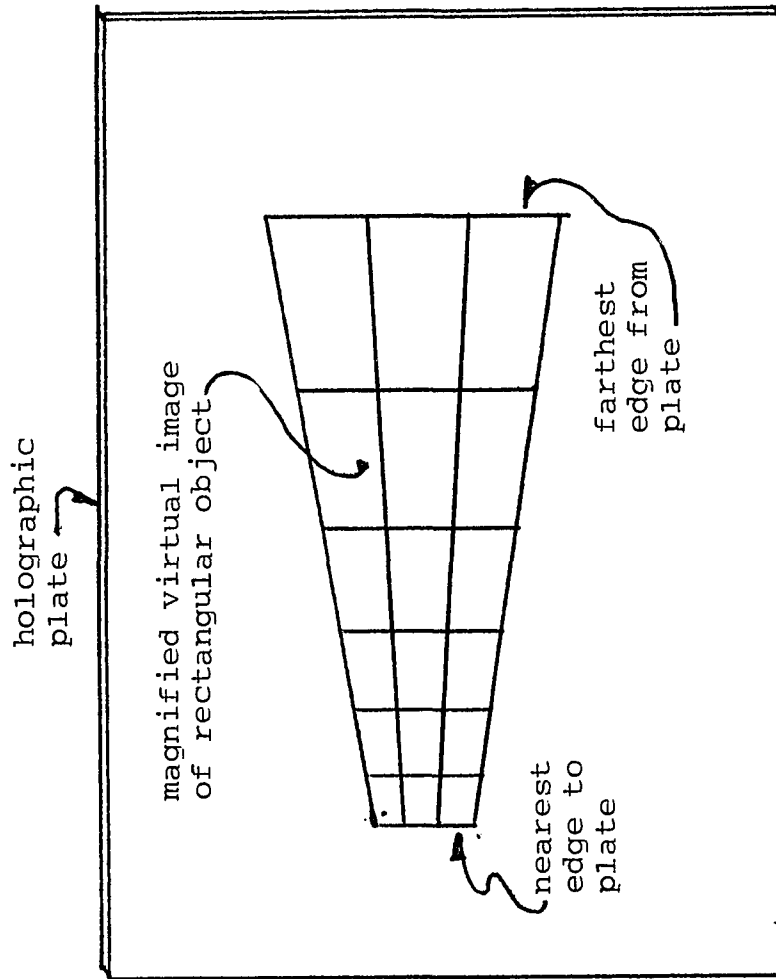
identifies another serious source of distortion.

For the previous application it was required only that a two dimensional rectangular plane, with parallel orientation to the plane of the photographic plate, be magnified. In that case, Z_1 was very conveniently equal to a constant and therefore the magnitude of $M_V \text{ lat}$ was determined by the values of Z_C and Z_R only, and $M_V \text{ long}$ was of no consequence since the object had no depth.

Consider now the magnified virtual image of this same two dimensional rectangular plane if it were not originally parallel to the photographic plate. The magnified image would more resemble a trapezoid laying on its side than a rectangle, as depicted in Figure V-4.



Plan view
orientation when
recording hologram



Reconstructed hologram

Figure V-4
Longitudinal distortion in magnified image

The severity of this condition is easily identified by re-examining, from Chapter II, the value of Z_1 for which the discontinuity occurs in the plot of ' Z_V/Z_1 vs Z_1 ', and the suggested set of operating parameters for maximum vernier control of lateral magnification, i.e.,

$$Z_1 = Z_C Z_R / (Z_C - Z_R) ,$$

and $Z_1 = Z_C = -1.0, -0.5 > Z_R > -1.0 ,$

(these results were developed with $\mu = 1$). Under these conditions, the value of lateral magnification is

$$M_{V \text{ lat}} = \frac{Z_R}{2Z_R + 1} .$$

Setting $Z_R = -2/3$, arbitrarily, produces a lateral magnification, by a factor of 2 at the original object point $Z_1 = -1$. However the discontinuity, i.e., $M_{V \text{ lat}} \rightarrow \infty$, for these values occurs at $Z_1 = -2$.

Therefore if the object of the hologram were such that its nearest point to the photographic plate were at $Z = -1$, and its furthest point were located at $Z = -2$ or beyond, then the following condition would result during reconstruction. The nearest point of the object would be located at $Z = -2$, enlarged laterally by a factor of 2. That portion of the objection originally at $Z = -2$ would be located at a point $Z \rightarrow -\infty$, enlarged laterally by a factor approaching , and any portion of the object that was beyond $Z = -2$, originally, would be located on the opposite side of the holographic plate from the above, with an inverted and

equally distorted appearance.

This type of image distortion might appear to be a serious potential limitation, but it is not a real consideration due to the nature of the task at hand. The dimensions of the desired reconstructed image are known fixed values, equal to the dimensions of the missing portion of the full scale set. Since these values will always be finite, the value of lateral magnification will be also. This therefore identifies the need for predistorting the miniature set and having this predistortion compensated for by the magnification process.

The method to be used for the proper construction of the miniature set is similar to the technique of false perspective and requires the selection of only two parameters; the scale of lateral magnification (2 or 5 or 10, etc.), and the location of the nearest point of the reconstructed image to the holographic plate, i.e., the Z component of the nearest point of the full scale set that the reconstructed image is to be adjacent to. All other parameters are fixed by these two values.

A simple example of determining the dimensions of a miniature set will best clarify the procedure. Assume that it is desired to have an image of a 45° triangle located in the XZ plane, as shown in Figure V-5, and that lateral magnification of the nearest plane of the image will be equal to 2.

The dimensions of the miniature set required to produce the desired image will be developed on a unit value

magnification
factor desired = 2

point	X	Z
1	+5	-10
2	-5	-10
3	-5	-20

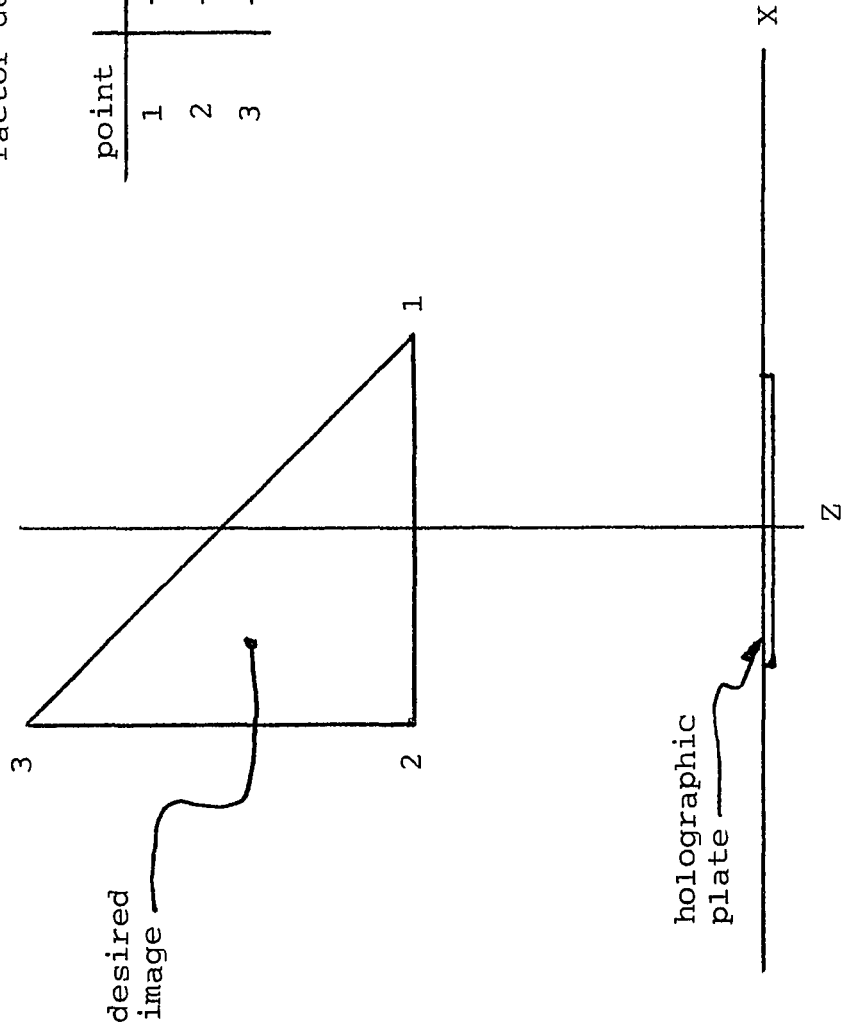


Figure V-5
Starting point for construction of
a predistorted miniature set

basis, with M_V again equal to 1. Setting $Z_C = Z_1 = -1$, where Z_1 represents the closest point of the miniature set to the photographic plate, then $Z_R = -2/3$ for $M_V \text{ lat} = 2$. From the previously developed formulas,

$$Z_V = Z_1 \cdot M_V \text{ lat}$$

substitution provides

$$Z_V = (-1) \cdot 2 = -2.$$

Applying a scaling factor of 1/5 to all coordinates of the desired image provides its unit values.

point	X	Z
1	-1	-2
2	+1	-2
3	-1	-4

The coordinates of points 1' and 2' of the miniature set are obviously equal to 1/2 the values of points 1 and 2, for this case. Point 3' is found from

$$Z_3 = Z_3' \left[1 + Z_3' \left(\frac{1}{Z_C} - \frac{1}{Z_R} \right) \right]^{-1}$$

where substitution provides

$$-4 = Z_3' (1 + Z_3' / 2)^{-1}$$

$$\text{or} \quad -4/3 = Z_3' \quad ,$$

$$\text{and} \quad X_3 = X_3' \left[1 + Z_3' \left(\frac{1}{Z_C} - \frac{1}{Z_R} \right) \right]^{-1}$$

where substitution provides

$$-1 = X_3' (1 - 4/6)^{-1}$$

$$\text{or} \quad -1/3 = X_3' \quad .$$

Therefore the miniature set has the unit value coordinates

point	X	Z
1'	-.5	-1
2'	+.5	-1
3'	-1/3	-4/3

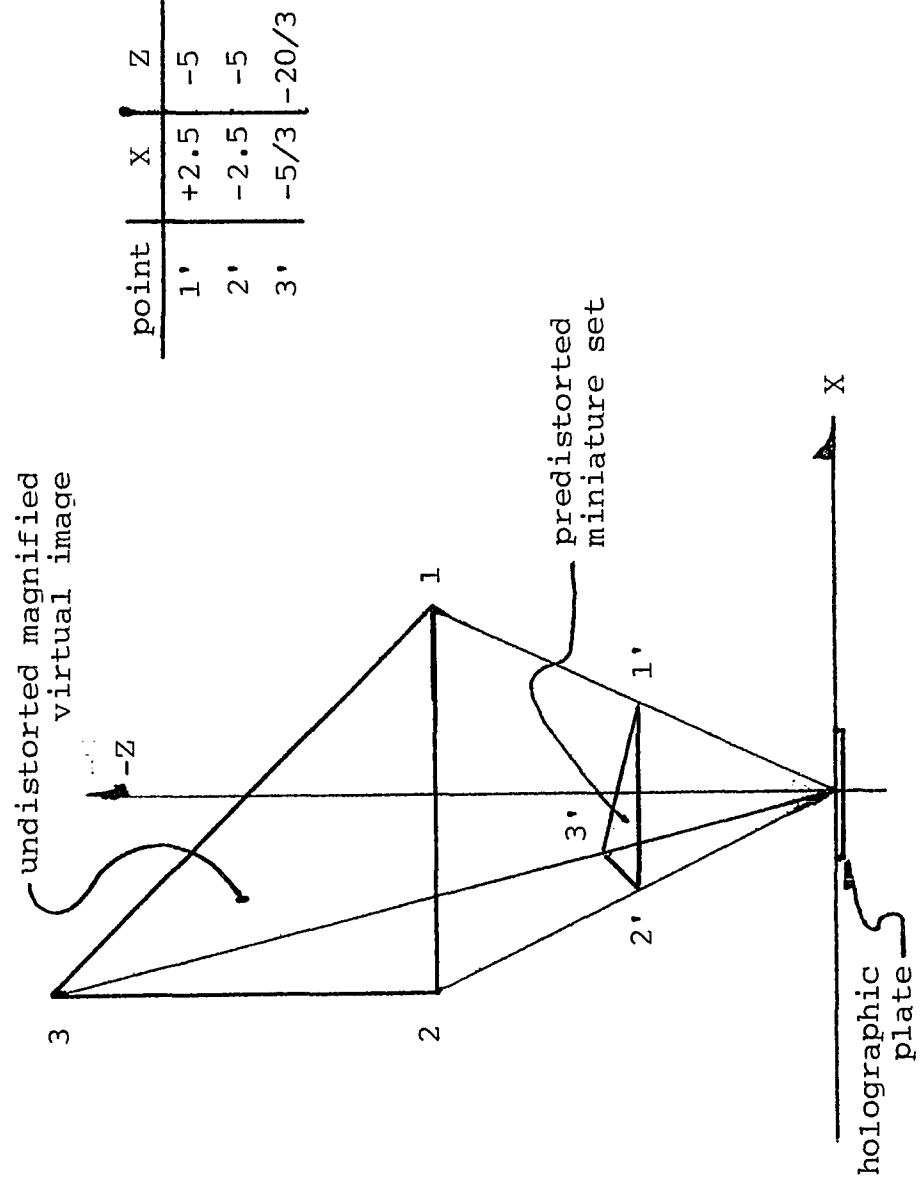
Multiplying each value by the reciprocal scaling factor, 5, produces the actual coordinates of the miniature set that would provide the desired reconstructed image, under the conditions stated, as shown in Figure V-6.

It was mentioned in chapter II that angular magnification can be used to reduce the distortional type differences between longitudinal and lateral magnification. This is true if careful attention is given to the factor of color in this application. Since the reconstructed image might be required in white light, and if differences in wavelength (color) are to be utilized, then the selection of the reference light source wavelengths must be based on the required white light reconstruction light source.

The laboratory work performed on the application presented was done using only a red laser. The results were very promising but future work is required in the use of three lasers for recording and reconstruction (white light) and also the area of miniature set construction must be explored for sets requiring more than just simple structures. The benefits offered by the application of holographic techniques to special effects are substantial enough to warrant the required effort.

magnification
factor = 2

point	X	Z
1	+5	-10
2	-5	-10
3	-5	-20



point	X	Z
1'	+2.5	-5
2'	-2.5	-5
3'	-5/3	-20/3

Figure V-6
Preditorted miniature set and
undistorted magnified hologram image

CHAPTER VI

CONCLUSIONS AND SUGGESTIONS FOR FUTURE INVESTIGATION

In this thesis an investigation has been conducted regarding several different phenomena and techniques. These were primarily optical effects of turbulence, distortions in holographic image magnification and others. A theory was consequently developed which permits the practical implementation of several novel techniques of generation and use of optical imaging.

Two possible applications are discussed in some detail and have indeed motivated this work: a novel procedure for conducting a survey of an airport runway and an alternate method for obtaining miniature special effects as used by the motion picture industry. Both of the new processes offer substantial improvements over the results produced by the standard techniques that are presently employed.

Magnification of the reconstructed image of a hologram is an essential element in each of the processes; therefore the previously developed theory on magnification was reviewed and analyzed and specific techniques for its application developed.

In particular the effects of the locations of the equipment used in making a hologram and in reconstructing and magnifying the hologram's image were investigated to determine the optimum conditions for application in the two

new processes (cfr. Chapter II). Experimental verification was presented showing how the hologram's image can be magnified to the prescribed accuracy and how the image can be spatially located at any desired position within the tolerances required.

This experimental verification was presented via the photographs in Chapters III and IV. In future work, if larger values of magnification are anticipated than those encountered here, then the target value initially selected should be greater than the factor of five (5) which was used in this study.

In the course of this investigation a detailed method of design was developed and a set of "unit value" parameters were introduced. These were used in the subsequent feasibility study and were shown to lead to very accurate reliable results.

During the course of the study, many factors of magnification were used (from 1 to 12) and in each instance a relatively small adjustment in the position of the reconstruction light source, accomplished within a maximum limit of adjustment of 24 inches, provided the exact increase in magnification that was sought.

The subject of lateral distortion of the magnified image was investigated and two methods were presented for avoiding this source of distortion. Each of these methods was tested in the laboratory and it was shown that they did successfully control the occurrence of lateral distortion.

In particular it was shown that there is a distinct difference between the two methods. Four physical components are involved in viewing a hologram's reconstructed magnified image: the hologram plate, the reconstruction light source, the optical instrument, i.e., the camera, and the three dimensional holographic spatial image.

To avoid lateral distortion, two of these system components must physically move in a prescribed manner as the observation point on the hologram plate is changed.

In the first method tested, the reconstruction light source was moved as the observation point was changed, with the hologram plate and camera held at their original locations (the camera was moved only to change the observation point). The spatial location of the image therefore changed, but was viewed without lateral distortion at its new position. This method can be used in any case where the reconstructed image is the only thing being observed or movement of the image relative to some background is acceptable. This method can be easily implemented by the construction of a precise mechanical movement that provides for pivotal motion of the camera and reconstruction light source about a fixed hologram plate, (cfr. Chapter II).

The second method required moving the hologram plate and the camera while the reconstruction light source and the spatial location of the image remain fixed. This method also permits viewing the magnified image from any point on the hologram plate free of lateral distortion, and

must be used when the spatial location of the image has to be maintained, as is the case in the two new processes presented herein. Here again a precision mechanism can be constructed that will provide the proportional lateral movement of the hologram plate and the camera, in response to the movement of the camera to a new observation point.

A second type of distortion associated with the magnification of a hologram's image, i.e., longitudinal, was investigated. A method for compensating for this type of distortion prior to the making of the hologram was presented together with the mathematics for computing the amount and type of predistortion required in the small scale subject of the hologram, based on the factor of magnification and the geometry of the image desired (cfr. Chapter V).

Identifying the accuracy achievable in spatially locating the hologram's image was the second objective of the study. The methods used for positioning an image at an exact location were described in Chapters II and III, and were then successfully applied throughout the course of the experimental investigation. Verification of the accuracy of these results achieved was presented in the photographs of Chapters III and IV.

The next objective of the feasibility study was to record data observed through turbulent medium. Two techniques for accomplishing this were described in Chapter III. One of these, multiple exposures on a single photograph, was tested in the laboratory as part of the

study, the successful results of which were presented in Chapter IV. The second method described, i.e., using a computer based system, offers superior results in a more timely fashion, and should be the subject of future efforts.

The concept of digitally recording and analyzing data is well within the software capabilities of the present state of the art, and its implementation is a matter of financing rather than technology. The obvious benefits of this approach were enumerated in Chapter III and are most certainly worthy of pursuit.

The final objective of the feasibility study was the applicability of time averaging statistical methods to data observed through turbulent mediums. Time averaging of the photographically recorded data was reported in Chapter IV and the results substantiated the predictions of the theory presented in Chapter I. In the cases reported, when the data sample was statistically valid, the difference position vector, y , was shown to be stationary, within the limits of the measurement techniques used. Conversely, as predicted by theory, when the sample was insufficient, the experimental results proved that the technique failed, as stationarity was not achieved.

These reported results strongly support the use of time averaging statistical techniques for removing the distortion from recorded data obtained under turbulent conditions.

Having successfully accomplished the four

objectives of the feasibility study, i.e., demonstrated the practicality of magnification of a hologram's image to an exact size, demonstrated the achievement of high accuracy spatial positioning of this image at a predetermined location, demonstrated one of the techniques for the recording of suitable data, and demonstrated the applicability of time averaging techniques to the correct determination of true position, by removing the image displacements and distortions resulting from observation through a turbulent medium, it is to be concluded that the feasibility study was successful.

The techniques of magnifying and spatial locating a hologram's reconstructed image used in the above investigation were also employed in presenting a novel procedure for accomplishing the miniature special effects utilized by the motion picture industry (cf. Chapter V).

This procedure was employed in a laboratory simulation where a small set was constructed with a portion of it missing. The magnified hologram image of the miniaturized missing portion of the small set was spatially located on the small set so as to provide, optically in proper scale, the missing portion of the small set. A ten minute film on the prominent characteristics of this approach to miniature techniques and an article describing the process were presented to the 14th Congress of UNIATEC and were enthusiastically received. A condensation of the article was later presented to the 1981 Congress of SMPTE.

The laboratory test of this procedure was conducted with a single laser output of red light, and the results showed conclusively the merit of the techniques used. However, for implementation of this approach on other than a test basis, the simultaneous use of lasers with red, green and blue light outputs must be investigated in the future to provide a reconstructed image appearing in white light illumination. Also, it is felt that the use of multiple lasers will reduce the effects of speckling, which are so apparent in single laser applications.

Based on the results of the feasibility study, it is recommended that a survey be performed under real world conditions using the photographic method and the results of this be used to acquire funding for the computerization of the technique presented, as this was not possible given the limited resources and constraints under which the feasibility study was conducted.

A rigorous analysis should be conducted on the order of magnitude of accuracy that is obtainable by the methods presented.

This is of paramount importance to all further development of the methodology for immediate application in the conduct of a full scale survey using photograph and for later development of a real time analysis computer based system.

Computations of the size of a sufficient statistical sample, under different turbulence conditions

should be performed to provide theoretical constraints for the photographic application.

Computerization of the process, of course, would obviate the need for sample size parameters. The computer software would continually compute the variance of the samples being taken and identify instantly when a sufficient sample had been obtained.

A deterioration of the hologram's image can be noticed in the photographs of the magnified image. This is mostly caused by speckling, a well known property of coherent light illumination. Future work should be performed to determine if this can be avoided by the use of two lasers, of the same wavelength, during recording and reconstruction, or if the use of the three prime colors, to produce white light, will remove this deterioration.

Appendix A

Computation of expected values of Points A and B in Photograph IV-3

The computation of the expected values of Points A and B in Photograph IV-3 was performed in the following manner.

The 1/16" grid that has been burned into the photograph provides the boundaries for individual matrix arrays of black dots within each grid element.

The dot matrices are the result of the off-set screening process which automatically transformed the grays of the original negative into an array of weighted black dots, which when viewed with the naked eye, reproduces the shapes and tone contrasts of the original photograph.

Using a medium lens magnifying glass, the dot matrix contained in each grid element was examined, and based on the quantity and size of the black dots contained therein, each element was assigned a value of from 10 to 0, (10 for no black dots and 0 for all black dots).

The assigned element values for those elements which contained a portion of either Point A or Point B are shown in the tables on page 135.

These assigned values in the tables were then summed for each row and column. The centers of mass were then identified horizontally and vertically. These two centers then formed the coordinates of the center of gravity of each point.

The center of gravity is actually the density center of the exposed area for each point and represents the center of the location that was occupied for the longest time by the point image on the negative during the multiple exposures of the photograph.

		2	2	5	7	8	8	7	4		
		5	9	10	10	10	10	10	8	4	
		3	9	10	10	10	10	10	8	6	1
		2	6	10	10	10	10	10	7	4	
1	2	6	9	10	10	10	10	8	5	2	
	2	5	6	7	7	6	5	2	2		
1	6	20	41	48	52	53	53	50	47	32	16

↑

		3	7	9	10	10	10	7
		3	5	10	10	10	10	8
		1	5	9	10	10	10	8
		3	8	10	10	10	10	8
		3	5	6	8	9	8	2
		2	3	3	3	3	1	
9	24	34	48	51	52	49	42	32

↑

43
76
87
89
83
42

56
66
73
77
51
18

Grid element values and column
and row totals for Point A

Grid element values and column
and row totals for Point B

Computation of expected values of
Points A and B in Photograph IV-3

Selected Bibliography

- Born, M. and Wolf, E., Principles of Optics, third edition, Pergamon Press, New York: 1965, p. 453.
- Champagne, E.B., Nonparaxial Imaging, Magnification and Aberration Properties in Holography, J. Opt. Soc. Am., 57, 1967, p. 51.
- Collier, R.J., Burckhardt, C.B., Lin, L.H., Optical Holography, Academic Press, 1971.
- David, Foote & Kelly, Surveying: Theory and Practice. Fifth Edition, New York: McGraw-Hill, 1968.
- Feldman, S.I., The Effects of Optical Path Perturbation During Recording On A Reconstructed Holograph Image, Doctoral Thesis, New Jersey Institute of Technology, 1976.
- Fowles, Grant R., Introduction to Modern Optics, Holt, Rinehart and Winston, Inc., 1968, p. 144.
- Gabor, D., Nature, vol. 161, 1948, p. 777.
- Gabor, D., Nature, vol. 162, 1948, p. 764.
- Gaskill, J.D., J. Opt. Soc. Am., vol. 58, 1968, p. 600.
- Goodman, J.W., Huntly Jr., W.H., Jackson, D.W. and Lehmann, M., Appl. Phys. Letters, vol. 8, 1966, p. 311.
- Leith, E. and Upatnieks, J., J. Opt. Soc. Am., vol. 52, 1962, p. 1123.
- Leith, E. and Upatnieks, J., J. Opt. Soc. Am., vol. 53, 1963, p. 1377
- Leith, E. and Upatnieks, J., J. Opt. Soc. Am., vol. 54, 1964, p. 1295
- Meier, R.W., Magnification and Third-Order Aberrations in Holography, J. Opt. Soc. Am., vol. 55, 1965, p. 987.
- O'Neill, Edward L., Introduction to Statistical Optics, Addison-Wesley Publishing Company, 1963, ch. 3.
- Stone, J.M., Radiation and Optics, McGraw Hill Book Company, 1963, p. 299.
- Tatarski, V.I., Wave Propagation in a Turbulent Medium, McGraw-Hill Book Company, 1961.

Zambuto, M. and McGovern, P., Composite Miniature
Special Effects by Holography, Actes du XIV
Congres UNIATEC, Varna, Bulgaria, 1980.